Investigations of Natural Radioactivity Levels in Cement, Cement's Raw Materials and Some Related Environmental Samples using Gamma Ray Spectrometer

A Ph.D. Dissertation Submitted to the Department of
Physics Addis Ababa University
In Partial Fulfillment of the Requirement of the Degree of
Doctor of Philosophy in Nuclear Physics

Hailu Geremew

Addis Ababa University
Addis Ababa, Ethiopia
© *February 18, 2020*

Declaration

This Ph.D. dissertation has been submitted to Addis Ababa University Department of Physics as my original work, with the approval of my supervisor.

Name: Hailu Geremew

Signature: ——————

This Ph.D. dissertation has been submitted for examination with my approval as a Student's advisor.

Name: Prof. A. K. Chaubey

Signature: ——————

Place and date of submission:

Addis Ababa University

Department of Physics

February 18, 2020

Addis Ababa University College of Natural Sciences

Department of Physics

Investigations of Natural Radioactivity Levels in Cement, Cement's Raw Materials and Some Related Environmental Samples using Gamma Ray Spectrometer

by

Hailu Geremew

Approved by the Examination Committee

_____, External Examiner _____

_____, Internal Examiner _____

Prof. A. K. Chaubey, Advisor _____

_____, Chairman _____

Dedication

This dissertation is dedicated to Father♠ and Mother♡ of the Author.

Statement of the Author

I, the author born in 1987 G. C. and completed school level education in 2007 G. C. I graduated from University of Gondar in BSc degree in Physics in 2010. I owned MSc degree in Nuclear Physics in 2012 from Addis Ababa University by thesis work titled “Thermal Neutron Capture in Bromine”. I am teaching different physics courses in Wollo University since 2013 G. C. I joined Addis Ababa University for Ph.D. follow ship under same supervisor of MSc, Prof. A. K. Chaubey in 2016.

Acknowledgment

Before all and above I am deeply thankful to “Waaqa Tokkicha!”, by the grace of whom the progress and success of this work was possible.

I would like to express my deepest gratitude to Prof. A. K. Chaubey, Professor of Nuclear Physics at Department of Physics, Addis Ababa University, for supervising this research work, stimulating discussions, valuable comments, continuous encouragement and reading throughout the manuscript. Special thanks to Dr. Tilahun Tesfaye for providing advice with technical issues, for his useful comments and illuminating constructive discussions, even for my future life.

I have also a great respect for my wife♡ and son, kid. Keraajum♣, and all families and friends who had contributed for my help.

I am grateful to Physics Department, Addis Ababa University, for providing the financial support in the form of research project and every facility used for the success of this dissertation. I am also thankful to Wollo University for sponsoring me for this study.

I would like to give special thanks for Ethiopian Radiation Protection Authority (ERPA) for providing their full laboratory without any cost. I have great thanks for the whole staff of the authority, specially Mr. Eshetu Tilahun and Mr. Birhanu Turi, for their guidance in the laboratory and encouraging me for the future work in this field of study.

Finally, I would like to express my cardiac gratitude and sincere appreciation to the staff members of Physics Department, Addis Ababa University, for their generous help and continuous encouragement throughout this work.

Abstract

Natural radioactive materials can be originated from various geological materials enriched with radio elements. Commonly known natural radioactive materials are primordial radionuclides, $^{238}_{92}U$, $^{235}_{92}U$, $^{232}_{90}Th$ and $^{40}_{19}K$, which are known for their long half lifetime. Parts of the earth or earth surface like sedimentary rock, limestone and sandstone, and clay rocks are the known geological materials in hosting such radioactive materials. The distribution of radio elements in earth crust depends on geo-chemical conditions of their hosts, weathering, human actions, and the like factors. Therefore, their distribution in and/or on earth surfaces is not homogeneous, vary from places to places. Radionuclide hosting materials can be used for different purposes in different factories as a raw material. Cement factories are the known consumer of such raw materials in the production of Portland cement. In this study, the levels of activities and health hazard indices in raw materials and final products of Portland cement samples were measured at cement factories in west Shoa Oromia regional state, Ethiopia. Besides, activities and health hazard indices of related environmental samples, soil, were measured.

The study had been accomplished using high efficiency gamma ray spectrometer with Digital Signal Analyser, (DSA) coupled with High Purified Germanium detector and high efficiency gamma ray spectrometer with modular detector electronics, coupled with Thallium activated Sodium Iodide (NaI(Tl)) detector. The gamma ray spectrometers are controlled by GENIE2K-high channel number performance, computer software, and out put results are displayed on coupled personal computer.

The activity levels and corresponding health hazard indices of $^{238}_{92}U$, $^{232}_{90}Th$ and $^{40}_{19}K$ in the main cement raw materials (Limestone, Sandstone, and Clay rocks), additive raw materials (Coal, Pumice and Gypsum) and final cement product (Ordinary Portland cement, Pozzolana Portland cement and semi-processed cement called clinker) samples were measured. As the main cement raw materials, maximum activities were measured in clay samples, 50.58 ± 2.42, 150.40 ± 7.41 and 365.00 ± 17.11 Bq/Kg, for $^{238}_{92}U$, $^{232}_{90}Th$ and $^{40}_{19}K$ respectively, where low activity concentrations were measured in Limestone samples, 7.43 ± 0.35, 1.75 ± 0.29 and 17.02 ± 1.56 Bq/Kg respectively, for $^{238}_{92}U$, $^{232}_{90}Th$ and $^{40}_{19}K$.

In additive cement raw material samples, maximum activity concentrations were measured in pumice samples as 78.00 ± 4.00, 107.53 ± 5.49 and 1307.65 ± 60.70 Bq/Kg, for

$^{238}_{92}U$, $^{232}_{90}Th$ and $^{40}_{19}K$ radio elements respectively. Low activities were measured in gypsum samples, 1.56 ± 0.14, 1.79 ± 0.33 and $28 \pm 2.0\ Bq/Kg$, for $^{238}_{92}U$, $^{232}_{90}Th$ and $^{40}_{19}K$ respectively. In the same way, the final product of cement, Portland cement, got a maximum reading of 31.63 ± 1.46, 45.87 ± 2.30 and $369.71 \pm 16.94\ Bq/Kg$ for $^{238}_{92}U$, $^{232}_{90}Th$ and $^{40}_{19}K$ respectively. The related environmental samples, collected from floriculture industry near Holeta town, Oromia special zone, gave activity concentration readings for $^{238}_{92}U$, $^{232}_{90}Th$ and $^{40}_{19}K$, as 197.18 ± 16.88, 8.00 ± 0.29 and 360.40 ± 21.20 respectively.

The elemental concentration values for natural radio elements in above were also calculated for additive cement raw material and floriculture soil samples. The results have a direct relation with activity concentrations, maximum activity concentration will give maximum elemental concentration values. The health hazard indices, Radium equivalent activity (Ra_{eq}), Absorbed dose (D_R), Annual dose rate (AD_R), External hazard index (H_{ex}) and Internal hazard index (H_{in}) were calculated for each studied sample. These parameters have a direct relation with activity concentrations that maximum activity concentrations will induces maximum health hazards to the environments.

The measured activity values were compared with other's work investigations for the same sample types and world average values given by United Nations Scientific Committee on the Effects of Atomic Radiation (UNSCEAR-2000). It was found that results from some samples (Pumice, Coal and Clay) were crossed the values given by the committee, and others are with in the permissible values given by this committee.

List of Publications

1. Hailu Geremew and A. K. Chaubey, Estimation of Minimum Counts for an Acceptable Pulse Shape Using Scintillation Detector from 200 to 2000 keV Energy, International Journal of Innovative Science, Engineering & Technology, Vol. 5 Issue 11, November 2018.

2. Hailu Geremew and A. K. Chaubey, Investigations of Natural Radioactivity Levels and The Possible Radiation Hazards in Floriculture Soil, Holeta, Shoa, Ethiopia, using Gamma Ray Spectrometry, International Journal of Current Research Vol. 11, Issue, 02, pp.1535-1540, February 2019, DOI: https://doi.org/10.24941/ijcr.34403.02.2019.

3. Hailu Geremew, A. K. Chaubey, Birhanu Turi "Measurements of Natural Radio activity Levels and Associated Health Hazard Indices in Some Portland Types of cement, Ethiopia" Vol 2-Issue 5 (96-101) November - December 2019, International Journal of Scientific Research and Engineering Development (IJSRED) :ISSN:2581-7175, www.ijsred.com.

List of Prepared Manuscripts

1. Hailu Geremew, A. K. Chaubey, Birhanu Turi "Natural Radioactivity Levels and Their Associated Health Hazard Indices of Main Cement Raw Materials Using HPGe Detector"

2. Hailu Geremew, A. K. Chaubey, Birhanu Turi "Investigations of Natural Radioactivity Levels and Corresponding Elemental Concentrations in Additive Cements Raw Materials Using HPGe Detector"

Contents

List of Figures

List of Tables

1

Introduction

Natural radioactivity is wide spread in the environment and exists in various geological formations in soil, rocks, plants, water and air. So the knowledge of the distribution patterns of both anthropogenic and natural radionuclides in soil plays an important role in radiation protection and measurement. The activity concentration of these radio nuclides above the permissible level is harmful to the human body and other life [1].

Therefore, measurements of radioactivity levels in such environmental materials are important for recording the radiation impacts on the environment, population and occupational personal exposed to radiation [2]. The most common forms of radiation emitted have been, traditionally, classified as alpha (α), beta (β), and gamma (γ) radiation, after named by Ernest Rutherford. Nuclear radiation can also occur in other forms, including the emission of protons or neutrons or spontaneous fission of a massive nucleus [3]. This study shows the activity levels of radioactive materials in cements and cements raw materials, some environmental samples and their corresponding health hazard indices, like dose rate, internal and external hazard indices, by using the emitted gamma radiation.

Gamma-ray spectrometer can be used for different energy levels of radiation measurements, specially for weak environmental radiations caused by nature and artificial. High resolution germanium detector assembly and thallium activated sodium iodide detector coupled with modular detector electronic are used for measurements of weak environmental radiations. Measurements of the amounts of radionuclide present in a given sample require the knowledge of the efficiency of a detector in the counting geometry and energy resolution [4]. In this study High Purified Germanium detector (HPGe) of 77% relative efficiency (as compared to 3 by 3 inch (7.62 cm) NaI(Tl)) and Thallium Activated Sodium Iodide (NaI(Tl)) detector of 6% efficiency and 7.5% energy resolution at 662keV energy, were used for measurements.

The methodology is widely applied for same work at different areas and is the best estimates of activity concentrations of environmental radioactive materials.

1.1 History of Environmental Radioactivity Measurements

The history of environmental radioactivity measurements started with the onset of the nuclear age, in particular with the atmospheric nuclear weapons tests. It was driven by the concern of global radioactive pollution and the resulting human radiation exposure [5]. Wilhelm Roentgen in (1895) and Henri Becquerel (1896) are recognized peoples in producing human made radionuclide when they had been trying X-ray experiments. Such radiation sources can be considered as background radiation sources, which are emitted from both natural (air, soil and water) and human-made radionuclides or radioactive chemicals [3,6,7].

Some naturally occurring radionuclides are found in the earth beneath the last top surface of the earth, while others are produced in the atmosphere by radiation from space. More percentage (82%) of the global average human radiation exposure is attributed to the natural sources of environmental (terrestrial) and cosmic origin [6, 7]. The terrestrial component results from the long-living radionuclides in the earths crust like, ^{40}K, ^{238}U, ^{235}U and ^{232}Th, known as also primordial radionuclides. They contribute an exposure to the environment including their progeny. Almost all primordial, short-lived radioactive nuclei have decayed during the aging of the Earth. The cosmic part is made up of cosmic rays coming from the outer space like ^{3}H, ^{7}Be, ^{14}C and ^{22}Na as a result of nucleon synthesis in atmosphere [7,8].

The other is human-made radionuclides, that can entered the environment from activities such as nuclear weapons tests, medical procedures that use radionuclides to image the body and electricity generation that uses radioactive fuels [6].

1.2 The Statement of Problem

Humans are one of the creation that exposed to environmental radiations in their life. The finally processed and raw materials of building materials are the known sources of environmental radiations. Those materials contain naturally occurring radioactive materials and if the radiation dose from such materials crosses the permissible value, it may be dangerous for life. The levels of natural activity concentration of primordial radioactive materials in cements and cement's raw materials in west Shoa Oromia regional state of Ethiopia has not studied so far. Knowing the activity levels of naturally occurring radioactive materials in environment has ensures the health condition of environment, for life, specially for materials that have a direct contact with human beings.

1.3 Objectives of The Study

1.3.1 General Objective

The objective of this dissertation is to investigate the levels of primordial natural radio activities and corresponding health hazard indices, like Radium equivalent activity (Ra_{eq}), Absorbed dose (D_R), Annual dose rate (AD_R), External hazard index (H_{ex}) and Internal hazard index (H_{in}) in cement's raw materials (main raw materials and additive raw materials), final and semi-final processed cements, and related environmental samples made from sedimentary and clay rocks, using gamma ray spectrometer coupled with HPGe detector and NaI(Tl) with electronic modular circuit detector.

1.3.2 Specific Objectives

The specific objectives of this dissertation are;

1. To investigate the natural radioactivity levels and corresponding hazard indices in main cement's raw materials like Limestone, sandstone and Clay stone

2. To measure activities and elemental concentrations of primordial radionuclide in cements additive raw materials, Pumice, Coal and Gypsum.

3. To investigate natural radioactivity levels and corresponding health hazard indices in final and semi-final cement products from study areas.

4. To measure the natural activity concentrations and elemental concentrations in environmental soil samples exposed to artificial fertilizers.

1.4 Motivation of The Study

The author was interested in this work from preliminary study on cement factories like Mugher, Dangote and Habesha cement factories. In the factories materials like volcanic ash and coals are used as raw materials and energy sources. In addition, we observed other raw materials like clay and the final products are used for sheltering and different constructions that have a direct contact with humans. Such materials are known in hosting radionuclide from earth centre and earth crust. Up to this study, there was no report about the natural radioactivity levels and hazard indices from such materials used in a factory and related

environmental samples, and we were interested to measure the activities and corresponding health hazard indices in such environmental samples.

1.5 Scope of The Study

This study, Ph.D. dissertation include all raw materials and final products of cements produced at three cement factories in west Shoa Oromia regional state, Ethiopia. In addition to this, floriculture farm found in Holeta administrative town and final product of cement from Derba cement factory, Ethiopia and Mosobo cement factory, Ethiopia were also included. The three cement factories in west Shoa Oromia regional state are Mugher Cement Factory (under chemical industry) Gov., Dangote Cement Factory (Ethiopia branch) Plc., and Habesha Cement Factory SC. In fact factories are in west Shoa Oromia regional state, but some of their raw materials are from other places.

1.6 Limitation of The Study

Limitations of this study were from research, dissertation, design and methodology of our study.

In the study plan, the collected samples have a limit in representing sampling area. We took samples from one season deposit of factories. We did not cover even annual deposit. Information about collecting of raw materials were also not clarified for us when we collect samples. Some factories collect from depth where others collect from surface of the earth. Time of study and willingness of industries at some places in sample collection were another barrier in our study.

The methodology constraints are mainly originated from limited access of gamma spectrometer for laboratory work. We did the experiment at Ethiopian Radiation Protection Authority, which is a single laboratory for the country. So the time allocated for us is not sufficient to repeat same measurements for each sample. We measured one sample only one time, and no opportunity to try again for the reduction of statistical errors. So the author used the possible research delimitation techniques to accomplish this dissertation.

2

The Studie of Environmental Natural Radioactivities and Their Detection Mechanisms

Natural radioactive materials are responsible for most of the total radiation dose received by humans and other life. They originated from many diverse sources. Some of these sources are natural; from various geological materials enriched with radio elements (uranium 238 and uranium 235, thorium 232 including their decay progeny and potassium 40), can be generated in stars and from cosmic rays. Others feasible contributors are the results of human activities as explained in section 1.1. Therefore, the magnitude of these natural exposures and composition depends on geographical, geo-chemical conditions and some human activities [9–11].

Soils produced from weathering of radioactive rocks and minerals, food we eat, water we drink, and air we breathe contain radioactive materials. But they exhibit a low level of natural radioactivity that can be attributed to one or some combinations of these radioactive materials. Therefore, the amount of these materials (radiation sources) that are present in environment are measured in parts-per-million (ppm) and percent [12]. So for their detection, detectors of high efficiency and large, in size, are more preferable. For gamma rays from such sources, the low level gamma counting systems, High Purified Germanium detector (HPGe) and Thallium Activated Sodium Iodide detector (NaI(Tl)) are commonly used laboratory requirements for measurements [1].

2.1 The Study of Environmental Radioactivity

In the environment, one may get radiation from different radioactive materials performing radio-activity, and accelerated particle(s) from nucleon synthesis. So, we are continuously bombarded by high-energy electro-magnetic radiation from outer space, and long-lived radionuclides which are parts of the earth.

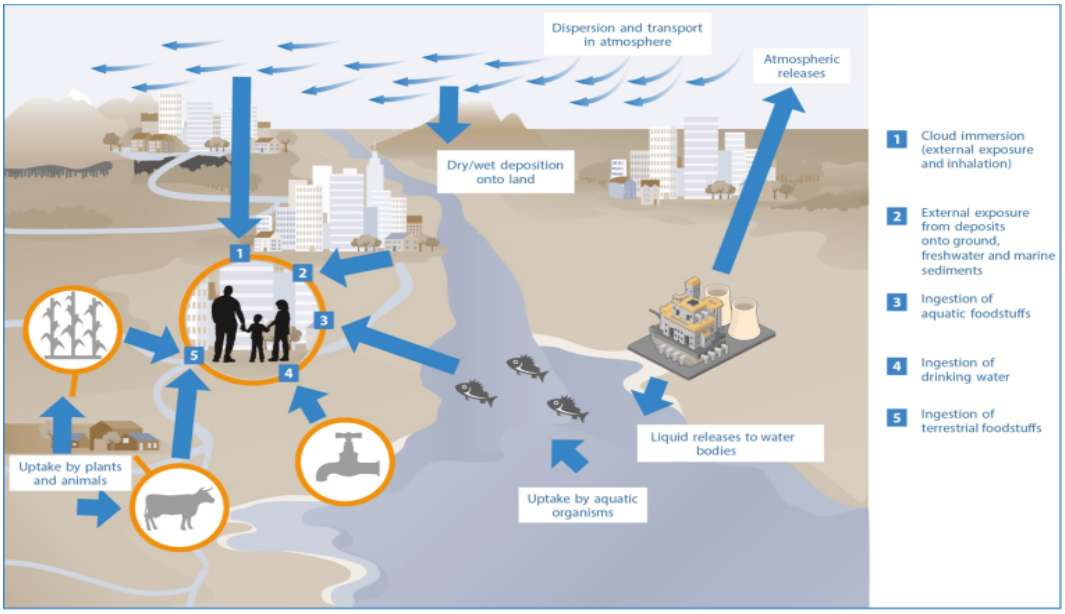

Figure 2.1: Possible sources of environmental radiation, Re-printed from UNSCEAR-2016 Report

The particles and/or elementary particle emissions are caused by radioactive decay of atoms that disintegrated spontaneously and transformed into different atoms. Most of the lighter radionuclides like ^{14}C, ^{40}K, emit only electrons or/and photons, whereas many of the heavier radionuclides like ^{232}Th, ^{238}U emit alpha particles. The decaying radionuclides create new progeny, which may be stable or may decay also [6, 14].

Most environmental radioactivity originates from natural sources, but radionuclides and ionizing radiation are also created through human activities. Spontaneous fission occurs naturally in terrestrial systems at a low rate, but induced fission is mostly by human actions which exploited in commercial nuclear reactors. Cesium-137 with half-life more than 30-years and energy 662 keV is commonly known fission product. Energy from such processes/man action, can activate other atoms to create radionuclide by-products (such as tritium and carbon 14), from nuclear reactors [10].

2.1.1 Natural Radio-activity in Environment

Natural radioactive materials has always been an integral part of our environment and release particle(s) continuously. It is part of our every day as visible light and heat of the sun's rays. These are from outer space, immerse us in a constant flux of radiation and low level emanating from minerals and rocks that comprise the Earth's crust [6, 14].

2.1.1.1 Cosmogenically Produced Radionuclides

Radio nuclides produced from cosmic-energy interactions are usually formed in the atmosphere where cosmic radiations are most intense. The spatial variability of these radionuclides are due to their variations in fluxes of cosmic radiation, which varies spatially with altitude and latitude and temporally with changes in cosmic-ray production rates. Out of the produced cosmogonies' radionuclide, only a few radionuclides are formed in sufficient quantities and are long-lived enough to contribute sufficient radiation in environment as some of them shown in Fig. 2.2 [14].

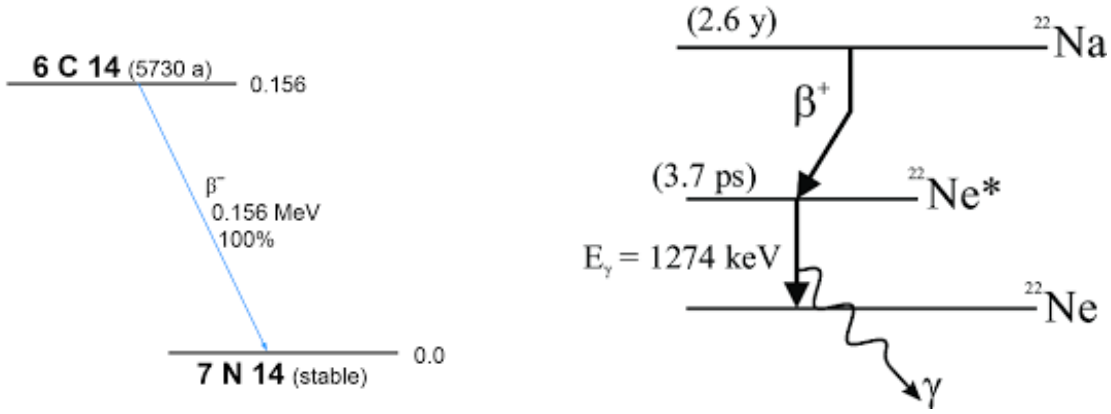

Figure 2.2: Decay scheme of Carbon-14 and Sodium-22, cosmogenically produced radio nuclides.

Tritium and Carbon-14 are the known long-living cosmogenic radionuclides. These are formed cosmogenically by interactions of their stable isotopes with atmospheric nitrogen. Less amounts of ^{26}Al, ^{32}P and ^{14}Si are other heavier radionuclide produced in cosmogenic process by nature. Noble gases such as ^{39}Ar and ^{81}Kr are also formed in the atmosphere, remain most of the time in atmosphere because of their chemical inertness [14].

2.1.1.2 Primordial Radio nuclides

Primordial radionuclides are those that were present when the earth was formed and have always been a part of the earth decaying over time such that they contribute lower radiation than in the past. Most of the rocks and minerals that form the earth's crust and the surficial materials derived from them contain long living natural radioactive elements. They are found around the globe in igneous and sedimentary rocks. From rocks, these radionuclides migrate into soil, water, and even air [6]. The most common and important for man uses are the one that contain uranium, thorium, potassium and their daughter isotopes [12, 14]. The main concern of this study is to evaluate their activity levels and health hazard indices in

environmental samples.

Uranium (U)

The average content of uranium in the Earth's crust in reference of igneous and sedimentary rocks, is approximately $2 \ to \ 4ppm$; and for thorium, $7 \ to \ 13ppm$. It's concentration depend on geochemical differences in environment during volcanic magma differentiation at the time of crystallization. Most of the uranium however, moves from the rock in hydro thermal solutions. It can easily oxidize and taken into solution after primary crystallization of volcanic magma. Therefore, uranium can be carried over long distances and redeposited in other rocks, in many cases, at higher concentration than the original occurrences. This is in a combined chemical or mineral system, not freely, uraninite, brannerite and carnotite. It is also present as an accessory element in zircon, apatite, allanite and monazite, and in complexes with organic matter and phosphatic ironstone [12, 15]. Such mobility is not the same for thorium and thorium is about three times more abundant than uranium in nature [16].

Uranium and thorium has no known biological function. They are chemo-toxic, radiotoxic and a carcinogen. Long-term exposure to such nuclide increases the chances of getting health problems [17, 18].

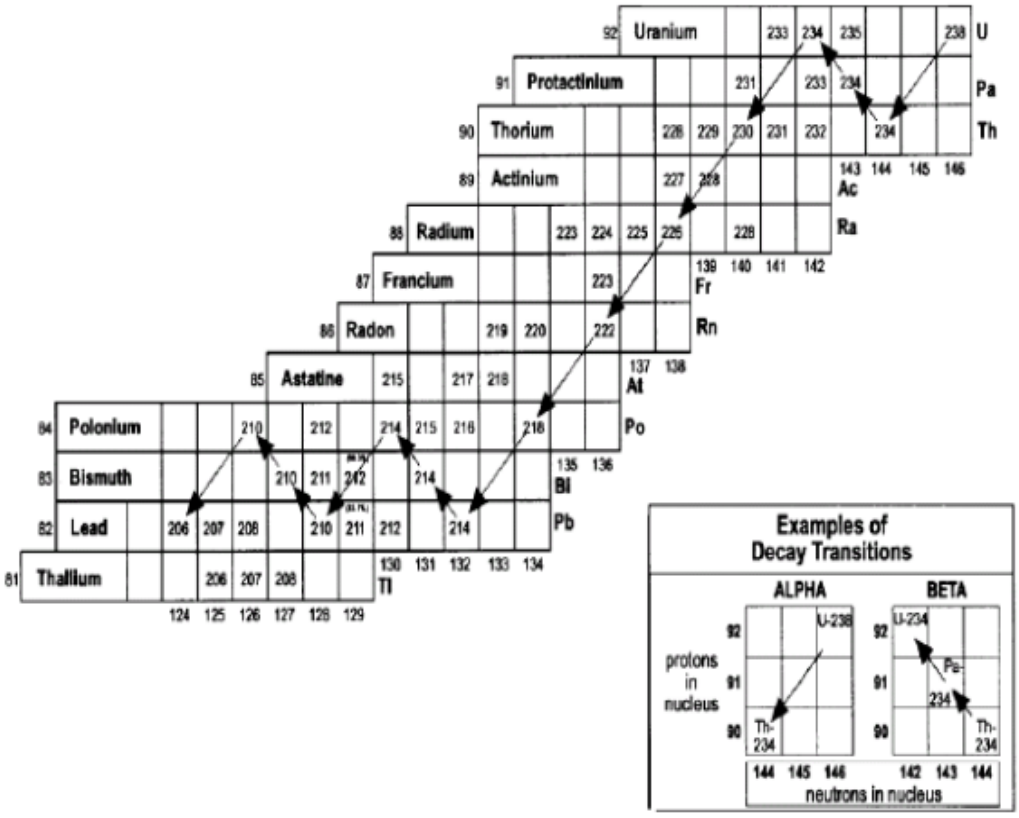

Figure 2.3: Schematic diagram of the Uranium-238 decay series, Re-printed from [19]

Uranium, ^{238}U, representing 99.2% of the total uranium in abundance, has two long-lived progeny, ^{234}U and ^{230}Th as seen from Fig. 2.3. Their decay products commonly referred to as radium (^{226}Ra). The decay progeny of ^{226}Ra is ^{222}Rn, commonly called radon, can cause about half the background radiation dose to humans, mostly through deposition in lung. This dose from radon progeny varies spatially, depending on soil and geo-sphere concentrations of ^{226}Ra [14, 19]. The progenies can also disintegrate through an emission of beta particles and gamma rays, and the most importantly used for the study of natural radioactivity levels are gamma emitters, commonly from ^{214}Pb and ^{214}Bi as seen from Fig. 2.4.

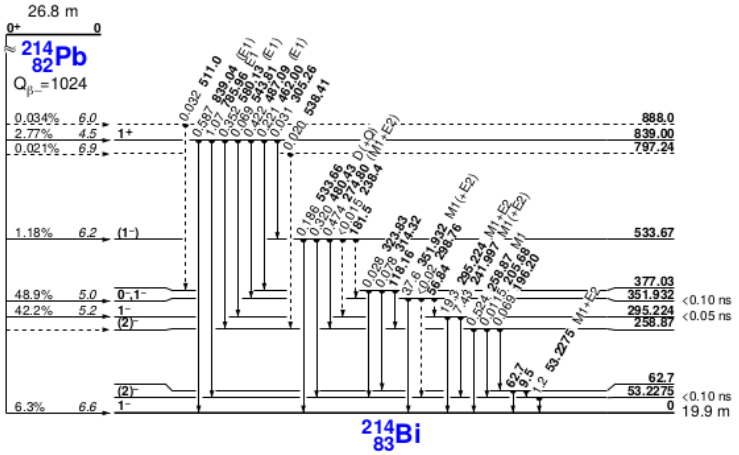

(a) Decay scheme of Pb-214

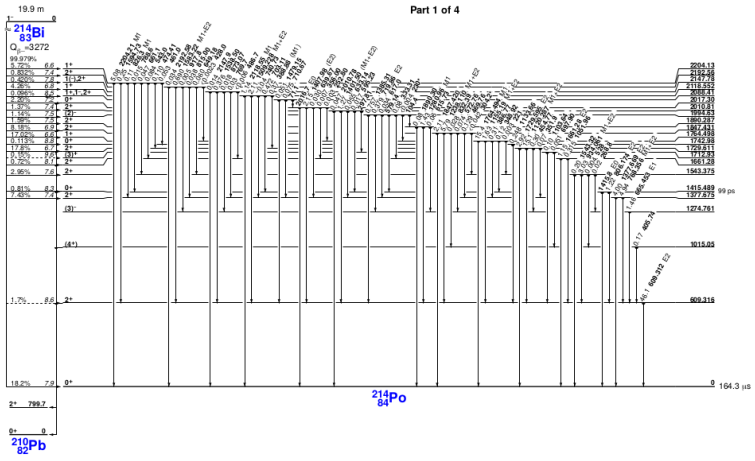

(b) Decay scheme of Bi-214

Figure 2.4: Decay scheme of gamma emitter nuclides from ^{238}U decay series, Re-printed from [20]

As observed from figure, 2.4, several gammas are emitted from these radio elements. In measurements, only gammas with high abundances are considered as background radiation

measurements.

Thorium (Th)

Thorium, ^{232}Th, is the most abundant of the heavy elements, that present in several minerals and contributes to the general background radioactivity. The minerals in which thorium mainly originated are igneous rocks, as disseminated and discrete minerals. It is not as soluble as uranium and is thus not as mobile in chemically solvent environments. Thorium is about three times more abundant than uranium in nature. The more important minerals that contain thorium are monazite, thorite, thorianite, uranothorite, and thorogummite [12]. Thorium and its radioactive progenies decay through the emission of alpha, beta and gamma until it's stable end product, ^{208}Pb as shown in Fig. 2.5 [14, 19, 21].

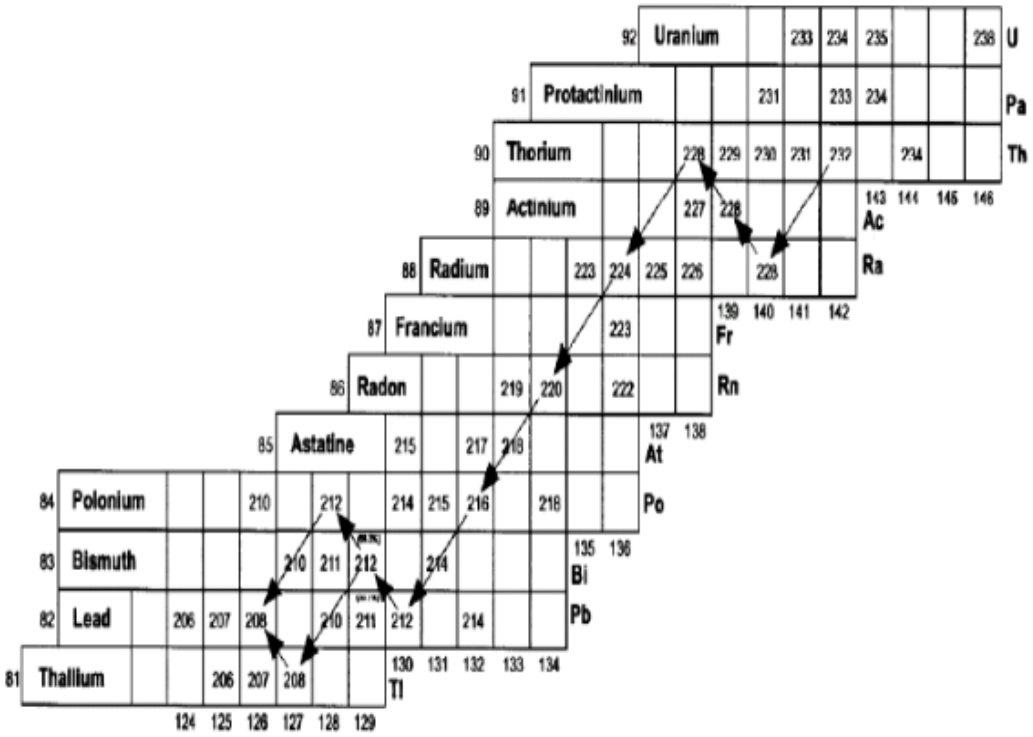

Figure 2.5: Schematic diagram of Thorium-232 decay series, Re-printed from [19]

The common gamma emitters of it's progenies are ^{212}Pb, ^{212}Pb and ^{228}Ac which are considered in this study. They emit gamma energies of different energy levels and most commonly gammas with more abundant are used to determine activity concentration, as seen in Fig. 2.6.

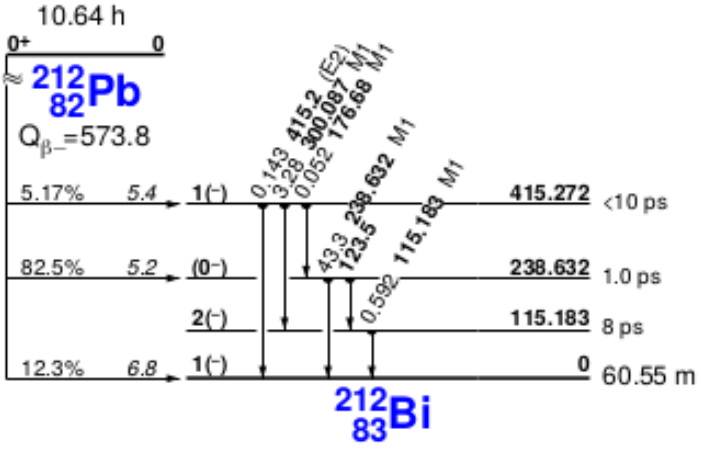

(a) Decay scheme of Pb-212

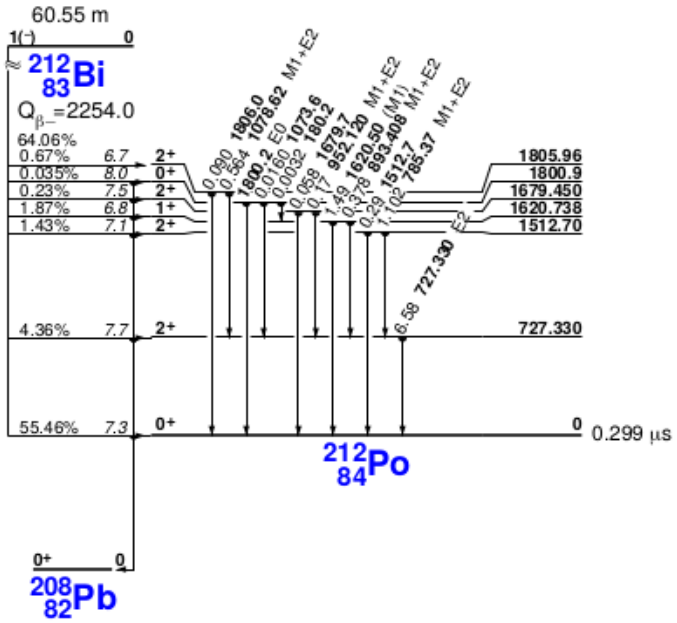

(b) Decay scheme of Bi-212

Figure 2.6: Decay scheme of gamma emitter nuclides from thorium 232 decay series, Reprinted from [20]

As observed from figure, 2.6 the gamma emitted from Pb-212 carry 238.632 keV energy which is 47% abundant as seen in (a). For Bi-212 seen in (b), gamma with 727.330 keV energy has more than 37% probability of emission.

Potassium (K)

Potassium is a major constituent in many igneous rocks, and their petrographic classification where potassium-40, (^{40}K) represents about 0.0119% of the total potassium inventory on Earth. It is one of the major radiation dose contributors from natural sources, with both electron and photon emissions as in Fig. 2.7.

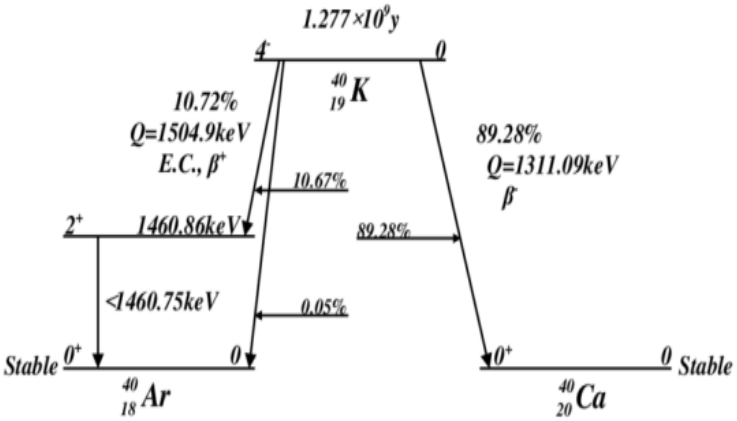

Figure 2.7: Decay scheme of Potassium-40, Re-printed from [19]

Since potassium is a basic nutrient required for life, ^{40}K also cycles and accumulated freely in the biosphere. The combined dose from internal and external exposures of ^{40}K is estimated to be about 8% of the total radiation dose from all sources. It is found in nature in rock forming minerals that contain potassium feldspars (orthoclase and microcline) and muscovite mica [12, 14, 19].

2.2 Radiation Detectors and Detection of Low Level Natural radiations

Radiation detectors are an analytical method that allows the identification and quantification of radio-elements in a variety of matrices. In one single measurement and with little sample preparation, radiation detectors allows us to detect several radiations/particles emitting radio nuclei in samples. The rough measurement outcome may give lines of spectra, quantified particles or in any other form which is proportional to the activity of their sources [22].

2.2.1 Radiation Detectors

Radiations from natural environmental radio-elements are low level energy, as observed from their facts of long term effects on life. So large volume radiation detectors have become dominant over other detector types because of their inherently good resolution and linearity in detecting low energy level radiations [23]. The sensitivity of such detectors' system depends on several factors, like detector efficiency, detector resolution, background radiation, sample constituency, sample geometry and counting time [22]. Scintillator detectors and semiconductor detectors are commonly used radiation detectors in measuring photon energies emitted from environmental samples. Such photons are the main concerns of this dissertation. Virtual experiments and standardized radiation sources can be used

to check the performance of such detectors. The commonly used standardized radiation sources are like ^{137}Cs, ^{60}Co, ^{152}Eu and others with long life-time and known strength which are also used in our measurements.

Virtual laboratories are developed by using Monte Carlo simulation in different machine languages. GEometry ANd Tracking4 (GEANT4) and Monte Carlo N-Particle simulation are the frequently used computer programs developed by C^{++} computer code and any other computer language, if geometry of a detector is clearly identified. GEANT4 is the common computer program used at CERN international laboratory for particle accelerating. In other sites, the computer codes are used for optimization of radiometric experiments and calibration purposes. The program uses Monte Carlo simulation following the trajectory of particles in the active region of particle detectors. It is a methodological way of doing what if analysis is true. From the result, it is possible to optimize the detectors and determine efficiency of detectors if geometry is clearly designed [24].

2.2.1.1 Scintillator Detectors

When a γ-ray interacts with a scintillator materials, it produces a pulse of light, which is converted to an electric pulse by a photo-multiplier tube. The photo-multiplier consists of a photo-cathode, a focusing electrode and large number of dynodes that multiply the number of electrons from photo cathode, as shown in 2.8 below [25].

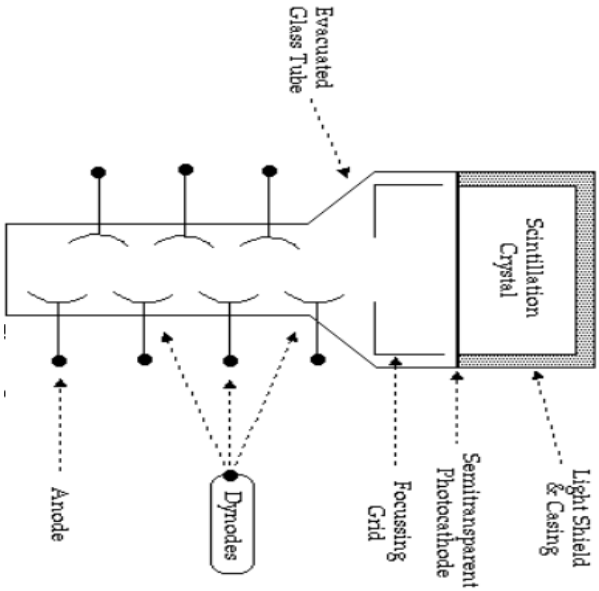

Figure 2.8: Schematic diagram of scintillation detector, Re-printed from [25]

Good scintillation detectors are transparent, have a large light output that is proportional

to γ-ray's energy, and are available in large size. Commonly used scintillators for low level environmental radiation measurement are thallium activated Sodium Iodide, NaI and Cesium Iodide, CsI crystals. The high atomic number of iodine (I), in $NaI(Tl)$ and CsI gives better efficiency for γ-ray detection. A small amount of Tl is added in order to shift the wavelength of the scintillation photons, so they are not re-absorbed by the crystal. A photomultiplier tube converts a weak photon signal to a detectable electric pulse [22, 25, 26].

2.2.1.2 Semiconductor Detectors

A semiconductor detector is fabricated from either elemental or compound crystal materials having conduction band gap in the range of approximately 1 to 5 eV. The band gap is created by a pn junction at one electrode and no current passes through when there is no ionizing radiation in the region. This creates a region called depletion layer as shown in Fig. 2.9.

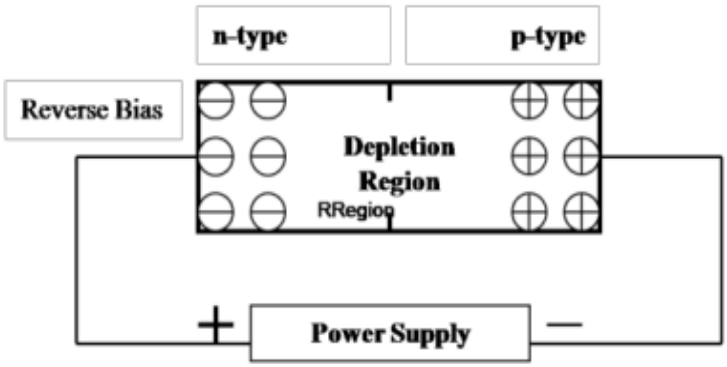

Figure 2.9: Creation of depletion region in semiconductor crystal, Re-printed from [27].

Silicon and Germanium are the most commonly used semiconductors with an impurity of valence 3 (acceptor) or 5 (donor). These impurities lower the energy necessary to create electron-hole pairs [25, 27]. These systems provide much better energy resolution than scintillators. This can be attributed to the small amount of energy required to produce a charge carrier and the subsequent large output signal. Only $3eV$ is required to produce an electron-hole pair in Ge and $3.61eV$ for Si. So, low temperature of around -200^0C is required to avoid thermal charge carrier generation during the interactions of intrinsic (I) region by incoming photons from low level gamma energies [22, 25].

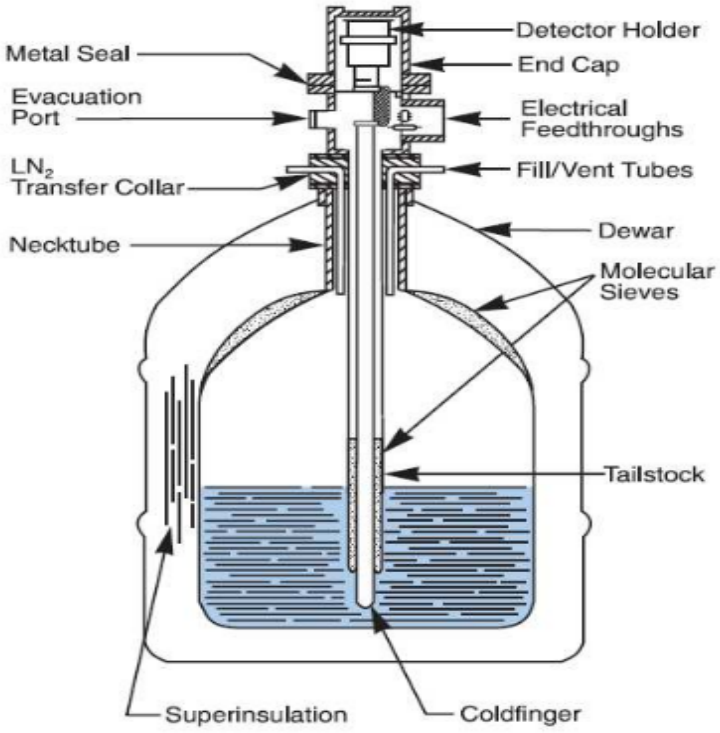

Figure 2.10: Schematic diagram of semiconductor detector with freezing liquid containing Dewar, Re-printed from [22]

Higher mass number of semiconductor material is more advantageous than lower mass material type. This will increase the probability of interaction (efficiency) in between incoming photons and atoms of detector materials. Therefore, Highly Purified Germanium (HPGe) semiconductor, with impurity concentration of 10^{10} atoms * cm^{-3} is more efficient than Silicon semiconductor.

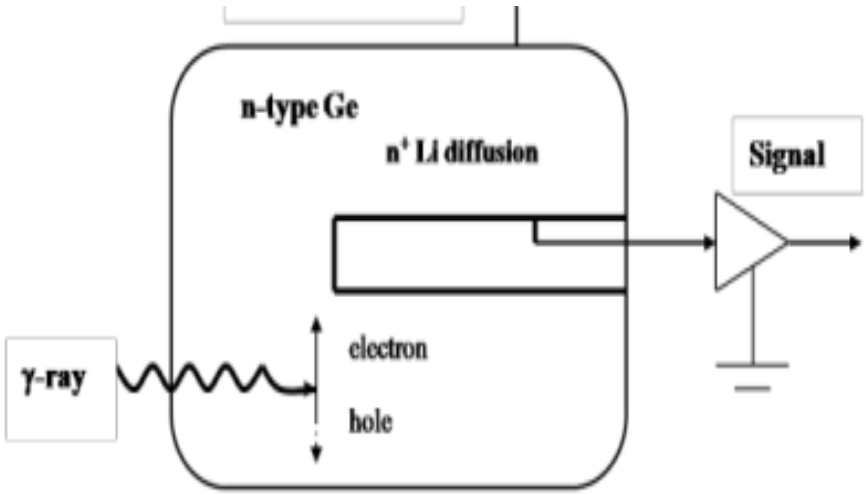

Figure 2.11: Configuration of an n-type intrinsic germanium closed-end co-axial detector, Re-printed from [27].

Therefore, the major characteristics of HPGe detector are high atomic number, low impurity concentration (large depletion depth), low ionizing energy required to produce an electron-hole pair, high conductivity, compact size, high resolution and relative simplicity of operation [22, 25, 27].

The standard specifications, Full Width at Half Maximum (FWHM), Full Width at Tenth Maximum (FWTM), Peak-to-Compton ratio, and relative efficiency are useful in guiding the user to an appropriate detector choice for the intended measurement. FWHM is a measure of resolution of a single energy peak at a specific energy, either expressed in absolute keV or as a percentage of the energy at that point (Semiconductor materials are more advantageous). Relative Efficiency of HPGe detectors are almost universally specified in terms of their relative full-energy peak efficiency compared to that of a 3 *by* 3 *inch* NaI(Tl) scintillation detector at a detector to source distance of 25 cm of 1.33 MeV energy. This shows that NaI(Tl) is more efficient due to its large mass number of Iodine atom and activator, thallium atom [22].

2.2.2 Detection of Low Level Natural Radiations

Radionuclide in a sample of study emit one or more specified energies carried by alpha, beta, gamma or any other particles. These particles are detected by detectors, coupled with electronic setup, and observed in a form of energy spectrum. In this dissertation, low level gamma radiation from environmental samples had been measured using gamma spectrometer [22].

After radionuclide has emitted particles, alpha or beta, it is still slightly unstable and will get rid of its excess energy by emitting a gamma ray immediately afterwards, from meta stable state. The time delay between the two emissions is so short (less than a billionth of a second) that we look upon them as being simultaneous, and as being only one disintegration [22]. So, detection of such gamma ray will depend on the effect of a γ-ray interacting with material of a detector [27].

The main concern for gamma spectrometer is the energy of photon from emitter, which is to be measured. The amount of energies deposited in the detector materials will be equal to the initial photon energies. The energy can be deposited in three commonly known events.

a. *Photoelectric event*; an interacting photon gives all of its energy to the recoil electron. As a result, the recoil electron ejected from the shell of atom and hence produce the

electron-hole pairs in the detector that yield the output pulse. This output pulse, from the detector, is proportional to the energy of photon that made the interaction.

b. *Compton scatterings followed by a photoelectric event*; the photon will transfer only part of its energy to an electron. The remaining energy is taken away by a new gamma photon of lower energy. The new photon is scattered, because it will take off in a new direction. This photon may cause other events, photoelectric effect, because it has sufficient energy to create an electron-hole.

c. *Pair production followed by photon absorption*; produced by gamma energy from the source of minimum energy 1.022 MeV. This is to obey the law of energy conservation in production of electron-positron pair after interaction.

In each of these cases the sequence stops in a photoelectric event. The three effects through which γ-rays interact directly with detector material can transfer energy simultaneously at one lattice point, which is called combined effects. The photo-peak efficiency of a detector is dependent of the energy of the photons at different interaction events, which is commonly named as Full-Energy Peak (or Photo peak) Efficiency (FEPE) [22, 27].

2.2.2.1 Low level gamma counting system

The sensitivity of a gamma spectrometer depends on several factors, like detector efficiency, detector resolution, background radiation, sample constituency, sample geometry and counting time.

- *Efficiency*; It is a measure of how many pulses occur for a given number of gamma rays, the fraction of all the photons that are emitted by the source in all direction, which cause an event in the detector [22, 27].

- *Resolution*; Higher resolution means that spectral line widths are smaller, and fewer background counts are involved in calculating peak integrals [22, 25].

- *Background radiation and sample constituency*; If the sample being analysed has a high content of high-energy gamma emitting radioisotopes, the Compton-produced background will easily outweigh the environmental background. For extremely weak samples, the environmental background becomes more significant.

- *Sample geometry*; For a given sample size, the sample should be distributed over the surface of detector to minimize the distance between the sample and the detector to increase the geometrical efficiency. The absorption of γ-rays inside the sample material itself, and the influence of the dimensions of the sample container affects the measurement of low level gamma ray emitted from sources [22, 25–27].

2.2.3 Cement and Its raw Materials as Environmental Radiation Sources

Cement is a powdery substance made with calcined lime, clay and sand as major ingredients. Clay provides silica, alumina, and iron oxide, while calcined lime basically provides calcium oxide. In cement manufacturing, raw materials of cement are obtained by blasting rock quarries by boring the rock and setting off explosives. These fragmented rocks are then transported to the plant and stored separately in silos. They are then delivered, separately, through chutes to crushes. Depending on the type of cement being produced, required proportions of the crushed clay, lime stones, sandstone, and any other required materials; like volcanic ash, gypsum, are mixed by a process known as pre homogenization and milled by steel mill. It is then homogenized again and calcined (dissociation of calcium carbonate into calcium oxide and carbon dioxide), at an average of 1300^0C, in rotary kilns for the raw material to be a clinker [28, 29].

The combinations of these raw materials produces different types of cement according to the raw materials proportion in the mixed final product. The commonly known and considered in this study are types known as Ordinary Portland cement and Pozzolana Portland cement, and semi-processed cement called clinker. These three types of cement are made from environmentally available geological materials at different geological formations that can host natural radioactive materials like granite, known by its high natural radioactive materials' composition. The geochemical properties of raw materials is another factor that determine the concentration of natural radioactive materials, specially for long living radioactive materials. So, Portland cements that produced from such materials can be rich in such radioactive materials. It is also rich in chemically toxic elements like Hg, Cd, Tl, As, Sb, Pb, Cr, Co, Cu, Mn, Ni, and V in considerable amounts [29, 30].

As shown in table 2.1, an X-ray Florescence (XRF) analysis result is not showing long living radioactive materials like U and Th, and all chemically toxic elements. The results of XRF analysis are in percentage per kilogram, and radioactive materials are in parts per

million or part per billion [31].

Table 2.1: XRF analysis results of chemical composition for Portland Cement, Reprinted from [31].

Chemical Name	Common Name	Chemical Notation	Abbreviated Notation	Mass Content %
Calcium Oxide	Lime	CaO	C	58-66
Silicon dioxide	Silica	SiO_2	S	18-26
Aluminium oxide	Lumina	Al_2O_3	A	4-12
Ferric Oxide	Iron	Fe_2O_3	F	1 -6
Magnesium oxide	Magnesia	MgO	M	1-3
Sulphur trioxide	Sulphurican	SO_3	S	0.5-2.5
Alakaline Oxides	Alkalis	K_2O & NaO_2	A+N	< 1

3

Methodology and Method of the Study

3.1 Gamma Ray Spectrometer

Gamma ray spectrometer is an analytical method that allows an identification and quantification of gamma emitting isotopes in a variety of matrices. In one single measurement and with little sample preparation, gamma ray spectrometer allows us to detect several gammas emitting radio nuclei in the sample. The measurement gives a spectrum of lines, the amplitude of which is proportional to the activity of the radionuclide and its position on the horizontal axis gives an idea on its energy and pulse height.

A typical high performance gamma ray spectrometer Canberra system consist of Digital Signal Analyser (DSA) with High Purified Germanium detector, (HPGe) and gamma spectrometer Canberra system consist of Pre-amplifier, Amplifier and Multi-Channel Analyser (MCA) with Thallium activated Sodium Iodide, (NaI(Tl)) crystal detector were used in this study. The two spectrometer systems are preferable due to their high performance in detecting low level gamma energies of environmental radiation sources [22].

3.1.1 Gamma Ray Spectrometer with HPGe Detector

Germanium detectors are semiconductor diodes having a $p-i-n$ structure in which the intrinsic (i) region is sensitive to radiations like, X-rays and γ-rays. Under reverse bias, as seen in section 2.2.1.2, an electric field extends across the intrinsic or depleted region. When photons interact with the material within the depleted volume of a detector, charge carriers (holes and electrons) are produced and are swept by the electric field to the p and n electrodes. This charge, which is in proportion to the energy deposited in the detector by the incoming photon, is converted to a voltage pulse or signal by an integral charge sensitive pre-amplifier [22].

This integrated charge sensitive device is coupled to Digital Signal analyzer (DSA) consists of a pulse height analysis system to transform pulses, which are collected and stored by a computer installed GENIE2K-based software, as shown in Fig. 3.1.

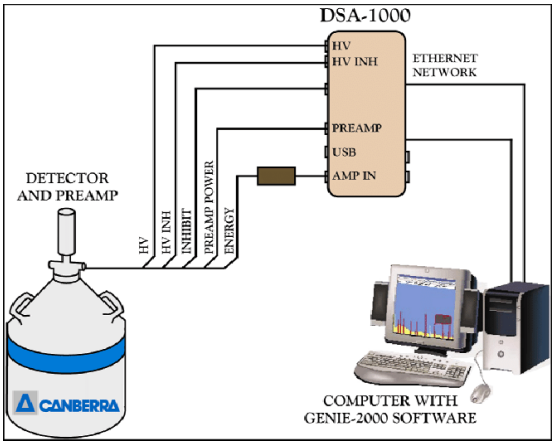

(a) Gamma spectrometry full set up with DSA

(b) DSA system

Figure 3.1: Gamma spectrometry system with DSA and HPGe detector.

Pulse shape is determined by calculating ratio of Full Width at Tenth Maximum (FWTM) to Full Width at Half Maximum (FWHM) and ratio of Full Width at Fiftieth Maximum (FWFM) to FWHM. The theoretical acceptable ratio for FWTM/FWHM is 1.82 and should be less than 1.9 in practice. While for FWFM/FWHM is 2.38 for Gaussian peak and should be less than 2.5 in practice [32].

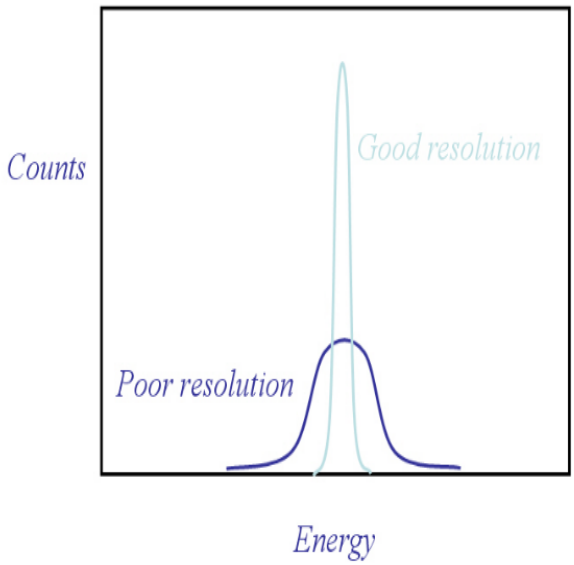

Figure 3.2: Energy Resolution, Re-printed from [22].

From this facts, energy resolution of photo peak is calculated using Eq: 3.1.

$$E_R = \frac{FWHM}{E_{centroid}} \tag{3.1}$$

where FWHM is calculated using the relation given in Eq: 3.2, in GENIE2K computer

program/code.

$$FWHM = 2\sigma\sqrt{2ln2} \tag{3.2}$$

Where σ is standard deviation which is not a constant because it is a function of the photon energy. In the same way, same relation as in Eq: 3.2 is used for the calculation of FWTM and FWFM by putting in place of $ln2$, $ln10$ and $ln50$ respectively.

The FWHM of a peak in the pulse height spectrum shown in Fig: 3.3 is used as a measure of energy spread. This is a quantitative indication of the expected resolution of a detector, which is, its ability to distinguish two peaks that are close together. Energy resolution becomes good if centroids of two consecutive peaks are 3FWHM of a peak apart [33].

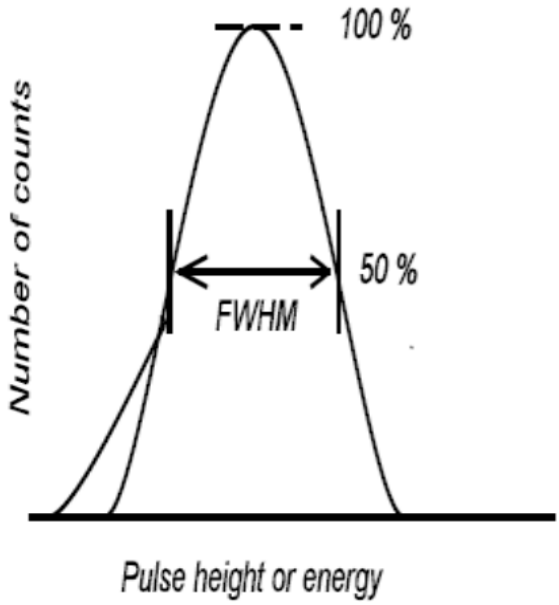

Figure 3.3: Counts vs pulse height/energy, Re-printed from [22].

The FWHM increase with the energy of a photon, and is dependent on intrinsic properties of the detector, the type and setting of electronic modules being used, and the layout of the cables.

After checking for such equipments, a standard Marinelli beakers of $0.5 Litter$, volume were used as sample holders. Range of peak locating channel were used from 180 keV to 8192 keV with nuclide energy identification tolerance of 1 keV. The dead time of cascaded DSA, as its high performance, is 0.4% in average, for 36000 sec live time, which means approximately 144 sec difference of real time [34].

Operating parameters of the system are governed and controlled by the installed GENIE2K computer program, Canberra System. The information from prepared samples has been established in a reference of calibration measurements performed for Marinelli's geometry and standard sources listed in section 2.2.1. Calibration measurement is a measure of the relationship between gamma energy and channel number. Additionally, the spectrum of laboratory background has been established from prolonged measurements and subtracted from sample's measurements. The resulting values allows us to perform nuclide identification and activity analysis, by referring to the information located in a nuclide library file, typically ISO-11929 MDA Report [34, 35].

So, cement and cement's raw materials were analysed using this gamma spectrometry system. The DSA and large volume HPGe detector in a system makes it more interesting in our study.

3.1.2 Gamma Ray Spectrometer with NaI(Tl) Detector

A gamma ray interacting with a scintillator produces a pulse of light, which is converted to an electric pulse by a photo cathode and multiplied by multiplier tube that consists of a focusing electrode and dynodes that multiply the number of electrons striking them several times each. The properties of scintillation material required for good detectors are transparency, availability in large size, and large light output proportional to gamma ray energy. Relatively few materials have good properties for such detectors like NaI(Tl) as discussed in section 2.2.1.1 [22, 25].

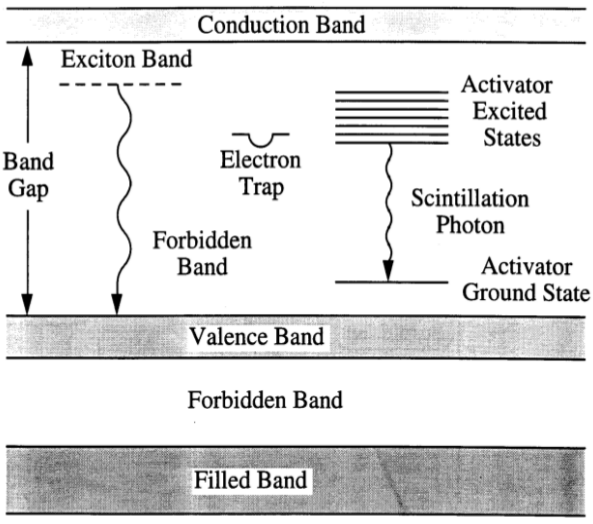

Figure 3.4: Band gaps of inorganic Scintillation NaI(Tl) detector.

A small amount of Tl is added in order to activate the crystal or to shift the wavelength

of the scintillation photons, so they are not re-absorbed by the crystal. The best achievable resolution, ranges from 7.5%-8.5%, as compared with high resolution gamma spectrometer, for 662 keV gamma rays from ^{137}Cs at zero distance from source to detector, for 3 inch diameter by 3 inch long crystal, and is slightly decreasing as energy is increasing as seen in Eq: 3.1 [22, 25].

A typical gamma ray spectrometer coupled with NaI(Tl) detector used in this study is as shown in Fig: 3.5 block diagram, which includes all components shown in the figure.

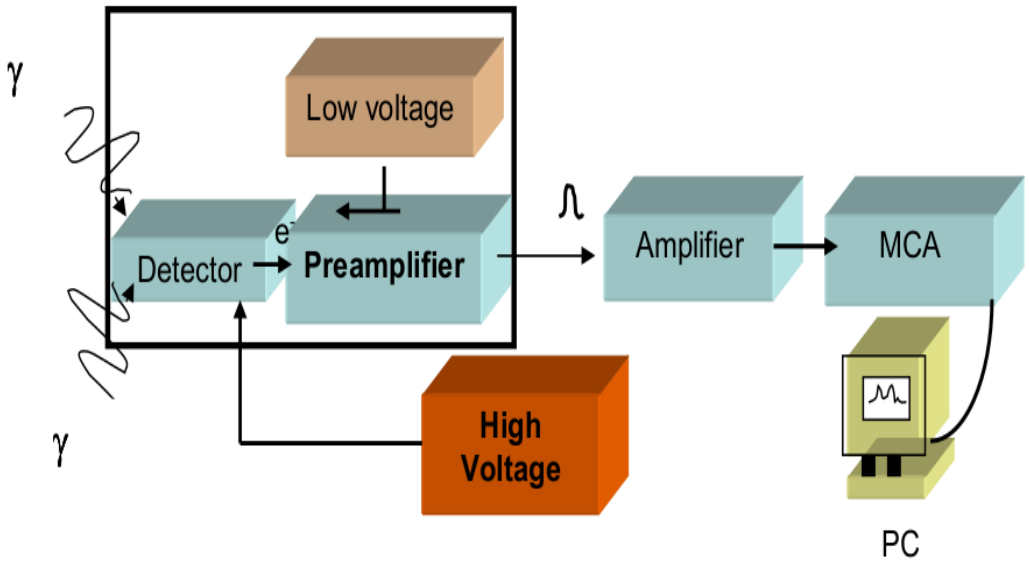

Figure 3.5: Block diagram of a basic gamma spectrometer system with MCA, Re-printed from [22]

The detector is the centre of energy loss of incoming photons in region of the gamma spectroscopy system. The gamma photons interact with the detection material and transfer their energies to electrons or to positrons in the case of annihilation as discussed in section 2.2.2. These produced particles lose their energy within the detector, creating charged particles and further creates ionized atoms and ion pairs by Coulomb interaction. These secondary entities form the basis of the detector signal.

The charge created within the detector after the photon interaction with the detector crystal, is collected by the preamplifier. Additionally, the preamplifier also serves to provide a match between the high impedance of the detector and the low impedance of coaxial cables to the amplifier. In charge-sensitive preamplifiers, an output voltage pulse is produced that is proportional to the input charge. To maximize performance, the preamplifier should be located at the detector [22].

The High Voltage Power Supply unit, supplies the necessary voltage to the photo-multiplier tube to create potential difference in between photo-cathode and anode. These units are usually able to supply up to 500 Voltage.

The amplifier serves to shape the pulse and further amplify it. In this module the size (height) of the pulses are increased, and they carefully manipulate problems with electronic noise, shifts in the baseline, and pulses riding on the tails of those preceding them.

The multichannel analyser (MCA) is the heart of most experimental measurements. It performs the essential functions of collecting the data, providing a visual monitor, and producing output, either in the form of final results or data for later analysis. This electronic module consists basically of an Analog-to-Digital Converter (ADC), control logic, memory and display. The multichannel analyser collects pulses in all voltage ranges at once and displays this information in real time. All these electronic devices shown in Fig: 3.6 are coupled to each other and give an out put pulses initially started by the detector [22, 25].

Figure 3.6: Modular detector electronics (High voltage supply, preamplifier, amplifier and multichannel analyser)

3.2 Materials and Methods of the Study

3.2.1 Samples and Sampling Area

The origin of samples of study were mainly from great rift valley in Ethiopia as shown in Fig. 3.7. So, we collected from store houses of cement factories for the study of cement and cement's raw materials, and from the field for related environmental samples study. The

materials from store houses are used in the factories as raw materials and energy sources. These samples were collected at few meter depth and top of earth surfaces, and our study is mainly for samples collected by means of surface sampling.

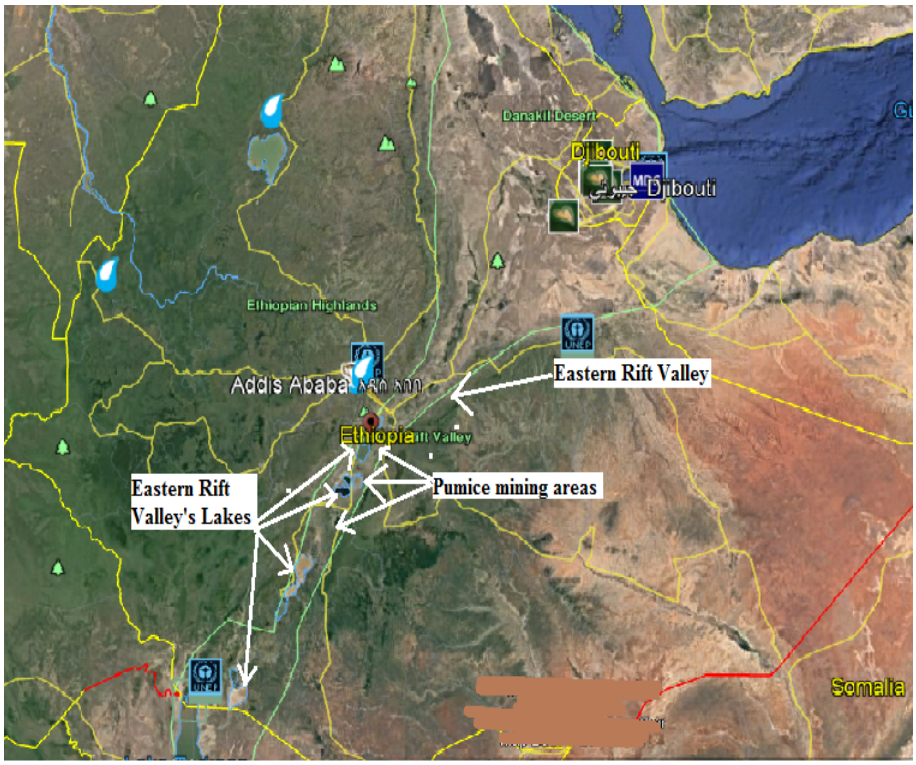

Figure 3.7: Eastern Ethiopian Rift-valley and Sampling area, (taken by Google Earth)

In this study, raw materials and final products of three cement factories were considered. In addition, final product of two cement factories from open market were used. The three factories we used are; Mugher Cement Factory (under chemical industry) Gov., Dangote Cement Factory (Ethiopia branch) Plc., and Habesha Cement Factory SC, in West Shoa, Oromia regional state, Ethiopia. The main mining areas of coal for these factories are from South Africa and from Jimma Seka, Ethiopia (specially for Habesha Cement Factory and Dangote). These factories (Mugher, Dangote and Habesha) are found in the north-western direction of the capital city, Addis Ababa, at distances of 90-KM, 83-KM and 40-KM respectively as shown in Fig. 3.8.

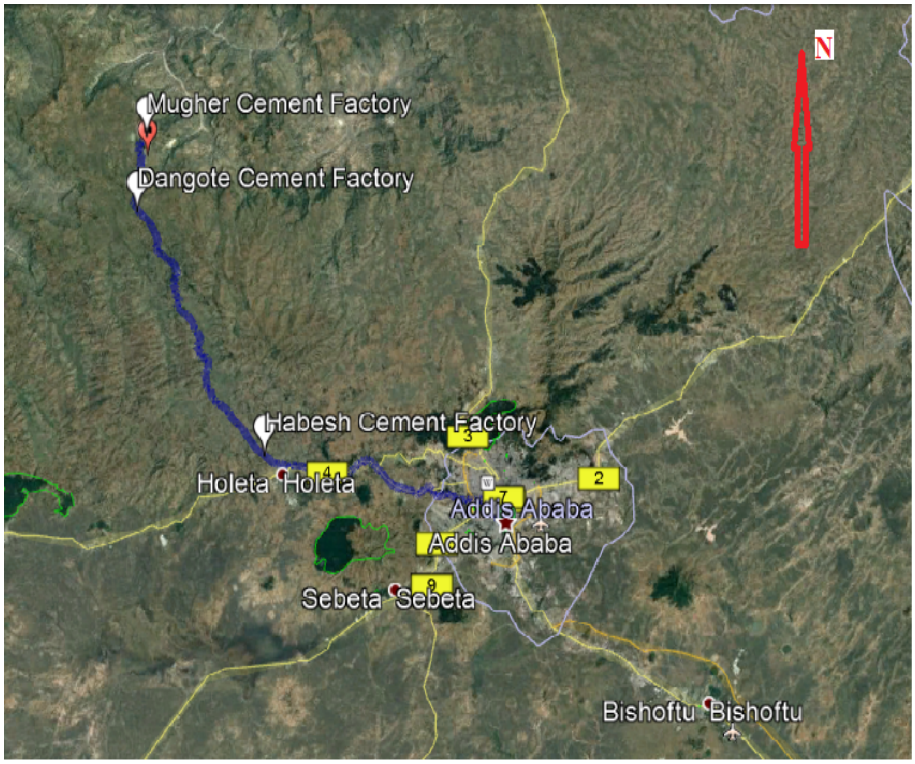

Figure 3.8: Locations of the three cement factories from capital city Addis Ababa, (taken by Google Earth)

From the sites, we collected all raw materials used by the factories and their final products which are supplied for the markets. Raw materials are materials like limestone, sandstone and clay used as main raw materials, Gypsum, pumice (volcanic ash) and coal with slag used as additive raw materials, and processed outputs like clinker and Portland cement (Pozzolana Portland and Ordinary Portland cement). In addition, soils from floriculture industry were used, which was enriched with fertilizer from sedimentary rocks, Holeta town, nearby the study area. Limestone and sandstone are from sedimentary rock type where clay is from igneous rock. Volcanic ash is a product of frozen cooled magma, and coal is from prehistoric plants.

3.2.2 Sampling and Sample Preparation

Samples named in section 3.2.1 had been collected from factories store house's that represent, nearly, their annual deposit and Pozzolana Portland Cement from open market as seen from Fig. 3.9.

(a) Clay Sampling

(b) Pumice Sampling

(c) Coal Sampling

(d) Environmental Soil Sampling

Figure 3.9: Sampling from the site.

The samples had been brought to nuclear laboratory by packing in polyethylene bags and oven dried to 110^0C to avoid moisture. Dried samples were grinded to a fine powder, sieved through 0.425-mm diameter mesh siever (ISO-9001 and ISO-2000 quality approved) which is seen from Fig. 3.10 (a), to the optimum size enriched in heavy mineral for the reduction of self-absorption. The sieved samples were sealed in polyethylene bags seen in Fig. 3.10 (b), until we set marinelli beakers. We provided marinelli beakers for HPGe detector which is a standard marinelli beaker and for NaI(Tl) detector we prepared manually from pvc plastic by the geometry of marinelli beaker that fit NaI(Tl) detector of FJ374 model size as shown in Fig: 3.10 (d).

(a) Mesh siever

(b) Packed samples

(c) Prepared samples for HPGe detector

(d) Prepared samples for NaI(Tl) detector

Figure 3.10: Samples for gamma spectrometer measurements.

The final samples were packed in standard marinelli beakers for HPGe detector and manually prepared sample holders for NaI(Tl) detector as in Fig. 3.10, (c) and (d), whose volume is 500ml at Ethiopian Radiation Protection Authority, (ERPA) laboratory and 150ml at Addis Ababa University nuclear laboratory. We let air space in merinelli beakers while sealing. Teflon tape and normal Vaseline were used to prevent radon gas leakage. Then, we stored for a minimum period of 28 days to allow an in-growth of uranium and thorium decay products and achievement of equilibrium with their respective progeny [11, 36]. Finally, the samples were counted for 10-hours using gamma spectrometer coupled with HPGe detector and 23 hours to 24 hours using gamma spectrometer coupled with NaI(Tl) detector. For analysis, we compared with a standardized soil samples, like SOIL-6 and SOIL-375 at the same geometries, measured at the same statuses.

3.2.3 Gamma ray Spectrometer Coupled with HPGe Experimental Setup and Measurements

The measurements were performed using a p-type high purity germanium (HPGe) coaxial detector with a relative efficiency of 77% and multichannel analyser of 8192 channel performance.

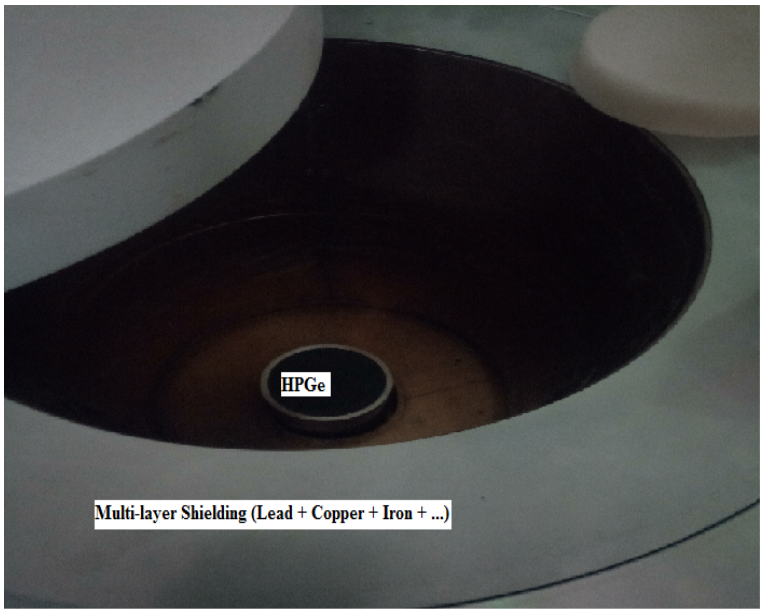

Figure 3.11: HPGe-detector and its shielding (Pb+Cd+Cu)

To minimize the number of photons whose their sources are out of sample of study, a detector is covered in a lead of 100-mm thickness, cadmium of 2-mm thickness, and copper of 2.5-mm thickness as seen in Fig. 3.11.

The 100 mm thick lead is used to reduce soft components of cosmic rays to a very low level. Copper layer suppresses X-ray emitted from the lead (specially with energy 73.9 keV), by its interaction with external radiation. The cadmium layer absorbs thermal neutrons produced by cosmic ray (Photo-neutron and alpha-neutron sources). There is also an effect of scattered radiation from shielding materials. This can be controlled by fixing the detector at a centre of shielding materials itself. After fixing all, we connected the detector to DSA and computer as in Fig. 3.12, so that we can see the amplified and resolved out put spectrum on a computer screen.

Figure 3.12: Gamma spectrometry mounted with HPGe detector and DSA circuit (ERPA Lab.)

Samples were placed over the detector for $36,000$ *sec* or 10-hours for measurements. Background radiation was also measured for an empty marinelli beaker for the same counting time and an effects of background radiation were subtracted from samples spectra [37, 38].

The spectra were analysed for energies; 911 keV of ^{228}Ac for ^{232}Th radionuclide identification, 351 keV of ^{214}Pb and 609 keV of ^{214}Bi for ^{238}U radionuclide identification, and 1460.9 keV gamma energy for ^{40}K radionuclide identification. Levels of activity were measured for these identified radio nuclides from their photo peaks. Our set up reports more than 99% confidence for the existence of these photo peaks exactly at channel number used for calibration. Energies; 238 keV, of ^{212}Pb and 727 keV, of ^{212}Bi were not observed in the region of spectrum fixed by our calibration that shows a straight line as seen from Fig. 3.13 [39].

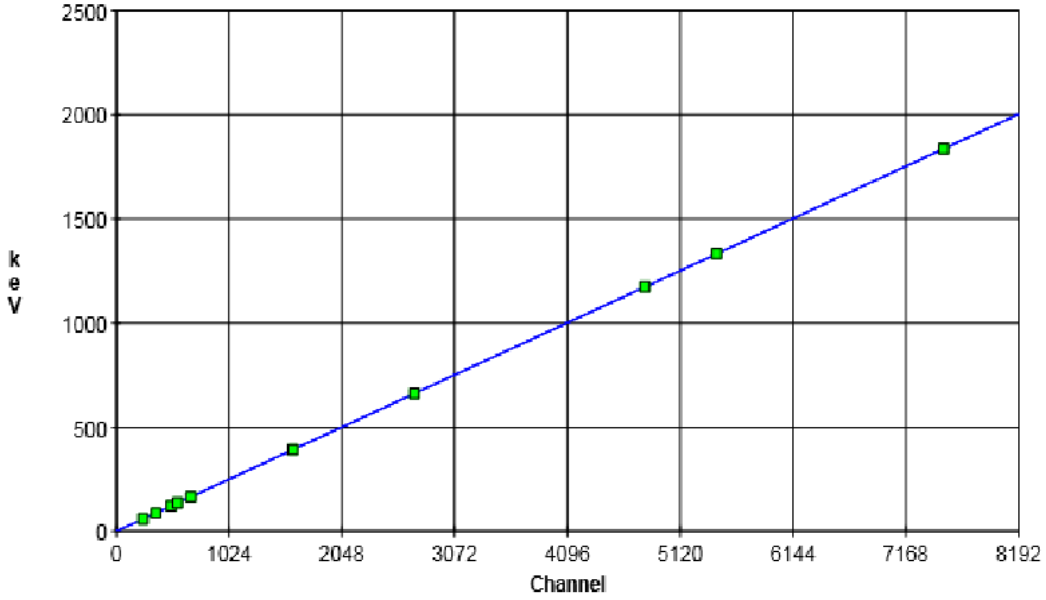

Figure 3.13: Calibration curve by standard check sources in the region of interests

After calibration, absolute efficiency (Full Energy Peak Efficiency) of the detector was measured using the same standard sources listed in section 2.2.1 for the same geometry as in Eq. 3.3

$$\varepsilon_i = \frac{A_i}{C_i * I_\gamma * t * M} \tag{3.3}$$

where A_i is net peak area corresponding to E_i, C_i is deduced activity by certified radionuclide, I_γ indicates probability of E_i photon emission per decay, and t is counting time, M mass of the radionuclide. The photo peak efficiencies from samples of measurement coincide with this efficiency curve and the curve is shown in Fig. 3.14.

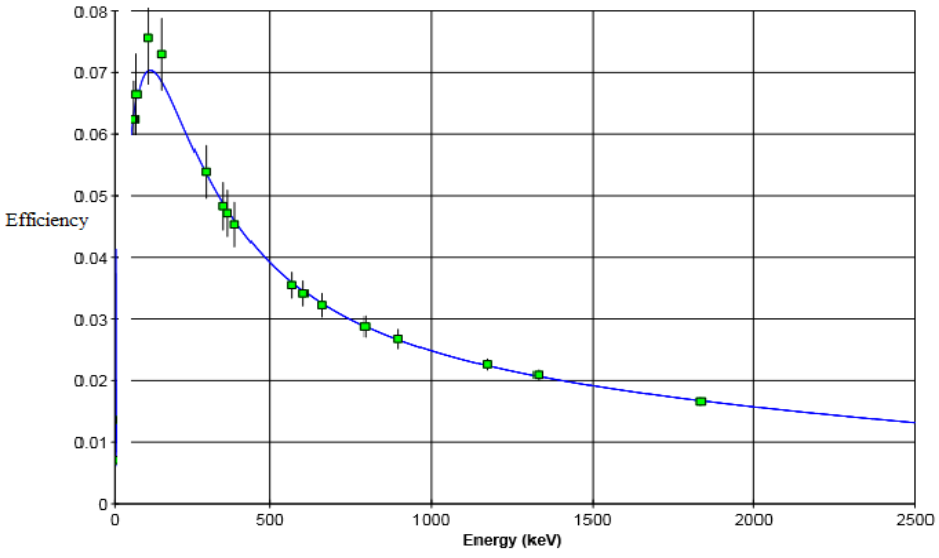

Figure 3.14: Efficiency curve by standard check sources in the region of interests

3.2.4 Gamma ray Spectrometry Coupled with NaI(Tl) Experimental Setup and Measurements

The measurements were performed using NaI(Tl) crystal of model known by FJ374. It is a 4cm by 4cm with a resolution up to 7.5% for ^{137}Cs source as calculated using Eq: 3.1 at $0cm$source to detector distance as compared with high resolution gamma spectrometer. To know the efficiency and energy resolution of this detector, ^{137}Cs standard source with activity 37 KBq were used which was supplied by PHYWE, German company. To confirm the findings, GEometry ANd Tracking of version 4 (GEANT4) Monte Carlo code, geant4.10.03.p02, was used for the same radiation source. GEANT4 Monte Carlo simulation is one of the commonly used method in particle simulation for an increasing of accuracy of measurements and calibration of gamma ray spectrometer. It is a reliable toolkit for particle simulation, if geometrical parameters of a detector and radiation sources are known [24]. It is a Monte Carlo method that uses a composition method if a condition is true, and rejection if the condition is false as dealt in section 2.2.1 [40].

3.2.4.1 Efficiency Checking for Gamma ray Spectrometer Coupled with NaI(Tl)

Gamma ray spectrometer efficiency is a measure of performance of detectors that quantify the number of photons that interact with its active region. Full Energy Peak Efficiency (FEPE) of a detector is a product of intrinsic efficiency of a device itself and geometrical efficiency determined by source position to a detector.

$$FEPE = \xi_{intrinsic} * \xi_G \tag{3.4}$$

Intrinsic efficiency is the ratio of total number of counted photons to a total number of photons entered to the detector. Analytically, it can be determined for an isotropic point sources and cylindrical NaI(Tl) detector with length L and radius R as shown in Fig: 3.15.

$$\xi_{intrinsic} = \frac{\int_0^{\theta_1}[1-e^{-\mu(E)(\frac{L}{cos\theta})}]sin\theta d\theta}{[1-cos\theta_0]} + \frac{\int_{\theta_1}^{\theta_0}[1-e^{-\mu(E)(\frac{L}{sin\theta}-\frac{d}{cos\theta_0}}]sin\theta d\theta}{[1-cos\theta_0]} \tag{3.5}$$

where, $tan\theta_0 = \frac{R}{d}$,

$tan\theta_1 = \frac{R}{d+L}$ and

$\mu(E)$ is the linear attenuation coefficient in NaI(Tl) [41].

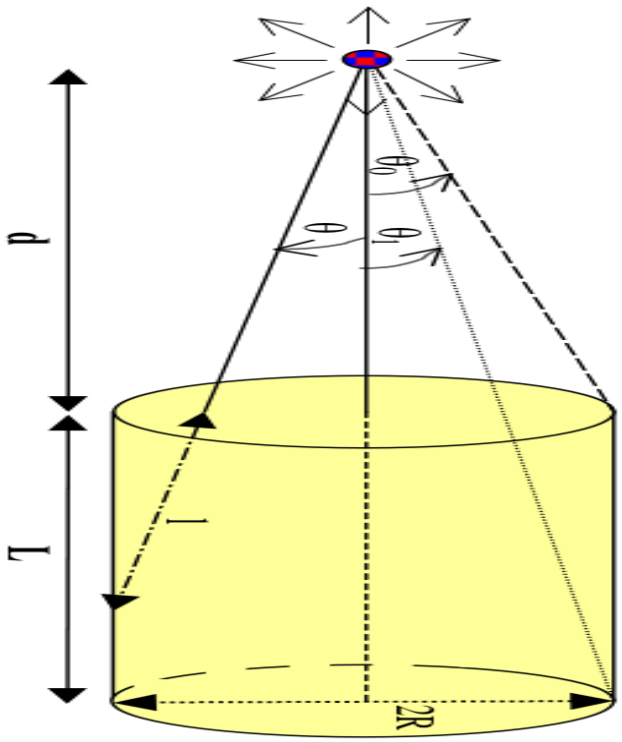

Figure 3.15: Symmetrical source position and geometry of NaI(Tl) detector.

The intrinsic efficiency was calculated using Eq: 3.5 for geometry shown in Fig: 3.15. This was calculated as 15.2% at 662keV energy source for which the linear attenuation coefficient in NaI(Tl) which is approximately $0.079cm^{-1}$.

To calculate geometrical efficiency of this detector, it is necessary to model the geometry of FJ374 NaI(Tl) detector using GEANT4 Monte Carlo simulation. This can be possible by considering all geometrical parameters and elemental compositions of detector material type. Some geometrical parameters are provided by manufacturer, where few of the others are from literature ([40]), which are given as NaI(Tl) crystal density, $3.667gcm^3$, Al_2O_3 reflector density, $3.970gcm3$ and aluminum density, $2.7gcm^3$. To account for back scattering, window of Photo Multiplier Tube (PMT) was modelled as being composed of glass, (SiO_2) layer, having an effective density of $0.94gcm^3$ [40].

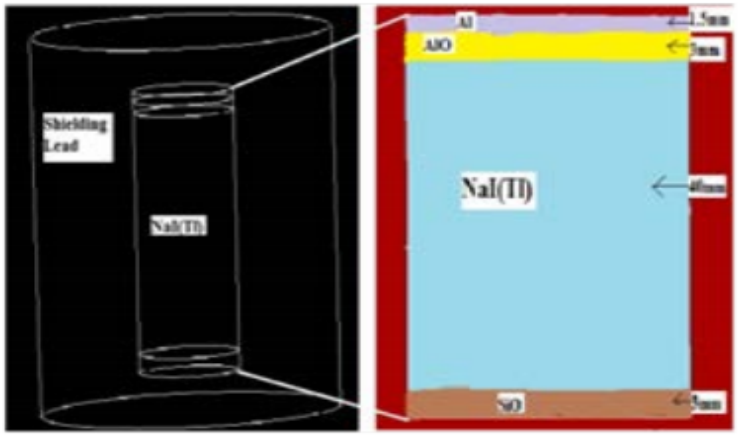

Figure 3.16: Cross sectional view of modeled FJ374 NaI(Tl) crystal and lead shield.

Geometrical efficiency depend on a solid angle covered by radiation towards an effective area of a detector modelled as in Fig: 3.16, can be calculated experimentally as;

$$\xi_G = \frac{\Omega}{4\pi} \tag{3.6}$$

where Ω is geometrical solid angle, given as $\Omega = 2\pi(1 - \frac{d}{\sqrt{d^2 - R^2}})$ for geometry shown in Fig: 3.15.

The simulation were performed for distances starting from $0cm$, to $16cm$. At $0cm$, on the top surface of the end cup of modeled detector, we found 42% geometrical efficiency for ^{137}Cs of energy 662keV using GEANT4 for modelled geometry shown in Fig: 3.16. The code considers both Eq: 3.5 and Eq: 3.6. Now, using Eq: 3.4, the theoretically calculated FEPE at $0cm$ for energy 662keV becomes 6.38%. As the distance from detector to source increase, Eq: 3.6 will reduce this result. At $10cm$ distance between source and detector, FEPE was found 0.22%, where for 3inch (7.62 cm) by 3inch (7.62 cm) detector at same distance for the same gamma energy measured by [42] was 1.04%.

Experimentally this measurement was done in laboratory for the same real geometry of FJ374 NaI(Tl) detector with 662keV energy ^{137}Cs source at distances from $0cm$ to $16cm$. The absolute efficiency, (FEPE) was measured by this energy using Eq: 3.3 is 5.4%, at $0cm$ distance from end cap of the detector to source. This efficiency value is affected by geometrical positioning of the source to detector, and measurements were done at symmetric axis of the detector. It is real as the distance between source and detector increases, FEPE decreases as shown from Fig: 3.17.

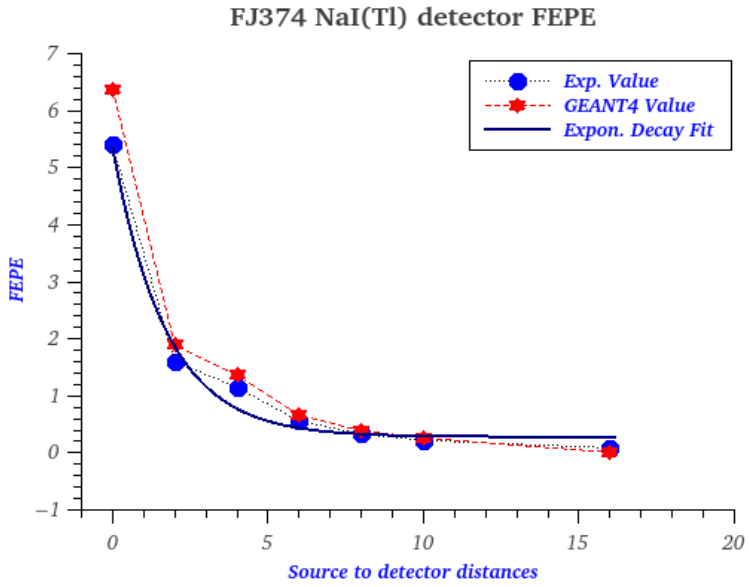

Figure 3.17: FJ374 NaI(Tl) FEPE vs end cap to source distances (d).

3.2.4.2 Resolution Checking for Gamma ray Spectrometry Coupled with NaI(Tl)

The high atomic number for iodine in NaI(Tl) gives good efficiency for γ-ray detection. But the resolution of this detector is less as compared with HPGe detector. The best resolution is up to 50 keV at 662 keV for a 3 inch (7.62 cm) diameter by 3 inch (7.62 cm) long cylindrical crystal. We measured resolution of FJ374 NaI(Tl) detector (4cm by 4cm) experimentally in the laboratory using Eq: 3.1 and 3.2 and using GEANT4 Monte Carlo simulation using Eq: 3.1 and 3.7.

$$FWHM = a + b\sqrt{E + cE^2} \tag{3.7}$$

where E is energy of radiation source, and constants a, b and c are equal to -0.0137257, 0.0739501, and -0.152982 respectively, which is obtained from experimental fitting of this equation [32,40]. Using GEANT4 Monte Carlo simulation, we calculated the energy resolution, for energy 662keV, 6.5%, where manufacturer gives 7.5% as compared to 3keV energy resolution HPGe detector. Experimentally observed fact is, for low count/photon intensity, resolution is very low and as count increases it also increases and at some finite energy it will be limited. That point is the maximum energy resolution for FJ374 NaI(Tl) detector and identified 6.5 in percent as shown in Fig: 3.18.

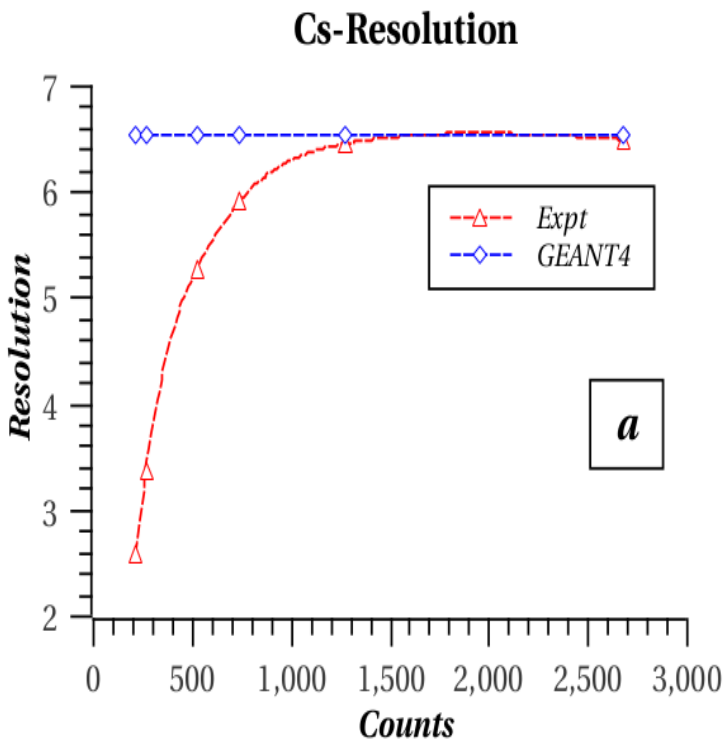

Figure 3.18: Energy resolution for FJ374 NaI(Tl) detector at 662keV.

Collected samples were measured by such gamma ray spectrometer cascaded with electronic circuits and GENIE2K multichannel analyzer of 4096 channels performance. The detector is shielded in a chamber of two layers starting with the inner part stainless steel of 3 mm thick and lead of 45 mm thick to reduce background radiations.

Figure 3.19: Gamma spectrometer with FJ374 scintillation crystal and Electronic circuits

The detector fixed in center of the chamber to minimize the effect of scattered radiation

from shielding materials. Then we kept sample over the detector for 23-24 hours.

The spectra were evaluated manually for the energies of 238 keV of Pb-212 for Th-232 identification, 351 keV of Pb-214 and 609 keV of Bi-214 for U-238 identification and 1460.9 keV gamma line for K-40 activity concentration [37–39].

3.2.5 Activity and Elemental Concentration Equations

Following the spectrum analysis, for photo peaks representing decay progenies of Uranium, Thorium and photo peak of Potassium, level of activities were calculated using eq. 3.8. The specific activity, C_{Ei}, (Bq/kg) of a nuclide i for a photo peak at energy E, is after rearranging Eq. 3.3, [43] is given by;

$$C_{Ei}(Bq/Kg) = \frac{A_i}{\varepsilon_{Ei} * I_\gamma * t * M_{Ei}} \tag{3.8}$$

Based on the activity levels, it is possible to calculate the elemental concentrations of Uranium, Thorium, and Potassium in sample of study according to Eq. 3.9.

$$F_E = \frac{M_E * C}{\lambda_E * N_A * f_{AE}} * \frac{1}{n} \sum_{i=1}^{n} C_i \tag{3.9}$$

where F_E is fraction of element E in the sample, M_E is the atomic mass in kg/mol, λ_E is the decay constant of parent nuclide in $1/s$, N_A is Avogadro's number in $atoms/mol$, f_{AE} is the fractional atomic abundance of ^{232}Th, ^{238}U or ^{40}K in nature, C is a constant (with a value of 100 or 1,000,000) that converts the ratio of the element's mass into a percentage or parts per million (ppm), and C_i is the radiological concentration or activity concentration of selected daughter radio nuclides in the decay series of ^{232}Th and ^{238}U, and ^{40}K. The value of n is equivalent to the photon number representing radioisotopes. The value is reported in ppm, whereas for potassium this value is one and reported in percent (%) [17].

3.2.6 Radiological Hazard Indices Equations

An exposure of population to environmental radiation sources increases appreciably as industries and natural disasters increases. Therefore, it is important to assess the radiological risks of radiation sources from environments like building materials and buildings. The widely used radiation hazard indices for assessment are radium equivalent activity, absorbed dose rate, annual dose rate, internal and external hazard indices and other parameters that give information about radiation exposure to population.

3.2.6.1 Radium Equivalent Equation (Ra_{eq})

Gamma radiation hazards from specific radio nuclides can be evaluated using different indices. (Ra_{eq}), is one of an indicator, which is the weighted sum of activities of the three radio nuclides based on the supposition that $370Bq/kg$ of ^{238}U, $259Bq/kg$ of ^{232}Th, and $4810Bq/kg$ of ^{40}K will give same gamma-ray dose rate. Therefore, Ra_{eq} can be calculated from this concept as;

$$R_{eq} = C_U + 1.43C_{Th} + 0.077C_K \tag{3.10}$$

where C_U, C_{Th} and C_K are activity concentrations in Bq/Kg of ^{238}U, ^{232}Th and ^{40}K respectively [44].

3.2.6.2 Absorbed Dose Rate in Air (D_R)

This parameter, (D_R) is measured at a distance of $1m$ above the surface that ensures a uniform distribution of the three radio nuclides for almost the same activities. At this distance the absorbed Dose rate (D_R) can be calculated as,

$$D_R = 0.427C_U + 0.623C_{Th} + 0.043C_K \tag{3.11}$$

Where the dose rate, D_R is in nGy/h and C is activity in Bq/Kg for ^{238}U, ^{232}Th and ^{40}K. This dose rate indicates the received dose at outdoors from radiation emitted by radionuclides in environmental materials. The limit for this dose is $59nGy/h$ [44, 45].

3.2.6.3 Annual Effective Dose Rate (AD_R)

Annual effective dose rate can be calculated to assess the health effects of the absorbed dose in a year. Mathematically it can be represented as;

$$AD_R = D_R(mGy/h) * 8760h/y * 0.2 * 0.7Sv/Gy * 10^{-6} \tag{3.12}$$

where AD_R is in mSv/y and $0.7SvG/y$ is to transform absorbed dose in air to the effective dose received by humans at $1m$ hight, 0.2 is an outdoor occupancy of 20% and 80% for the indoors [11, 44]. This factor may be changed according to the patterns of life by humans in the study area. The worldwide average annual effective dose is approximately $2.4mSv/y$ [44, 45].

3.2.6.4 External (H_{ex}) and Internal(H_{in}) Hazard Indexes

The external radiation hazard index, H_{ex} , corresponding to the investigated radio nuclides is calculated using the following equation;

$$H_{ex} = \frac{C_U}{370Bq/Kg} + \frac{C_{Th}}{259Bq/Kg} + \frac{C_K}{4810Bq/Kg} \tag{3.13}$$

The maximum value of H_{ex} should be 1 corresponding to the maximum value of R_{eq}, which is $370Bq/Kg$.

The hazard levels from inhaled alpha particles emitted from radon short-lived radio nuclides such as 222-Rn and daughter products can be quantified by internal hazard index, H_{in} as [46];

$$H_{in} = \frac{C_U}{185Bq/Kg} + \frac{C_{Th}}{259Bq/Kg} + \frac{C_K}{4810Bq/Kg} \tag{3.14}$$

.

4

Results and Discussions

4.1 The Study of Natural Radioactivity Levels and Their Associated Health Hazard Indices in Main Cement Raw Materials Using HPGe Detector

4.1.1 Introduction

Natural radioactive materials can be originated from various geological materials enriched with radio elements. Parts of sedimentary rock, limestone and sandstone, and clay rocks are the known geological materials in the formation of layers of the earth. They are used as a raw materials in different industries as building materials. Limestone, sandstone and clay are the main components used to make harden cement semi-product called clinker. This partial processed product is made after the three are mixed with each other and heated by a temperature more than $1,300^0C$. After that it will be grinded to a fine dust level and can be used as Portland Cement (PC) [5, 47].

Limestone and sandstone fall under the category of sedimentary rock which is made from mineral calcite (calcium ion and carbon dioxide) and silica (quartz) respectively. Sedimentary rock by itself is formed from shells, skeletons or secreted carbonate of wide varieties of organisms and a direct precipitation (crystallization) of carbonate in marine environments. These two families of sedimentary rocks are used as a raw material in many industries, as steel production, cement industry and as building raw materials [16, 47].

From the three known long living primordial radio active elements, uranium is expected to have more concentration due to its greater mobility in the form of oxidized (UO_2^{2+}) organic acid solution and deposited in limestone [15]. Thorium has low mobility under all environmental conditions, mainly due to its high stability of the insoluble oxide (ThO_2) and strongly resistive nature of its carrier minerals such as monazite and zircon. Therefore, the concentration of thorium in limestone is very low [12, 21]. The main composition of limestone is calcium carbonate $(CaCo_3)$ which is an organic composition. It is not formed

from mica or potash (potassium-bearing minerals, ores, and finished products), which means the potassium constituent of limestone is low. Any rock type that lack such minerals will show usually low concentration of potassium [21, 48].

Limestone ($CaCo_3$), crystal shown in Fig. 4.1 *(a)*, is a main basic raw material in cement industry. It covers more than 60% of the composition of finally processed cements and is a very hard rocky material. As it's ratio increases in cement processing, qualities of cement also increases, which means can resist more pressures. At the three cement factories, limestone is used for the production of Ordinary Portland Cement (OPC), with 42.5N strength and Pozzolana Portland Cement (PPC), with 32.5N strength [49].

(a) Crystal structure of Limestone

(b) Crystal structure of Sandstone

(c) Crystal structure of red Clay

Figure 4.1: Morphology of Limestone, Sandstone and Clay stones

Sand stone is free for the movements of oxygenated water, that can easily dissolve uranium. Therefore, the concentration of uranium in sandstone is expected to be less as com-

pared to other primordial radioactive materials. On the other hand, thorium is insoluble in water, highly stable and strong resistant to its carrier. Such behaviours are an indicator of more concentration of thorium in sandstone than uranium. Sandstone and/or siliceous sediments commonly contain optimum range of potassium as compared with clay, and this is a function of presence of the three minerals, potassium-feldspar, potassium-mica and glauconite [48]. It is possible to understand that as compared to other geological materials, like igneous rock, the concentration of natural radioactive materials in the two, lime and sand, is low, because of their large concentration of calcium and silicon in percentage composition and their morphological structure.

Sandstone (SiO_2), the crystal shown in Fig. 4.1 *b*, covers 15 to25% of the final products of a cement. Its content will determine the strength of cement in the reverse way of limestone [49].

Clay is another basic raw materials used in cement factory, which is a hydrous aluminosilicate that originate from igneous or metamorphic rocks. Igneous and/or metamorphic rocks have more concentrations of radioactive materials, because they are a product of harden cooled volcanic lava from core of the earth. Transformations in geometric arrangement of atoms and ions within igneous and metamorphic rocks on the earth surface due to weathering creates a clear geo-structure for clay that makes it differ from igneous or metamorphic rocks [50]. Its formation from igneous rock enhances uranium bearing minerals like granite, results of volcanic's lava flows and tuff ashes. The mobility of thorium in most case is limited by an absorption of clay minerals. Therefore, the concentration of thorium in clay minerals is more as compared to sandstone and other geologically related features. Quartz, mica and some feldspar are basic building blocks of clay minerals. The abundance of potassium-40 in quartz, feldspar and mica is generally more as compared to limestone and dolomite [12, 21].

Clay, (Al_2O_3), covers 5 to 10%. These three raw materials will form clinker, highly heated mixture of the three, to make a final product (OPC) [49].

4.1.2 Result and Discussion

From the experimental set up seen in Fig. 3.12, we found spectrum for each gamma emitters of our interest. The spectra were from primordial radioactive decay progenies and primordial radioactive given in 3.2.3. This was done for each sample of main cement raw materials

including back ground spectrum as shown in Fig. 4.2.

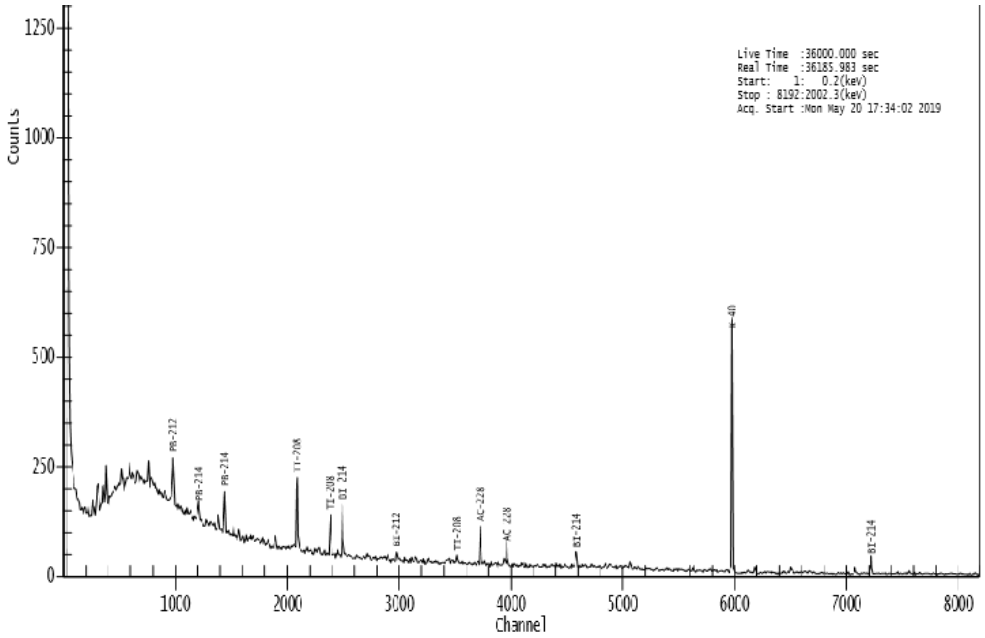

(a) Background Spectrum

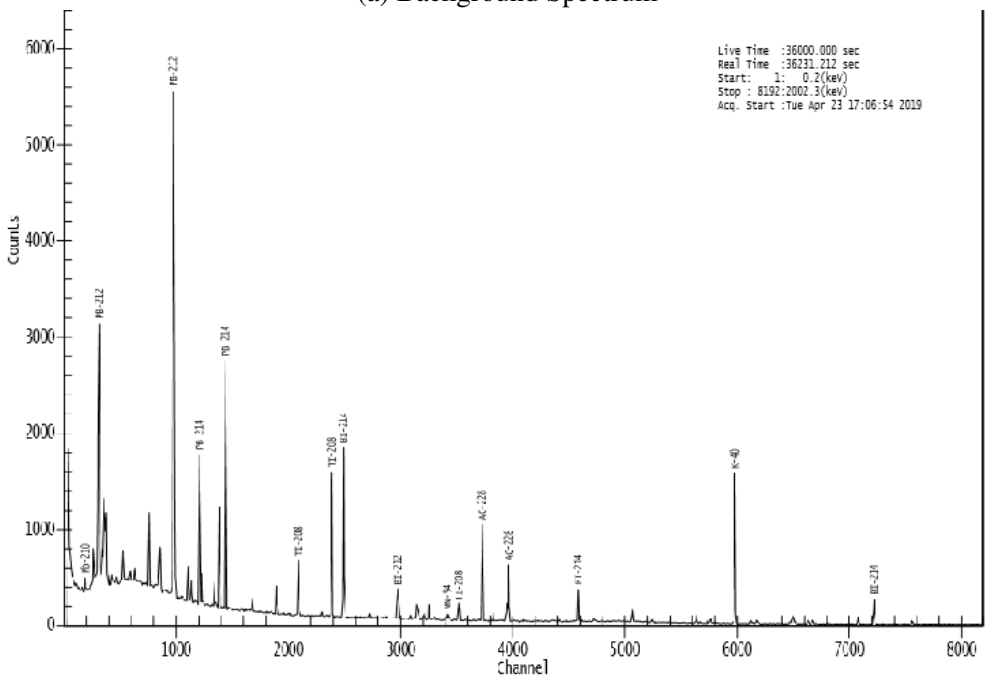

(b) Spectrum from Clay sample

Figure 4.2: HPGe background and samples output Spectrums

The spectra were observed for energies that indicate the existences of progenies of ^{238}U and ^{232}Th, and ^{40}K radio nuclides, as stated in section 3.2.3. These spectra were converted into activity concentrations using Eq. 3.8 as presented in table 4.1 below.

Table 4.1: Levels of activity concentrations measured in Clay, Limestone and Sandstone in Bq per Kg, M for Mugher cement, D for Dangote cement and H for Habesha cement factory

Sample Code	Sample Name	^{238}U $\frac{Bq}{Kg}$	^{232}Th $\frac{Bq}{Kg}$	^{40}K $\frac{Bq}{Kg}$
M01	Clay	35 ± 1.7	77 ± 3.8	200 ± 9.5
M02	Limestone N.	14.5 ± 0.74	3.8 ± 0.41	32 ± 2.1
M03	Limesone O.B	20 ± 0.95	17 ± 0.91	180 ± 8.1
M04	Sandstone	11 ± 0.78	28 ± 1.4	430 ± 19
D05	Clay	22.54 ± 0.95	43.37 ± 2.18	215.16 ± 10.04
D06	Limestone N	9.26 ± 0.47	1.75 ± 0.29	17.02 ± 1.56
D07	Sandstone	7.56 ± 0.36	24.47 ± 1.23	20.21 ± 1.58
H08	Clay	50.58 ± 2.42	150.40 ± 7.41	365.00 ± 17.11
H09	Limestone N	7.43 ± 0.35	2.34 ± 0.31	20.82 ± 1.68
H010	Sandstone	8.53 ± 0.36	24.17 ± 1.20	75.28 ± 3.47

Most of the activity concentrations for natural radioactive nuclides, ^{238}U, ^{232}Th and ^{40}K in the measured samples were seen in the world certified regions. But the concentrations of naturally occurring radioactive materials in clay samples collected from three factories explained in section 3.2.1, crosses above the permissible values given by [45], as reference in igneous rock.

As explained in section 4.1.1, limestone is part of sedimentary rock which is found at the lower part of the earth surface. The soluble radioactive materials deposited on such types of rock in the long period of time. So, the concentration of ^{238}U was seen more according to our measurements, but the whole readings showed below the permissible value. ^{232}Th, ores containing thorium are insoluble in water, and may not go to the lower layers of earth's crust. Therefore, the activity concentration of ^{232}Th in limestone is very low as compared to the world permissible values. In our measurements, same facts was observed about this radioactive material, ^{232}Th. Two types of limestone used as raw materials, Limestone N, and Limestone O.B, which is to mean Normal limestone and Overburden limestone respectively were collected. Overburden limestone is a mixture of normal limestone with other types of raw materials, used for controlling the contents of cement in processing. The reading observed in this sample type slightly violate our expectation and on the written literature. According to [12], sedimentary rocks are not a product of materials like mica or potash.

Therefore, the concentration of ^{40}K in measured samples is much lower than the world certified value, $400Bq/Kg$.

In the case of sandstone, its geological formation allows the movements of water than limestone. We can say that free for water movement comparatively. So, the concentration of ^{232}Th is more according to [12]. In our measurements, we found same fact in which the concentration of ^{232}Th is more than twice of the concentration of ^{238}U. But, the maximum recorded activity concentration of ^{232}Th is lower than world certified permissible value, $30Bq/Kg$ and ^{238}U is much lower than the limit, $35Bq/Kg$. The concentration of ^{40}K in silica of sandstone is optimum as discussed in sec 4.1.1, but the value was seen that slightly crosses the boundary condition given by [45]. The average value is almost as discussed in 4.1.1.

Clay is an hydrous aluminosilicate that originated from igneous or metamorphic rocks [50]. Such rocks are rich in radioactive materials specially for insoluble radioactive materials. As discussed in 4.1.1. The concentration of thorium in measured samples crosses the world certified limit value, $30Bq/Kg$. The activity concentration of ^{232}Th in sample $H08$ was measured almost five times greater than the world certified value. In other samples it is also more than twice of the limit value. In the same sample, $H08$, ^{238}U also crosses the average value given on [45], $35Bq/Kg$, where in other samples it is almost near the boundary. Such types of soil samples are used for a measure of optimum limit of elemental concentration in environmental soils according to [12]. The other radioactive material in clay is ^{40}K, and it is included in clay in the form of mica, quartz and feldspar. Those materials are rich in isotopes of potassium, and ^{40}K shares its abundance from the isotopes. In the collected samples of clay, it was seen more reading for sample coded as $H08$, and less in other types of samples. As a whole it was seen less than the world average value certified for ^{40}K as seen from fig: 4.3.

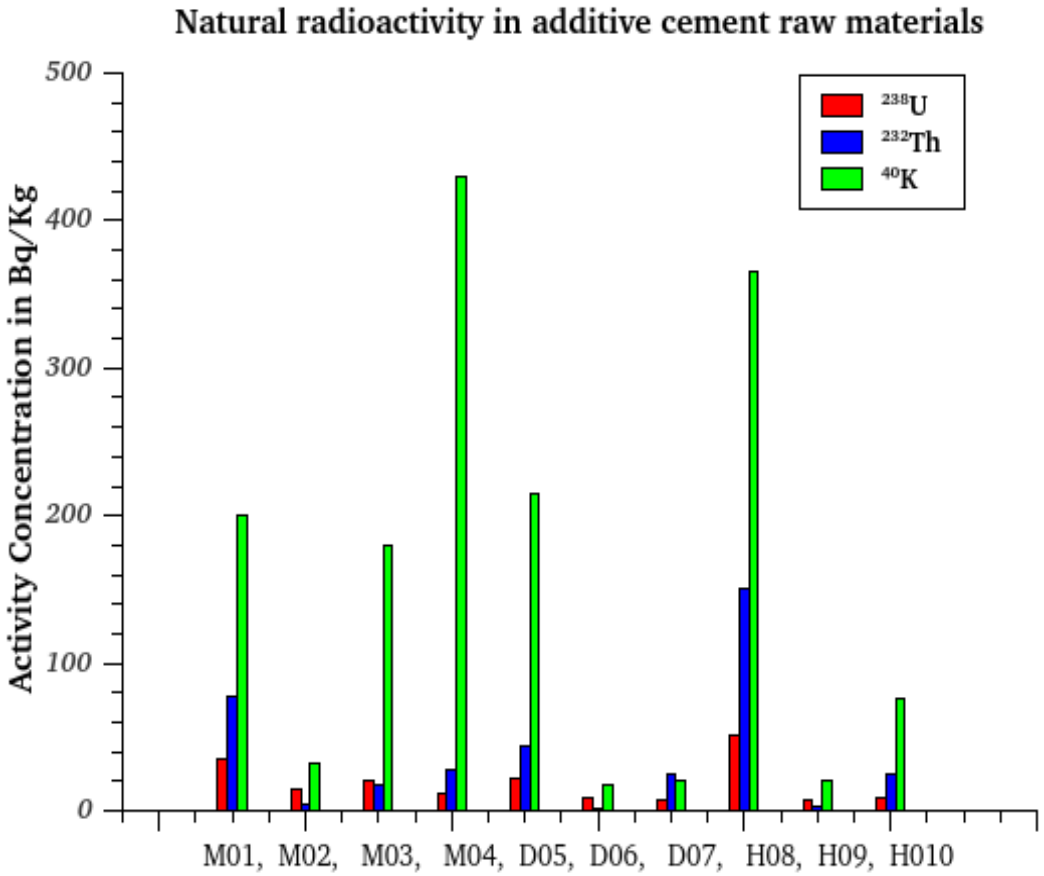

Figure 4.3: ^{238}U, ^{232}Th and ^{40}K activity in sampled cement's main raw materials

The activity concentrations of naturally occurring radioactive materials in samples identified as main cement raw materials is with in world permissible value in average as seen from Fig. 4.3. From the three sample types, clay shows more concentration of natural radioactive materials specially for ^{232}Th, which is up to $37ppm$, where the maximum expected value in clay is $13ppm$ according to [12]. The elemental concentrations of other radioactive materials were seen with in the limit according to the study by [12].

The limit of specific activity concentrations from building materials is higher than the environmental values for same radioactive materials, $50Bq/Kg$, $50Bq/Kg$ and $500Bq/Kg$ for ^{238}U, ^{232}Th and ^{40}K respectively [51]. The measured activities in table 4.1 can be converted to their corresponding hazard indices discussed in section 3.2.6 at dwelling and their mining areas. The hazard indicating parameters were presented in table below, table 4.2.

Table 4.2: Radio-logical hazard indices in Limestone, Sandstone and Clay used as main cement raw materials, M for Mugher cement factory, D for Dangote cement factory and H for habesha cement factory

Sample Name	Sample Code	R_{eq} in $\frac{Bq}{Kg}$	D_R in nGy/hr	AD_R in mSv/yr	H_{ex}	H_{in}
M01	Clay	160.51 ± 7.87	71.52 ± 3.50	0.088 ± 0.004	0.433	0.528
M02	Lime N.	22.40 ± 1.49	9.93 ± 0.66	0.012 ± 0.001	0.060	0.100
M03	Lime, O.B	58.17 ± 2.88	26.87 ± 1.32	0.033 ± 0.002	0.157	0.211
M04	Sand	84.15 ± 4.24	40.63 ± 2.02	0.050 ± 0.003	0.227	0.258
D05	Clay	101.13 ± 4.84	45.90 ± 2.20	0.056 ± 0.003	0.273	0.334
D06	Lime, N	13.07 ± 1.00	5.78 ± 0.45	0.007 ± 0.000	0.035	0.060
D07	Sand	44.12 ± 2.24	19.34 ± 0.99	0.024 ± 0.001	0.119	0.140
H08	Clay	293.78 ± 14.33	130.99 ± 6.38	0.161 ± 0.008	0.793	0.930
H09	Lime, N	12.38 ± 0.92	5.52 ± 0.41	0.007 ± 0.001	0.033	0.054
H10	Sand	49.89 ± 2.34	21.94 ± 1.05	0.027 ± 0.001	0.132	0.155

Radium equivalent activity, R_{eq} is a measure of activities of the three natural radioactive materials that can produce equal amount of radiation dose. The maximum limit for this parameter was given by [45] which is $370Bq/Kg$. In the collected raw materials, it was seen that R_{eq} much less than the given value. In clay sample coded as $H08$, thorium activity was measured five times more than the permissible value. Since the activity concentrations of other radio nuclide in the sample are not as thorium, R_{eq} shows less value.

The absorbed dose rate D_R from raw materials at $1m$ from homogeneous distribution of materials, is highly depending on the activity concentration and it is maximum for raw materials with high activity concentrations. The maximum value given by [45] is $59nGy/hr$ and it was found in the collected samples from $5.52nGy/hr$ to $130.99nGy/hr$. It was seen maximum value for sample number $H08$ for which its ^{232}Th activity value is five times more than the permissible limit. The total annual absorbed dose AD_R for public person from all environment was limited to $2.4mSv/yr$ according to [45]. It was measured from only the collected samples up to $0.16mSv/yr$ for a public man exposed to radiation of sampled material type.

The other hazard indicating parameters are external and internal health hazard indices, H_{ex} and H_{in}. The maximum values of those parameters are a unit value for the sum total of

the three radioactive materials. In the observed activity concentration results, these parameters were seen less than unit value. As in Eq. 3.13 and 3.14, the activities of ^{238}U, ^{232}Th and ^{40}K must be greater than $61.6Bq/Kg$, $86.25Bq/Kg$ and $1601.73Bq/Kg$ respectively to get values of H_{ex} and H_{in} greater than one (1).

In average, the median health hazard indices from cement's main raw materials from the selected cement factories were observed with in the world certified values. Some readings from some samples crossed the given values based on the fact from [45].

4.2 Investigations of Natural Radioactivity Levels and Corresponding Elemental Concentrations in Additive Cements Raw Materials Using HPGe Detector

4.2.1 Introduction

Coal, Pumice and Gypsum are parts of the earth's crust which contain concentrated radioactive materials. In cement factories, these materials are used for different purposes. Coal is used as energy source, pumice is used for quantity increasing and gypsum for setting time (for increasing of adhesive property of cement). The three cement factories under our study, Mugher cement factory, Dangote cement factory and Habesh cement factory are commonly using these additive raw materials in addition to main raw materials discussed in section 4.1, for same purposes.

Coal is formed from prehistoric plants, in marshy environments, some tens or hundreds of millions of years ago (70 million years). Some trace elements in a coal shown in Fig. 4.4 *(a)*, are naturally radioactive of primordial nuclide including radium (Ra) and radon (Rn). These radionuclides are added to a product in a factory as a by product of coal (slag). Such elements are less chemically toxic than other coal constituents, like arsenic, selenium, or mercury. Most of the time, thorium exist in coal in a form of phosphate minerals, such as monazite or apatite, where uranium is found in both mineral and organic fractions of coal. Some uranium may be added slowly over geologic time, because organic matter can extract dissolved uranium from ground water due to the solubility of uranium in water [52–54].

The average activity concentrations of ^{40}K, ^{238}U and ^{232}Th in coal is estimated to be 50, 20 and 20 Bq/kg, respectively, based on the analysis of coal samples from 15 countries [55]. The main mining areas of coal for these factories are from South Africa, ported to Ethiopia,

and from Jimma Seka, specially for Habesha Cement Factory. These coals are required to process 400 tons of raw materials in these factories, Mugher, Dangote and Habesha cement factories.

(a) Coal Samples

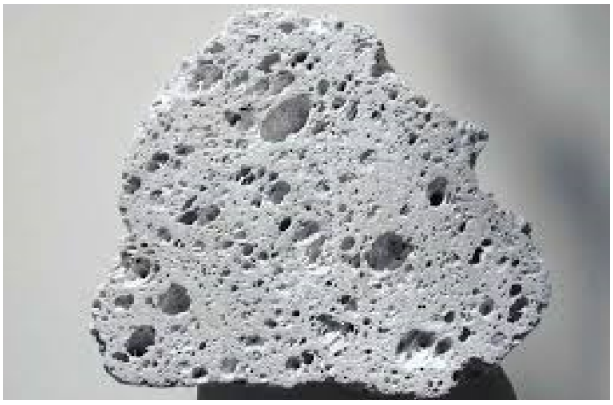

(b) Pumice Morphology

(c) Gypsum Morphology

Figure 4.4: Cement additive raw materials

Pumice, volcanic ash, is a very light, porous igneous volcanic rock that formed through the cooling of air-pocketed lava, that uses a steam and a gaseous material dissolved into the lava itself as seen in the structure from Fig. 4.4 *(b)* [56]. The light weight and some sticky properties of pumice are well suited for buildings and assorted building products.

This raw material is mined from East Shoa zone, local areas of Adama town. The three factories collects pumice from separated areas with in few tens of kilometres away from each other. These areas are in the Eastern rift valley region, surrounded by lakes, like Shala lake, Koka and the others. The historically formed pumice mining areas are shown in Fig. 4.5 *(a)* and *(b)*. This raw material is used up to 10% in cement production for quantity.

(a) Mugher cement Pumice mining area

(b) Dangote(Ethiopia) cement Pumice mining area

(c) Dangote(Mugher) cement gypsum mining

Figure 4.5: Satellite images of some mining areas of cement factories

The plastering properties of cement is mainly from the property of gypsum, which is a naturally occurring mineral made up of calcium sulfate and water ($CaSO_4 2H_2O$), some times called hydrous calcium sulfate, structurally shown in Fig. 4.4 *(c)*. Most of its constituents are calcium, sulfate and water, and is very soluble in water as compared to limestone. The concentration of water in gypsum takes more than 20%, that such materials are not suitable for hosting uranium, thorium and potassium as insoluble rock types like lime and clay. Therefore, the concentration of natural radioactive materials in natural gypsum used as an adhesive cement raw material is expected to be low [57]. This raw material is collected by factories from areas nearby factories, in Mugher gorge, mini Abay gorge, which is shown in Fig. 4.5 *(c)*. It can take up to 5% in cement production to increase plastering properties of final products.

4.2.2 Result and Discussion

The measurements of samples using experimental set up seen in Fig. 3.12, enables us to find spectra for all samples which indicate the presence of ^{238}U, ^{232}Th and ^{40}K. The areas of spectrum tell us the activity concentration of these parent sources after measurements. Some spectra look like as shown in Fig. 4.6.

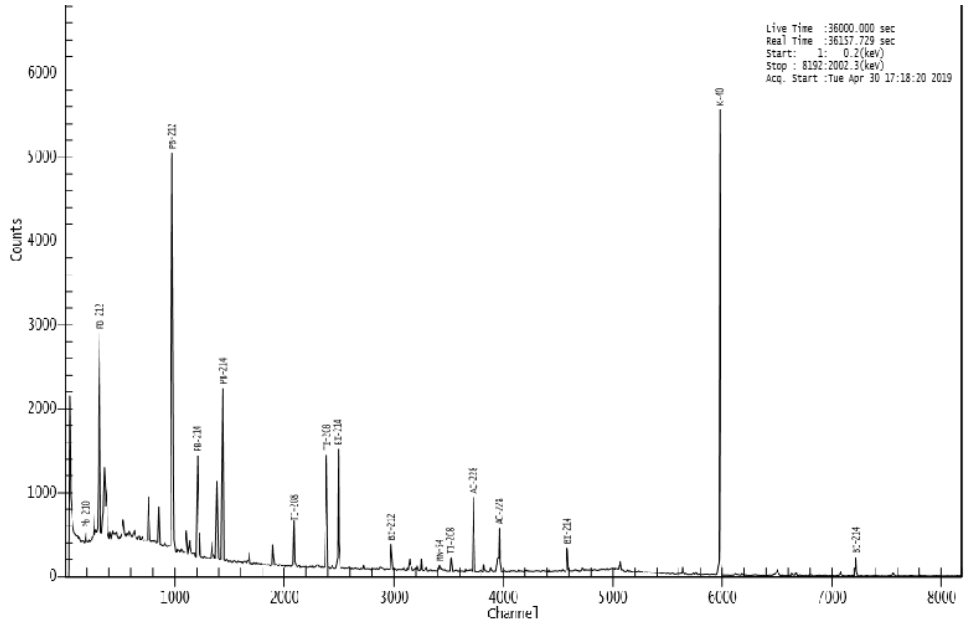

(a) Spectrum from Volcanic ash (pumice)

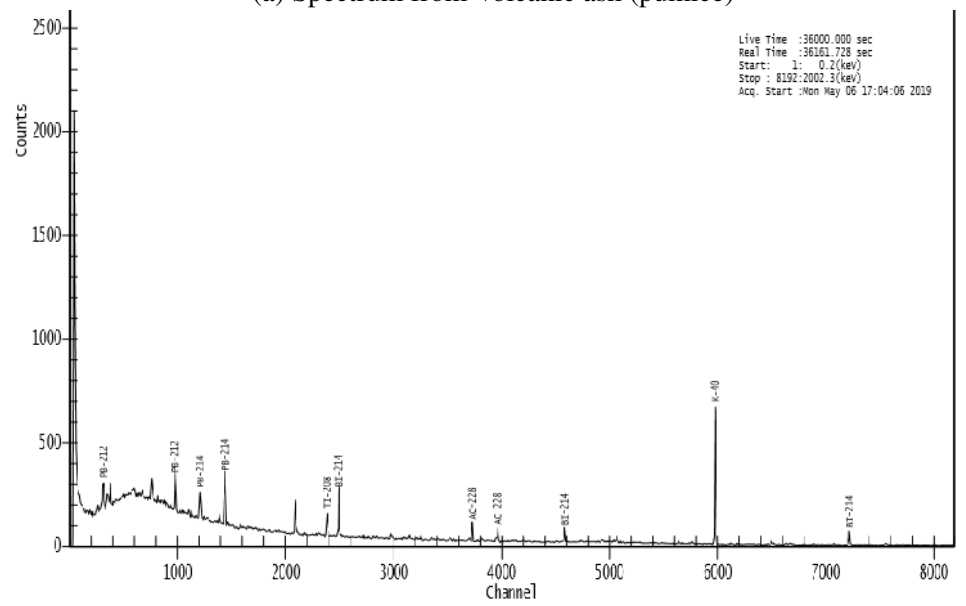

(b) Spectrum from gypsum sample

Figure 4.6: HPGe output Spectra

Analysis of peak area for each photo peak of interest were done for each sample. So,

activities of ^{238}U, ^{232}Th and ^{40}K were calculated using Eq. 3.8 for the corresponding gamma emitter progenies with a high confidence of nuclide identification, almost greater than 99% according to the pre-calibration information, and presented in table 4.3.

Table 4.3: Activity concentrations of natural radio nuclides in Bq per Kg for additive cement raw materials, M for Mugher cement factory, D for Dangote cement factory and H for Habesha cement factory

Sample Name	Sample Code	^{238}U $\frac{Bq}{Kg}$	^{232}Th $\frac{Bq}{Kg}$	^{40}K $\frac{Bq}{Kg}$
M. Pumice	M01	78.00 ± 4.00	32.00 ± 1.60	$1,100.00 \pm 51.00$
M. Gypsum	M02	2.55 ± 0.22	2.4 ± 0.44	28 ± 2.0
D. Pumice	D03	45.54 ± 1.58	107.53 ± 5.49	1034.76 ± 49.28
D. Gypsum	D04	2.26 ± 0.17	2.65 ± 0.34	33.22 ± 2.23
D. Coal	D05	30.52 ± 1.54	59.46 ± 3.14	23.04 ± 2.44
H. Pumice	H06	38.54 ± 1.54	90.08 ± 4.52	1307.65 ± 60.70
H. Gypsum	H07	1.56 ± 0.14	1.79 ± 0.33	31.99 ± 2.27
H. Coal (S.A)	H08	29.55 ± 1.60	58.29 ± 3.20	24.42 ± 2.78
H. Coal (L)	H09	28.54 ± 1.47	60.66 ± 3.15	82.70 ± 4.60

The activity concentrations of ^{238}U, ^{232}Th and ^{40}K seen in above table shows different radioactivity properties. In volcanic ash, pumice, the activity concentrations of the three radioactive materials shows almost above the permissible limit. The permissible values for environmentally distributed radioactive materials, for ^{238}U, ^{232}Th and $40K$ are $35Bq/Kg$, $30Bq/Kg$ and $400Bq/Kg$ respectively [45]. In our measurements,z we found more concentrations of the three natural radioactive materials specially for ^{40}K, in all collected pumice samples. It is three (3) times greater than the world certified value. In the same way, the activity concentration of ^{232}Th, in samples collected from Habesha and Dangote cement factories crosses the boundary limit in almost three (3) times that of world permissible value. The activity concentration of ^{238}U, in pumice samples crosses the boundary limit but not as much as the case of ^{232}Th and ^{40}K. This may differ from the geological and geochemical properties of mining area, that influence the mobility of thorium containing materials. ^{232}Th and ^{40}K are insoluble in water, and they sustain on the top surface land, formed by volcanic eruption. Therefore, their activity concentration were seen in measurements as indicated

from Fig. 4.7, which is three times the permissible value.

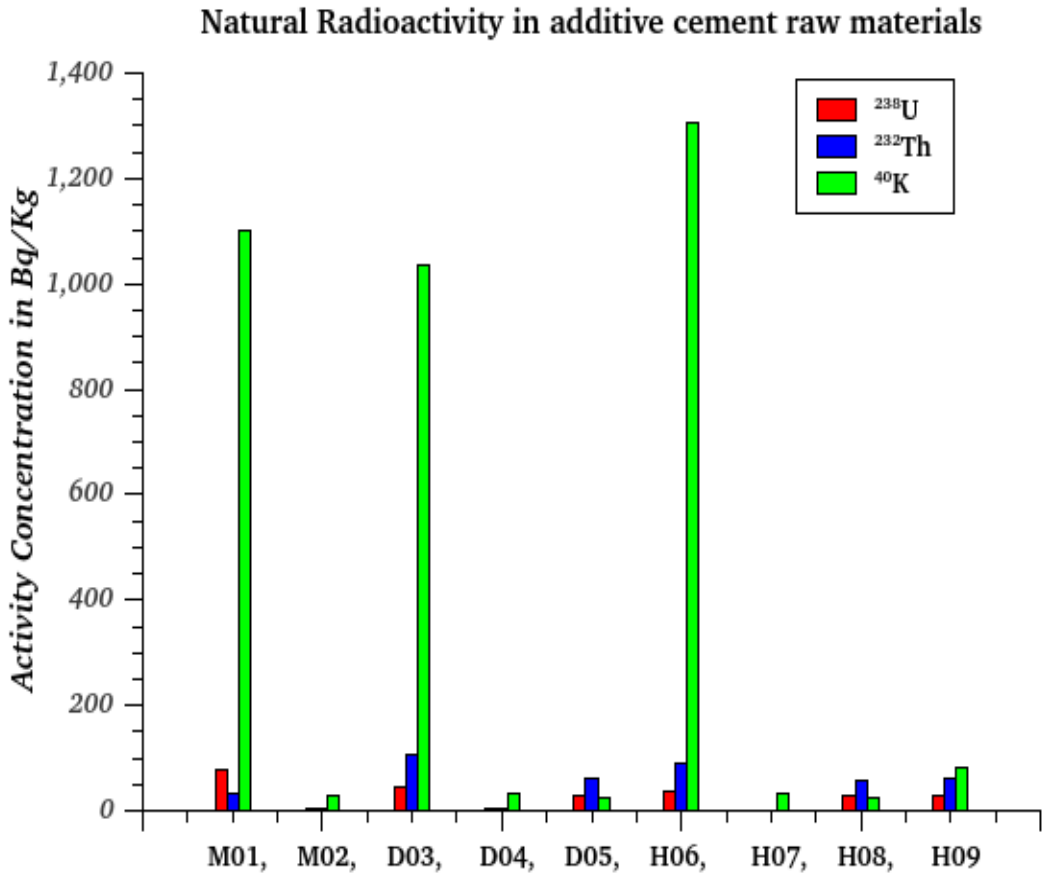

Figure 4.7: ^{238}U, ^{232}Th and ^{40}K activity in sampled cement's additive raw materials

Long leavings of coal in earth expose it to accumulate radioactive materials gradually. According to [55], the average limit of radioactive materials in coal is reported as $20Bq/Kg$, $20Bq/Kg$ and $50Bq/Kg$ for ^{238}U, ^{232}Th and ^{40}K respectively. In our measurements we found more than the average reported value on [55], specially, ^{232}Th became three (3) time greater than the reported value. ^{238}U also shows higher activity concentration value, which is almost half of ^{232}Th activity value. The activity concentration of ^{40}K in coal from Jimma Seka (Coal L) also crosses the value reported by [55], where coal from South Africa ranges below the value.

In gypsum samples, the natural radioactive materials measured in other samples shows extreme low reading as compared to the world average values for environmental samples activity concentrations. The results are the same as facts discussed in section 4.2.1, gypsum can not host concentrated soluble and insoluble radioactive materials, which means easily removed from it by water [57].

The measured activity concentrations in samples can be converted to elemental concen-

tration using Eq. 3.9 and presented in table 4.4 in parts per millions (ppm) and percentage (%) values per kilogram of samples.

Table 4.4: The elemental concentration of natural radio actives in additive cement raw materials, M for Mugher cement factory, D for Dangote cement factory and H for Habesha cement factory

Sample Name	Sample Code	^{238}U Concent. ppm	^{232}Th Concent. ppm	^{40}KConcent. %
M. Pumice	M01	6.32 ± 0.32	7.87 ± 0.39	3.540 ± 0.160
M. Gypsum	M02	0.21 ± 0.02	0.59 ± 0.11	0.088 ± 0.006
D. Pumice	D03	3.69 ± 0.13	26.45 ± 1.35	3.249 ± 0.155
D. Gypsum	D04	0.18 ± 0.01	0.65 ± 0.08	0.104 ± 0.007
D. Coal	D05	2.47 ± 0.12	14.63 ± 0.77	0.072 ± 0.008
H. Pumice	H06	3.21 ± 0.12	22.16 ± 1.11	4.106 ± 0.191
H. Gypsum	H07	0.13 ± 0.01	0.44 ± 0.08	0.100 ± 0.007
H. Coal (S.A)	H08	2.39 ± 0.13	14.34 ± 0.79	0.077 ± 0.009
H. Coal (L)	H09	2.31 ± 0.12	14.92 ± 0.77	0.260 ± 0.014

The elemental concentration in ppm, measured in pumice samples from the three cement factories exceeds the normal conditions of radioactive materials concentrations in igneous rocks which was given in section 2.1.1.2. ^{238}U measured to a maximum value of $6.32 ppm$, where ^{232}Th measured to a maximum value of $26.445 ppm$. The existence of ^{40}K in pumice sample of a kilo gram also ranges up to 4.106% as shown in Fig. 4.8 below. The elemental concentration in gypsum samples were observed very low, which is even less than $1 ppm$ for ^{238}U and ^{232}Th, and 1% for ^{40}K as seen in Fig:4.8.

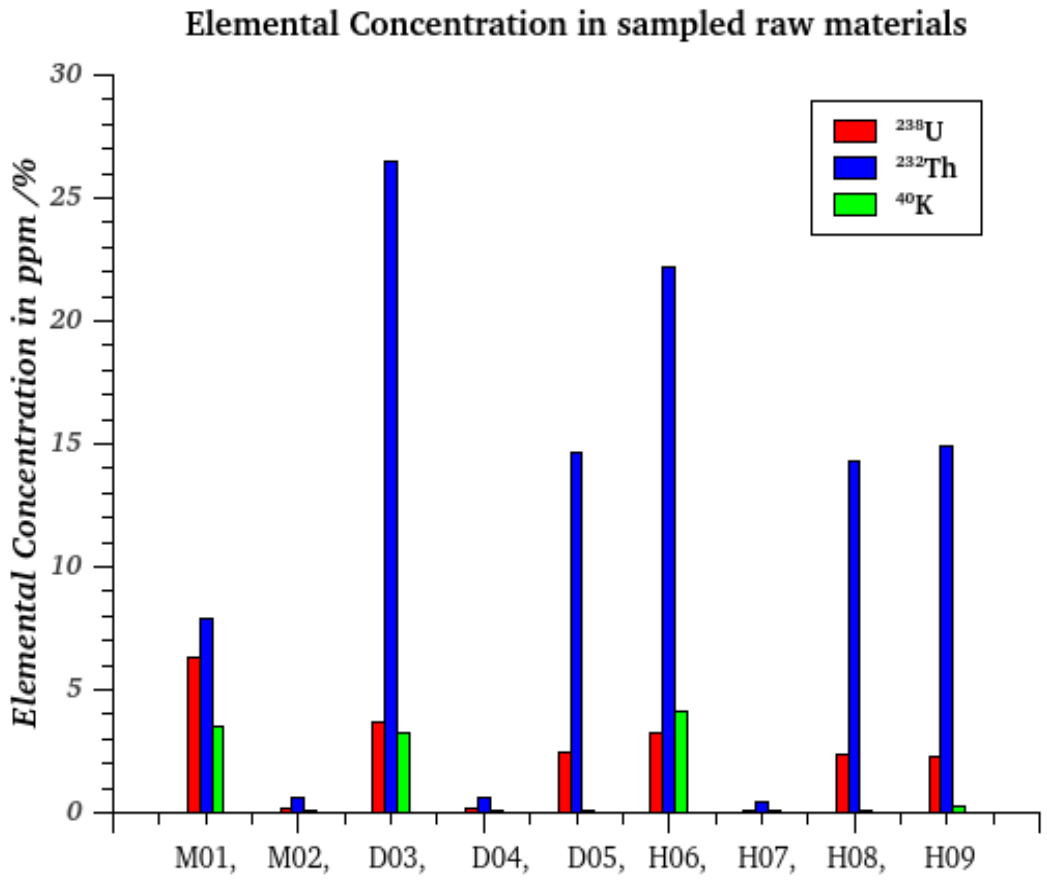

Figure 4.8: ^{238}U, ^{232}Th and ^{40}K elemental concentrations in additive cement raw materials

In collected coal samples the concentrations of long living natural radioactive elements were investigated higher than the average limit in igneous rocks as given by [12]. It is clear as given in Eq. 3.9, more activity concentration will produce more elemental concentration.

The possible health hazard measuring (indicating) parameters (indices), given in Eq. 3.10, 3.11, 3.13 and 3.14 were given in table 4.5 below to estimate the risks from radiation sources from cement additive raw materials.

Table 4.5: Calculated radiological hazard indices in samples of additive cement raw materials, M for Mugher cement factory, D for Dangote cement factory and H for Habesha cement factory

Sample Name	Sample Code	R_{eq} in $\frac{Bq}{Kg}$	D_R in nGy/hr	H_{ex}	H_{in}
M. Pumice	M01	208.46 ± 10.22	100.54 ± 4.90	0.56 ± 0.028	0.77 ± 0.038
M. Gypsum	M02	8.14 ± 1.00	3.79 ± 0.45	0.022 ± 0.003	0.03 ± 0.003
D. Pumice	D03	278.98 ± 13.22	130.93 ± 6.21	0.753 ± 0.036	0.88 ± 0.040
D. Gypsum	D04	8.61 ± 0.82	4.04 ± 0.38	0.023 ± 0.002	0.03 ± 0.003
D. Coal	D05	117.32 ± 6.22	51.08 ± 2.72	0.32 ± 0.016	0.40 ± 0.021
H. Pumice	H06	268.04 ± 12.68	128.80 ± 6.08	0.72 ± 0.034	0.83 ± 0.038
H. Gypsum	H07	6.58 ± 0.79	3.16 ± 0.36	0.018 ± 0.002	0.02 ± 0.002
H. Coal (S.A)	H08	114.78 ± 6.39	49.98 ± 2.80	0.31 ± 0.017	0.39 ± 0.022
H. Coal (L)	H09	121.65 ± 6.33	53.53 ± 2.79	0.33 ± 0.017	0.41 ± 0.021

Radium equivalent activity values in the measured samples have not crossed the value given by [45], $370 Bq/Kg$. Since those raw materials are partially managed by human body, dusts from raw materials can easily get a physical contacts and even can induce radiation dose at $1m$ distance from human body. In the studied samples, specially pumice samples, the possible induced radiation dose at $1m$ distance were observed twice as the limit given in section 3.2.6, $59 nGy/hr$. These can create some radio-health problems on human in the factories and even to the communities near mining area of these raw materials. For the remaining samples, coal and gypsum, it was observed in a range of world permissible value.

The internal and external hazard indices from these samples shows higher reading. If one worker from the factory got the value of indices listed in table 4.3, it may be difficult, because he/she can accumulate from other environmental areas and can easily cross the boundary limit, i.e 1.

4.3 Measurements of Natural Radioactivity Levels and Associated Health Hazard Indices in Portland Cements Using HPGe Detector

4.3.1 Introduction

Building materials, like cement, may contain various amounts of radiation sources, like cosmic and primordial radiation sources which are originated from different atmospheric layers and Earths crust [58].

The cosmic radiations which may happen in cement, like ^{22}Na, ^{14}C, ^{3}H, have short lifetime as compared with primordial radiation sources. Primordial radiation sources, which are expected in cements are long living, naturally occurring radio nuclides of uranium (^{238}U), thorium (^{232}Th) and their decay products, and the radioactive isotope of potassium (^{40}K). The two sources of radiations in cements can contribute to environmental radioactivity mainly in two ways, external and internal exposure. The external radiation exposure is caused by gamma radiation originating from (^{226}Ra), (^{232}Th) and their progenies, and (^{40}K). However, the internal radiation exposure is due to short-lived daughter product of radon (^{222}Rn) after the decay of radium, (^{226}Ra). This can be a permanent sources of internal radiation by sticking and accumulating themselves in respiratory systems and lung respectively. Decay product of (^{222}Rn), (^{218}Po) can also do same thing as (^{222}Rn) [58–60].

There has been an increasing demand for cement throughout the world due to the increasing of human civilization. In the present study, the analysed samples are mainly of Ordinary Portland cement (OPC), Pozzolana Portland Cement (PPC) and semi-processed cement called Clinker of brands shown in Fig. 4.9.

(a) Mugher cement

(b) Dangote cement

(c) Habesha cement

(d) Mosobo cement

Figure 4.9: Brands of collected cements samples from open market and factories

The products of five (5) cement factories, including Derba cement factory, covers almost all parts of the country and exported to some neighbour countries, like Kenya, Somali and others. There are other cement factories in the country, and all of them are producing Portland cements which is a basic ingredient of concrete, mortar, stucco and the like as a construction materials [61].

In factories, cements are made from grinded clinker and some additive raw materials discussed in section 4.2. Clinker is made by burning of a mixture of limestone, clay, and sandstone discussed in section 4.1 at high temperatures, $(1,300^oC)$, [62]. All, the main and additive raw materials are from the earth crust, that may contain fragments from igneous

and metamorphic rocks. Such rocks are rich in radioactive materials and can be a factor for the presence of radioactive materials in cements. In fact, the study in section 4.1 and 4.2 indicates final product or Portland cement gets radioactive materials from main raw materials and additive raw materials [61].

We collected samples of study, OPC, PPC and Clinker from market, and three factories, Mugher Cement Factory (under chemical industry) Gov., Dangote Cement Factory (Ethiopia branch) Plc., and Habesha Cement Factory, SC, at a distance of 90-KM, 83-KM and 40-KM respectively in West Shoa, Oromia regional state, Ethiopia as seen in Fig. 3.8. These factories were planted in the north-western direction of the capital city, Addis Ababa, which are seen in Fig. 4.10.

(a) Mugher Cement Factory, Gov.

(b) Dangote Cement Factory, Ethiopia, Plc.

(c) Habesha Cement Factory, SC.

(d) Cement at market

Figure 4.10: OPC, PPC and Clinker sampling areas

Portland Cement (PC) is a finely grinded, soft, powdery-type substance, mainly used to bind fine sand and coarse aggregates together in concrete. PC can be named by different names based on the grade given for them on their pressure resisting strength. We used

Ordinary PC and Pozzolana PC which is graded as 42.5N and 32.5N respectively. This is from raising or lowering the amount of limestone $(CaCo_3)$ added as main raw material, which means more limestone will take to OPC and other higher grade cements like 52.5N, and low limestone will produce PPC and any other lower grade cements [63]. As this raw material raised or lowered, the corresponding radioactive materials in limestone also raised and lowered.

Intermediate product, clinker, is basically a mixture of main cement raw materials. These raw materials are mixed with each other according to the cement grade they want to produce, and heated to a temperature more than $1,300^0C$.

Therefore, keeping in view the natural risks of radiations, it is necessary to measure the natural environmental radiation levels and this study will measure the radiation levels in cements and semi-processed cements used for making of dwellings and other constructions.

4.3.2 Result and Discussion

From the collected and prepared samples of Portland cements, spectra of each samples were recorded by using HPGe detector cascaded with the necessary electronic devices, DSA. From the observed spectra, energies representing daughters of long living radioactive materials and direct representing energy for ^{40}K were clearly identified.

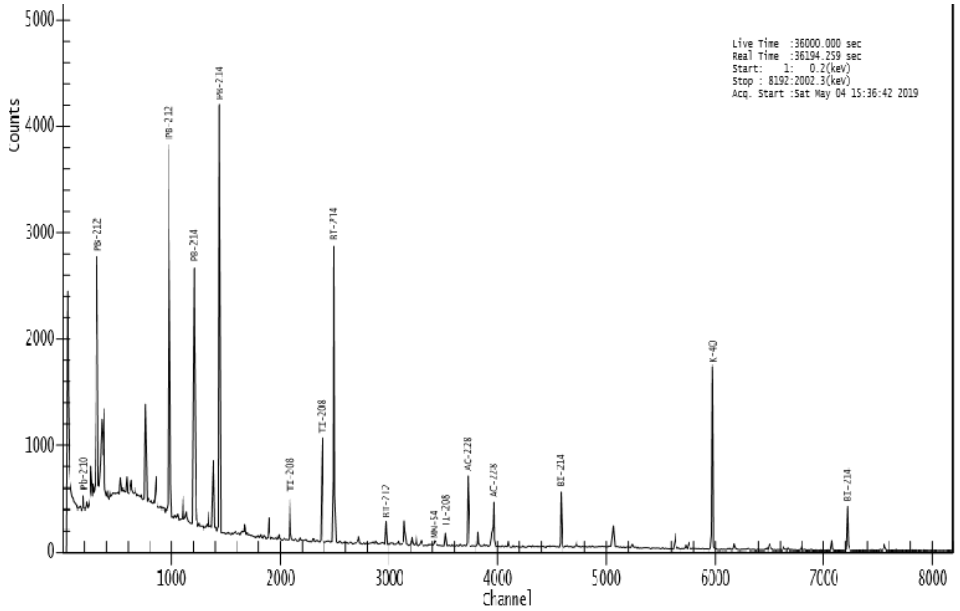

(a) Spectrum from Mugher PPC

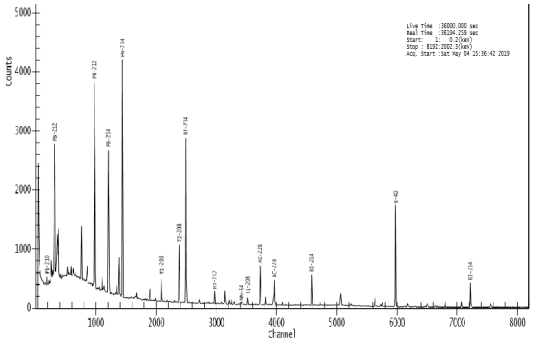

(b) Spectrum from Dangote OPC

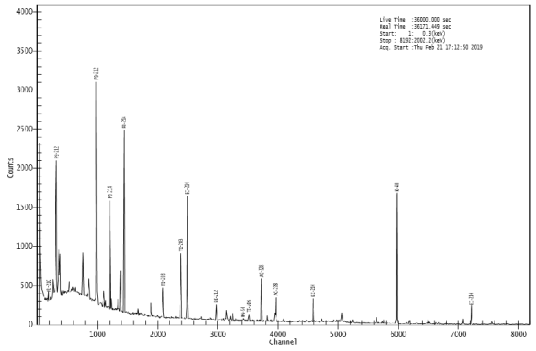

(c) Spectrum from Mugher Clinker

Figure 4.11: HPGe output Spectrums from some samples

The spectra in above figure were recorded for all collected Portland cements and activity concentrations for ^{238}U, ^{232}Th and ^{40}K were calculated, which are presented in table 4.6 below.

Table 4.6: Activity concentrations of natural radio nuclides in Bq per Kg for Portland cements and Clinker samples, M for Mugher, D for Dangote and H for Habesha cement factory

Sample Code	Sample Name	^{238}U $\frac{Bq}{Kg}$	^{232}Th $\frac{Bq}{Kg}$	^{40}K $\frac{Bq}{Kg}$
M01	Clinker	36.42 ± 1.51	32.19 ± 1.56	149.78 ± 6.68
M02	OPC	34.34 ± 1.65	31.18 ± 1.59	172 ± 7.98
M03	PPC	31.63 ± 1.46	39.49 ± 2.00	369.71 ± 16.94
D04	Clinker	22.58 ± 0.85	19.62 ± 0.98	101.96 ± 4.67
D05	OPC	20.53 ± 0.85	18.84 ± 0.99	102.35 ± 4.90
D06	PPC	27.54 ± 1.26	45.87 ± 2.30	333.25 ± 15.24
H07	Clinker	27.45 ± 0.95	30.51 ± 1.44	107.61 ± 4.79
H08	OPC	30.53 ± 1.45	34.14 ± 1.76	120.66 ± 5.90
H09	PPC	26.46 ± 1.11	30.60 ± 1.56	307.57 ± 13.91
Derba	PPC	28.57 ± 1.34	41.19 ± 2.03	334.66 ± 14.97
Mosobo	PPC	25.00 ± 0.94	30.00 ± 1.50	180.00 ± 8.20

The activity concentrations of ^{238}U, ^{232}Th and ^{40}K in partially processed and final products of Portland cements presented in table above shows below the world average values given for building materials, $50B/Kg$, $50B/Kg$ and $500B/Kg$ respectively [64]. To the environment, the certified world natural radioactivity concentration limit is $35Bq/Kg$, $30Bq/Kg$ and $400B/Kg$ for ^{238}U, ^{232}Th and ^{40}K respectively. Some activity concentrations measured in the collected samples crossed the permissible environmental activity values.

Clinker, the partially processed Portland cement is a mixture of limestone, sandstone and clay rock after heated by a temperature around 1300^oC. Therefore, the natural radioactivity concentration in clinker samples is the same as in the three main raw materials, lime, sand and clay. Out of these raw materials the first two are under the category of sedimentary rock in which concentrations of the three natural radioactive materials are low in concentration. So the concentrations of natural radioactive materials in clinker can be raised by clay rock since it is a part of igneous rock, which is rich in radioactive materials [12, 21]. In the measured value of activity in clinker samples, all recorded values were seen below the environmental permissible value listed in above, except for sample coded as $M01$. This may be from the more proportion of clay raw materials used during cement processing. In fact, in heating of the three main raw materials after mixing, coal used as energy source, and it's

slag can be easily added to clinker samples. Therefore, impurities in coal can also contribute in the concentrations of natural radioactivity in clinker.

Ordinary Portland Cement, (OPC) is a finally processed Portland cement in the factories. It is almost the same with clinker with a small amount of some additive raw materials. These additive raw materials, like volcanic ash can increase the levels of natural radioactivity in OPC. In measured values, these facts were seen for some OPC samples in which the levels of activity concentration is slightly greater than that of clinker. The three factories understudy have been using volcanic ash/pumice from the great rift valley in east Africa. This region is full of active volcano and radioactive materials easily comes to the top surfaces of the earth. So raw materials from such area will increase the activity concentrations of final products.

Pozzolana Portland cement, (PPC) is another lower grade cement produced in the factory under study. Its quality is lowered by adding more additive raw materials to clinker. This is to increase the quantities of cement and its adhesive property. The additive raw materials are mainly volcanic ash, gypsum and slags of coal. These materials are rich in radioactive materials from their geological and geochemical formations, may be gypsum can show low radioactive concentrations due to its more water contents. Therefore, the activity concentrations of natural radioactive materials in PPC samples were seen higher as compared to OPC and clinker, specially for ^{232}Th and ^{40}K. The ^{232}Th activity concentration in PPC crosses the environmental permissible limit, $30Bq/Kg$ as shown in Fig. 4.12.

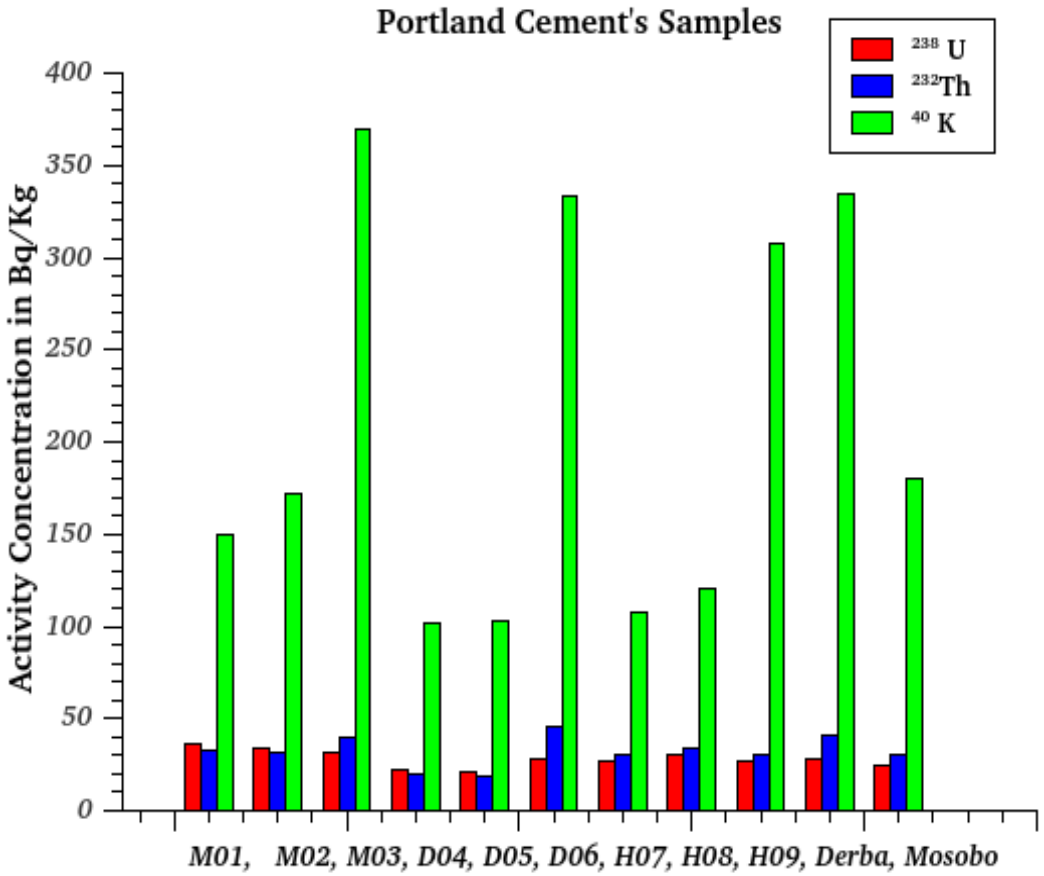

Figure 4.12: ^{238}U, ^{232}Th and ^{40}K activity in sampled types of Porland Cement

The natural radioactivity concentration in cement at Pakistan, Brazil, Grece, India, Iran and other countries [64], show almost similar findings as presented in table 4.6 and fig 4.12.

In table 4.7, maximum value of Ra_{eq} was recorded for PPC cement sample. The more activity concentration will give more Ra_{eq} as seen in Eq. 3.10. This value does not cross the world average value given in [45], at a distance of $1m$ from homogeneously distributed ^{238}U, ^{232}Th and ^{40}K, $370Bq/Kg$. In the same way, induced dose rate from these radioactive materials were not above the limit, which was calculated using Eq. 3.11 for almost same activities of ^{238}U, ^{232}Th and ^{40}K.

Table 4.7: Activity related radiological hazard indices in Portland cements of one kilogram M for Mugher, D for Dangote and H for Habesha cement factory

Sample Name	Sample Code	R_{eq} in $\frac{Bq}{Kg}$	D_R in nGy/hr	AD_R in mSv/yr	H_{ex}	H_{in}
M01	Clinker	93.98 ± 4.26	42.05 ± 1.90	0.052 ± 0.0023	0.26	0.35
M02	OPC	92.17 ± 4.54	41.48 ± 2.04	0.051 ± 0.0025	0.25	0.34
M03	PPC	116.57 ± 5.62	54.00 ± 2.60	0.066 ± 0.0032	0.31	0.40
D04	Clinker	58.42 ± 2.61	26.25 ± 1.17	0.032 ± 0.0014	0.16	0.22
D05	OPC	55.35 ± 2.64	24.90 ± 1.19	0.031 ± 0.0015	0.15	0.20
D06	PPC	118.79 ± 5.72	54.67 ± 2.63	0.067 ± 0.0032	0.32	0.40
H07	Clinker	79.36 ± 3.38	35.36 ± 1.51	0.043 ± 0.0012	0.21	0.29
H08	OPC	88.64 ± 4.42	39.49 ± 1.97	0.048 ± 0.0024	0.24	0.32
H09	OPC	93.90 ± 4.41	43.59 ± 2.04	0.054 ± 0.0025	0.25	0.33
Derba	PPC	113.24 ± 5.40	52.25 ± 2.48	0.064 ± 0.0030	0.30	0.38
Mosobo	PPC	81.76 ± 3.72	37.10 ± 1.69	0.045 ± 0.0021	0.22	0.29

Annual dose rate presented in table 4.7, were calculated using Eq. 3.12 considering the 20% outdoor radiation exposure from ^{238}U, ^{232}Th and ^{40}K. The remaining percent, 80% is a time considered for indoor duration. The samples of study, cement materials are mainly used for construction of dwellings and exposure can be raised to 80%. Therefore, the calculated value of AD_R in table 4.7 can be increased by four, (4) times. So the maximum value of AD_R for sample coded as $D06$, which is a PPC sample collected from Dangote cement factory, would be $0.27 mSv/yr$. The maximum annual value, permissible value is $2.4 mSv/yr$ as explained in section 3.2.6. External and internal hazard indices were not crossed the world average limit value, and maximum values were recorded 0.32 and 0.40 respectively. The internal hazard indices value is more than that of external due to radon gas from ^{238}U decay series, which is ^{222}Rn and ^{218}Po.

4.4 Investigations of Natural Radioactivity Levels and the Radiation Hazard indices in Floriculture Soil Using NaI(Tl) Detector

4.4.1 Introduction

Measurements of environmental natural radioactivity level will create an awareness for human beings to protect themselves from hazardous radiations. In most cases the levels are raised by the activities of human beings at different industrial areas and other places. Floriculture industry is one of the like places in which factors increasing the levels of environmental radiations are frequently used. The industry had been using excess, several types of fertilizers fabricated from similar sedimentary rocks, used for cement production, by adding of sulphuric acid and nitric acid [65].

By the processes, the two known types of fertilizers, Triple Super Phosphate (TSP) and Di Ammonium Phosphate (DAP) can be produced. The natural phosphates from sedimentary represent about 85% of fertilizer [66]. Such, fertilizers usually employed in the agricultural fields, contain traces of heavy metals and naturally occurring radionuclide, such as potassium, thorium and uranium with their decay products. Out of these radioactives, Uranium takes more concentration than remaining natural radiation sources [67].

The interested floriculture farms in this study had been using TSP and DAP fertilizers, and chemicals, more than two times per year to increase the productivity of flowers as interviewed with some employee. Such fertilizers from sediment (Lime and sand stone explained in section 4.1) are coming with naturally existing radioactive materials, and workers of the fields has the chance of getting radiations from fertilizers and chemicals used for flowers. Some studies had been done on floriculture industries and reports; floriculture industries have social and environmental impacts due to the uses of fertilizers and chemicals.

In Sebeta Floriculture, near by our area of study, 74.9% of the workers were females, with 93% of study subjects showing at least one health symptom. 67.8% had at least one skin problem and 81.1% had at least one respiratory health symptom in 12 months. These symptoms had been observed on those who did not have full personal protective equipment [68].

Many diseases such as Methemoglobinemia, Japanese encephalitis (JE), cancer etc, have been noted due to the use of chemical fertilizers [69].

Chemicals and fertilizers used for floriculture industries have a different character and

react differently when they applied to the soil and affect its texture, acidic value, and fertility by destroying nitrogen-fixing bacteria and many other micro- and macro- organism of the soil [68].

The floriculture industry were taken as a solution for economic development and the generation of employment, these advantages of the industry are at the expense of social and environmental disadvantage [70].

According to these reports, the social and environmental symptoms of health risks should be from fertilizers and chemicals used in the fields by actual contacts and radiations from them. In fact, the reports did not specify the specific consequences of those health risks.

The study area is near Holeta town, located at 30Km to the western part of the capital city of the country, Addis Ababa. Globally it is covering 1 KM radius to the Lat. $9^0, 04.2828^{'}$N and longtd. $38^0; 31.135^{'}$E in a maximum inaccuracy of $\pm 8m$.

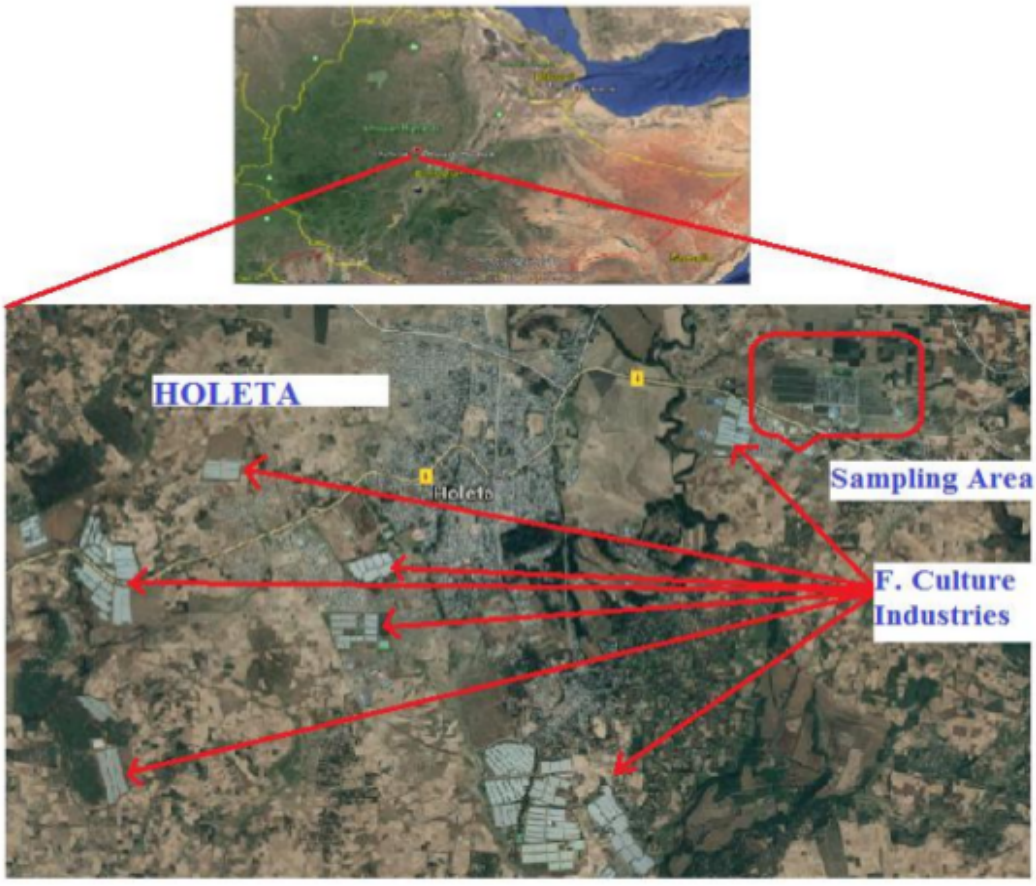

Figure 4.13: Holeta town and Its surroundings referring the sampling areas and floriculture industries (Satellite image taken from Google map)

The study area consists of fertile soil, basically local farmers have been using for the production of cereal crops. Farmers started using fertilizer since 1980s, as residents of the

area speaks. In nature, the soil types in the study areas are the same and variations of concentrations of radioactive materials may not be expected to the exaggerated difference. To see the effects of fertilizers in increasing of natural radioactivity concentrations, we used samples from normal farm land used by local farmers and virgin lands from the area.

4.4.2 Result and Discussion

The following spectra in Fig. 4.14, are the measured spectra from floriculture sample and virgin land sample.

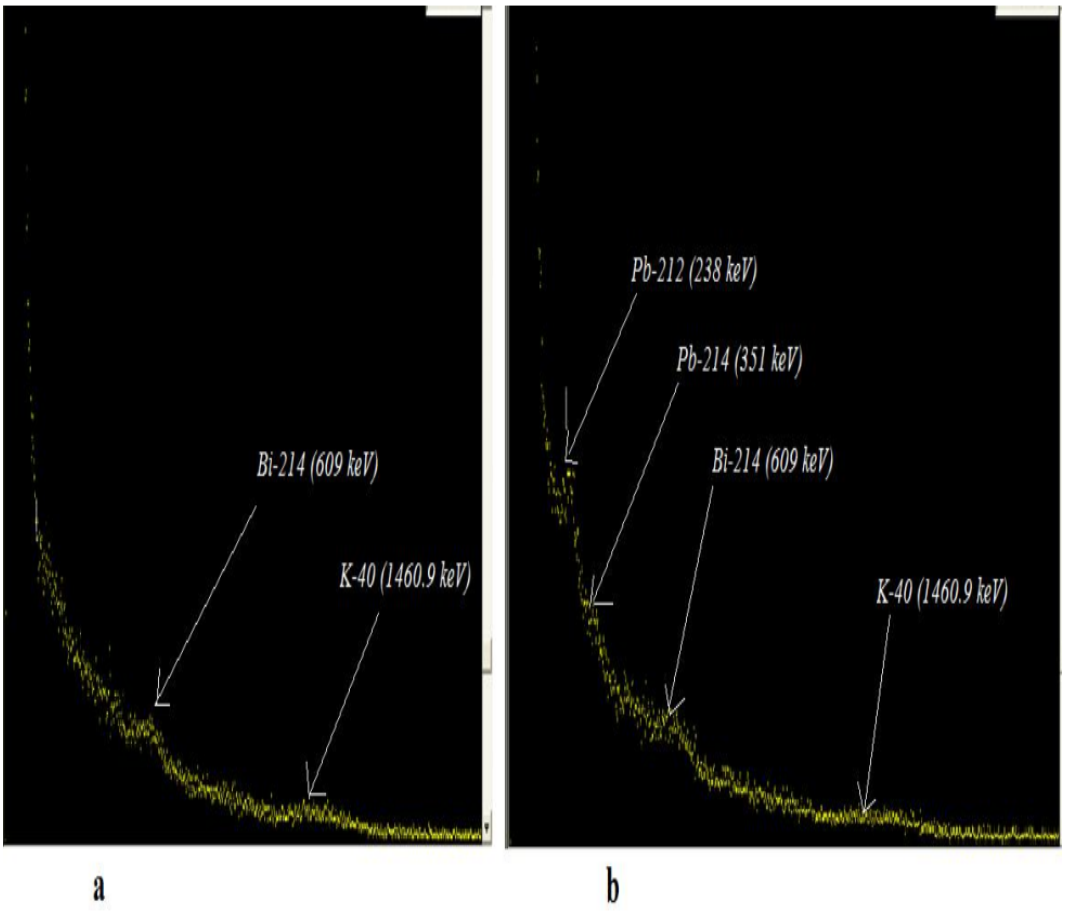

Figure 4.14: NaI(Tl) output Spectra from floriculture and farm soil samples

The activity concentration for natural radioactive materials for samples collected from floriculture, farm land and virgin land were calculated for each of the collected samples, at 20 cm depth using Eq. 3.8. These values are presented in table 4.8 below.

Table 4.8: The activity concentration levels of natural radionuclides per Kg sampled from Virgin, Agricultural and Floriculture soil, near Holeta town.

Sample Cite	Sample Code.	^{238}U $\frac{Bq}{Kg}$	^{232}Th $\frac{Bq}{Kg}$	^{40}K $\frac{Bq}{Kg}$
Virgin Land	1	34.98 ± 4.60	12.21 ± 0.67	73.27 ± 14.65
	2	26.04 ± 2.68	16.83 ± 1.55	127.31 ± 13.34
Agricultural Land	3	137.50 ± 12.42	—	272.97 ± 23.53
	4	130.20 ± 16.30	—	302.67 ± 26.82
F.Culture Land	5	122.18 ± 3.44	—	282.44 ± 20.84
	6	83.80 ± 8.62	7.64 ± 0.45	274.24 ± 20.78
	7	169.43 ± 14.38	8.00 ± 0.29	360.40 ± 21.20
	8	138.84 ± 13.72	—	214.12 ± 17.13
	9	197.18 ± 16.88	—	166.89 ± 20.35

The elemental (radioactive) concentrations of ^{238}U, ^{232}Th and ^{40}K in the three sites, virgin, agricultural and floriculture soils shows variations as compared with each other as in table 4.9.

Table 4.9: The elemental concentration of natural radioactives sampled from Virgin, Agricultural and Floriculture soil, near Holeta town.

Sample Cite	S. Code	^{238}U in ppm	^{232}Th in ppm	^{40}K in %
Virgin Land	1	2.83 ± 0.37	3.00 ± 0.16	0.23 ± 0.046
	2	2.11 ± 0.22	4.14 ± 0.38	0.40 ± 0.042
Agricultural Land	3	11.14 ± 1.01	—	0.86 ± 0.074
	4	10.55 ± 1.32	—	0.95 ± 0.084
F.Culture Land	5	9.90 ± 1.09	—	0.89 ± 0.065
	6	6.79 ± 0.70	1.88 ± 0.11	0.86 ± 0.065
	7	13.72 ± 1.16	1.97 ± 0.07	1.13 ± 0.066
	8	11.25 ± 1.11	—	0.67 ± 0.054
	9	15.97 ± 1.37	—	0.52 ± 0.064

The elemental concentrations were calculated based on Eq. 3.9, and values are showing maximum for uranium concentration and non exaggerated for thorium and potassium concentrations, which are in agreement with ideas in section 4.4.1.

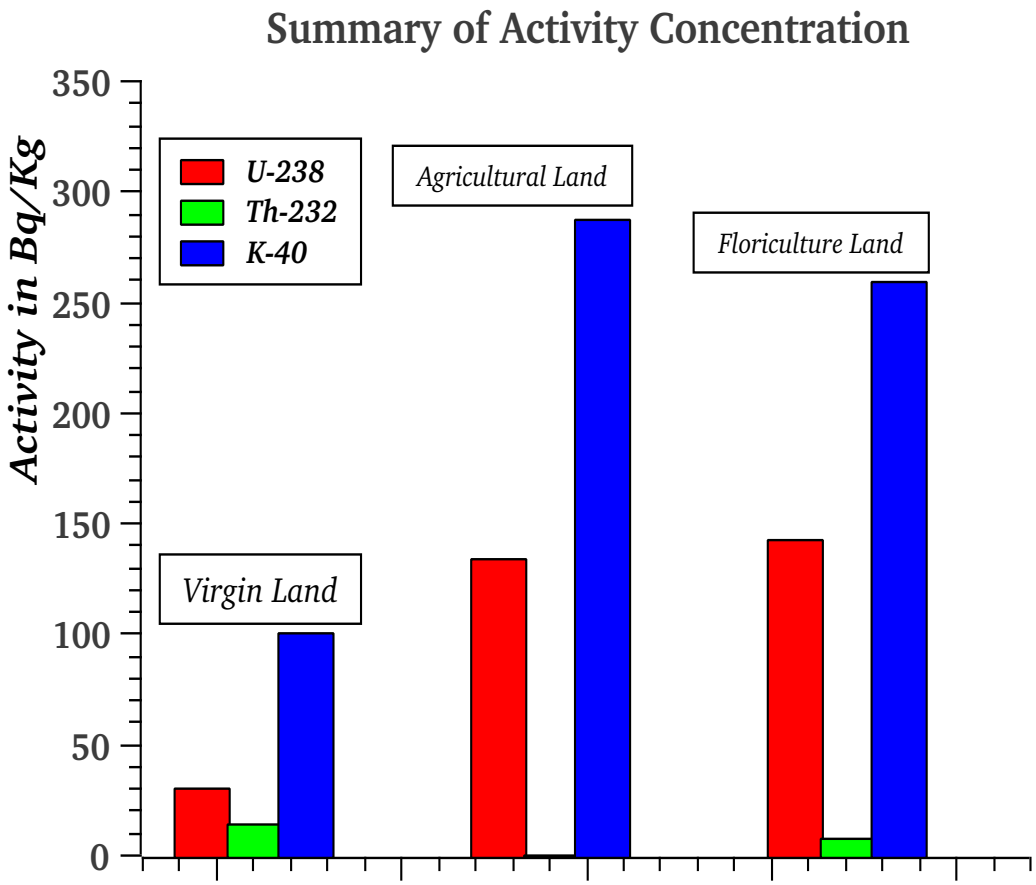

Figure 4.15: Histogram showing Activity concentrations of ^{238}U, ^{232}Th and ^{40}K in the three sites.

The average concentration of ^{238}U in virgin soil samples are less than that of agricultural soil samples for the same soil type and geological structures, homogeneously igneous clay type. In the agricultural soil samples, it is less than that of floriculture soil. Here the age of soils in getting fertilizers is longer than floriculture land, but the frequency of getting fertilizers and amount of fertilizers is the possible factor in raising concentration of ^{238}U.

The average concentration of ^{40}K is below the recommended value given by [45] in the whole samples of study. But it is more for the area that has been exposed to fertilizers. The remaining radio isotopes (^{232}Th) is Below Detection Limit (BDL) in agricultural land and very far from the recommended value.

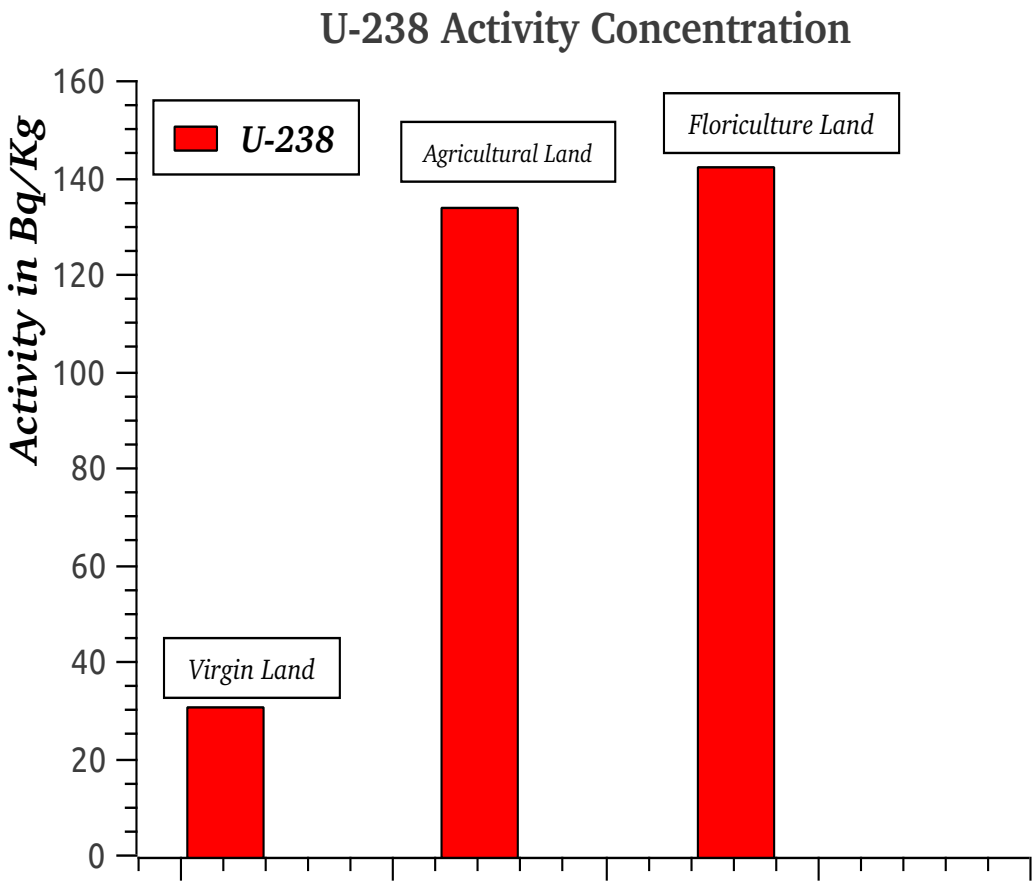

Figure 4.16: Histogram showing Activity concentration of ^{238}U in Virgin land, Agricultural land and Floriculture land.

The recommended reference levels of ^{238}U, ^{232}Th and ^{40}K in environmental soils are 35, 30 and 400 Bq/kg, respectively [45]. The average concentrations of ^{238}U obtained in the present study for agriculture and floriculture becomes 2.77 to 6.57 times of its permissible value. This may cause serious health problems as studied by [68, 69] in section 4.4.1.

In the area where the concentration of short and long living gamma emitters are maximum, all health problems reported in section 4.4.1 are expected. Not only gamma radiation, the problems can also happen from any ionizing radiations if the dose limit is above tissue weighting factors, crosses the limit.

The elemental concentrations in table 4.9 increases with the activity concentrations. The permissible ^{238}U concentration in environmental sample is from $2ppm$ to $4ppm$ and measured values in farm and floriculture land is more as activity concentrations.

The area is not safe even after the investor leave the places as shown in figure below.

Figure 4.17: Unsafe grazing of cattle in floriculture industry.

In the below table, hazard assessments indices are presented, which are useful for radiation hazard assessments.

Table 4.10: The radium equivalent (Ra_{eq}), absorbed doses (D_R), annual dose rate (D_R) the external (H_{ex}) and internal (H_{in}) hazard index of soil samples collected from Virgin, Agricultural and Floriculture near Holeta town

S. Code	R_{eq} in $\frac{Bq}{Kg}$	D_R in nGy/y	AD_R in mSv/y	H_{ex}	H_{in}
1	58.08 ± 2.86	25.69 ± 1.64	0.032	0.157	0.252
2	59.91 ± 2.36	27.07 ± 1.36	0.033	0.161	0.232
3	158.52 ± 12.55	70.45 ± 5.40	0.086	0.429	0.800
4	153.51 ± 16.43	68.61 ± 7.05	0.084	0.415	0.767
5	143.93 ± 13.53	64.31 ± 5.81	0.079	0.389	0.719
6	115.84 ± 4.26	52.33 ± 2.44	0.064	0.312	0.539
7	208.62 ± 5.94	92.83 ± 3.38	0.110	0.564	1.022
8	155.33 ± 13.78	68.49 ± 5.91	0.084	0.419	0.794
9	210.03 ± 16.95	91.38 ± 7.26	0.113	0.568	1.101

The above hazard measuring indices in soil samples from virgin lands were observed as low as compared to the world permissible values. For the case of agricultural land, samples 3 and 4, fertilizers were given to the land once per year or once in two years for the production of cereal crops. The R_{eq}, D_R, AD_R, H_{ex} and H_{in} in the samples taken from these sites are more than that of virgin land. The geographical and soil type of the two sites are almost the same. The difference can be from TSP and DAP fertilizers.

In the case of floriculture land, investors had been using fertilizers more than two times per year for the same floriculture farm. This condition increases the concentrations of radioactive materials in the soil artificially. Hazard indices in table 4.10 are higher than the values in other sites of study, virgin and agricultural land. In the long processes, this will produce a radioactive environment which can be difficult for the survival of human being.

In the site of study, workers stays for a minimum of 10-hours per day. In the calculation we used 20% for environmental exposure. But those workers will get more than 45% per day. This will increase the values of AD_R reported in table 4.10. This may cause the problems reported by [68, 69] in section 4.4.1.

As high radiation exposure rate affect human beings, it also affects microorganisms available in the soil. Microorganisms are essential organisms for the natural fertility of soil. According to [67], more fertilizers can reduces nitrogen fixing bacteria in a soil, which means acidic level of soil will increase. In general, as more fertilizers used in floriculture farm, more radioactive materials are added to the soil. This situation will be at the expense of social and environmental disadvantage [70].

5

Conclusions and Recommendations

5.1 Conclusions

The activity concentrations of primordial natural radio nuclides and their radiological health hazards indices in different types of cement and their raw material samples taken from Mugher, Dangote and Habesha cement factories in Ethiopia were measured using gamma ray spectroscopy coupled with HPGe detector. In addition, environmental samples which are exposed to materials made from cement's raw materials, fertilizer enriched soil samples from floriculture industry were also measured using gamma ray spectroscopy coupled with NaI(Tl) detector. Samples of cement's raw materials were categorized in two groups as main raw materials (Limestone, Sandstone and Clay rock) and additive raw materials (Pumice, Coal and Gypsum).

The average values of measured activity concentrations for ^{238}U, ^{232}Th and ^{40}K in limestone and sandstone samples are lower than the given world certified values, $35Bq/Kg$, $30Bq/Kg$ and $400Bq/Kg$ respectively. For clay rock samples, activity concentrations were measured almost higher than these limits. The radiation hazard indices from limestone and sandstone were also less than the world permissible value, due to their direct relations with measured activity values as given in section 3.2.6. For clay samples, absorbed dose rate crosses the world average limits even the limit given for building materials, $50Bq/Kg$, $50Bq/Kg$ and $500Bq/Kg$ for ^{238}U, ^{232}Th and ^{40}K respectively.

For additive raw material samples, pumice and coal samples, the activity concentrations of primordial natural radioactivity in above have crossed the world certified values. Transporting such radioactive environmental soils/minerals from mining to factories and using as a factory raw materials, can affect the rest of environmental areas under normal conditions by releasing energetic particles. Such radioactive environmental soils/minerals can produce a problem on human health by long term effects. Mixing such materials with other cements raw materials and producing a final product of cement also raise the radiation levels of cement, which are not good for humans/life's health.

The activity concentrations and health hazard indices measured in cement's samples were similar to findings reported by other investigators [58–62] from different parts of the world. In some final products, PPC samples, activity concentrations crossed the worldwide given permissible values. The main contributors to the overall specific activities in cement were attributed to volcanic ash and slags from coal as and additive raw materials.

For environmental soil samples from floriculture industry and nearby environmental soil samples, activity concentrations of natural radionuclide measured for floriculture soil samples were greater than virgin and agricultural soil samples under the same conditions. This can be from the phosphate fertilizers added to floriculture soil. In phosphate fertilizers, sedimentary rock cover more than 80% in which it is with natural radioactive materials as studied in section 4.1 for main cement's raw materials.

5.2 Recommendations

This study, dissertation has recommendations based on the findings, for cement factories and for responsible sectors on environmental biosphere near mining areas.

The average radioactivity levels measured in main cement's raw materials were with in safe limit as given for building materials. Additive raw materials like pumice and slags from coal minerals will raise the activity concentrations. If these additive raw materials are carefully monitored, the activity concentrations in final product of cement can be more safe for use as a building material. Other hazard indices from corresponding radio nuclides are with in the safe limit, and it is possible to use in construction without exceeding the world proposed radioactivity concentration levels.

It is interesting to recommend sectors responsible for mining and/or industries to give attention for human life, well inspections of working areas and take a care for the natural environments. Finally, industry management strategy should be implemented to avoid radiological negative impacts of the industry's raw materials and final products, and this study can be used as a baseline for the other similar works.

Bibliography

[1] A. H. M. Saadat et. al., (2013), Assessment of Natural Radioactivity and Radiation Hazard in Soil Samples of Rajbari District of Bangladesh, Jahangirnagar University Environmental Bulletin, Vol.2, 1-8, ISSN:2304-3326.

[2] A. Stochioiu, et. al., (2013), Environmental radioactivity assessment studies on placement area of the new extreme light infrastructure nuclear physics facility, Rom. Journ. Phys., Vol. 59, Nos. 78, P. 808816.

[3] Contemporary Physics Education Project (CPEP), (2018), Nuclear ScienceA Guide to the Nuclear Science Wall Chart, Chapter 3, Radioactivity.

[4] I. Hossain, et, al, (2012), Efficiency and resolution of HPGe and NaI(Tl) detectors using gamma-ray spectroscopy, Scientific Research and Essays Vol. 7(1), pp. 86-89, DOI: 10.5897/SRE11.1717.

[5] N. Todorovic, et, al, (2015), Natural radioactivity in raw materials used in building industry in Serbia, Int. J. Environ. Sci. Technol. 12:705716 DOI 10.1007/s13762-013-0470-2.

[6] Linnea E. Wahl, (2010), Environmental Radiation, Health Physics Society Specialists in Radiation Safety.

[7] Erol Kam, et. al., (2011), A Study of environmental radioactivity measurements for cankiri, turkey, Radiation Protection Dosimetry, pp. 17, doi:10.1093/rpd/ncr416.

[8] M.O. Isinkaye, et. al., (2018), Evaluation of radiological hazards due to natural radioactivity in bituminous soils from tar-sand belt of southwest Nigeria using HpGe-Detector, International Journal of Radiation Research, Volume 16, No 3.

[9] Boris Vakanjac, et. al., (2018), Natural Radioactivity of Intrusive-Metamorphic and Sedimentary Rocks of the Balkan Mountain Range (Serbia, Stara Planina), Minerals, 8, 6; doi:10.3390/min8010006.

[10] Laith Ahmed Najam, et. al., (2017), Evaluation of natural radioactivity in Selected Soil Samples from the Archaeological of Ur City by using HPGe detector, WSN 62 79-92.

[11] Khalil Mohammed Thabayneh, et. al., (2014), Measurement of activity concentration levels of radionuclides in soil samples collected from Bethlehem Province, West Bank, Palestine, Turkish Journal of Engineering & Environmental Sciences, 38: 113 125, doi:10.3906/muh-1303-8.

[12] Stanley S. Johnson, (1991), Natural radiation, Virginia division of mineral resources, Volume 37, No. 2, pp. 1-8.

[13] Canadian Nuclear Safety Commission (CNSC), (2012), Introduction to Radiation, Minister of Public Works and Government Services Canada (PWGSC) PWGSC catalogue number CC172-93/2012E-PDF ISBN 978-1-100-21572-3.

[14] Brian D. Amiro, (2002), Environmental Radioactivity, Encyclopedia of Physical Science and Technology, Third F..dition, Volume 5.

[15] http://weppi.gtk.fi/publ/foregsatlas/text/U.pdf

[16] J.A.H. Oates, (1998), Formation, Classification and Occurrence of Limestone, Lime and Limestone: Chemstryand Technology, Production and Uses.

[17] Michalis Tzortzis, et. al, (2012), Gamma-ray measurements of naturally occurring radioactive samples from Chttp://weppi.gtk.fi/publ/foregsatlas/text/Th.pdfyprus characteristic geological rocks, University of Cyprus.

[18] A. EI-Taher, et. al., (2004), Determination of traces of uranium and thorium concentration in some Egyptian environmental matrices, Proceedings of the Environmental Physics Conference, 24-28.

[19] Ali Abdulwahab Ridha, (2013), Determination of Radionuclides Concentrations in Construction Materials Used in Iraq, https://www.researchgate.net/publication/304677185.

[20] Richard B. Firestone, (1999), Table of Isotopes, 1999 Update with CD-ROM.

[21] http://weppi.gtk.fi/publ/foregsatlas/text/Th.pdf

[22] Nafaa Reguigui,(2006), Gamma Ray Spectrometry, https://www.researchgate.net/publication/259533588

[23] Hossein Tavakoli, (2009), Effects of Detector dimension on the NaI(Tl) Detector response function, Journal of applied sciences, 2168-2173.

[24] Samik Raychaudhuri, (2008), Introduction To Monte Carlo Simulation, Proceedings of the 2008 Winter Simulation Conference.

[25] Richard B. Firestone, (2005), Physics of Gamma-ray Spectroscopy Measurements, Lawrence Berkeley National Laboratory, Berkeley, CA 94720 USA.

[26] A. Das and T. Ferbel, (2005), Introduction to Nuclear and Particle Physics Second Edition, World Scientific Publishing Co. Pte. Ltd.

[27] Mayeen Uddin Khandaker, (2011), High purity germanium detector in gamma-ray spectrometry IJFPS, Vol.1, No.2, pp. 42- 46.

[28] Dr. J.D.Bapat et. al., (2014), History Of Cement And Concrete In India A Paradigm Shift, Research gate, https://www.researchgate.net/publication/274953585.

[29] Dunuweera and R. M. G. Rajapakse, (2018), Cement Types, Composition, Uses and Advantages of Nanocement, Environmental Impact on Cement Production, and Possible Solutions, Advances in Materials Science and Engineering, doi.org/10.1155/2018/4158682.

[30] Hendrik G. van Oss, (2005), Background Facts and Issues Concerning Cement and Cement Data, Science for changing world, http://www.usgs.gov.

[31] A. R. Abdunnabi, (2012), XRF Analysis of Portland Cement for Major and Trace Elements, Nuclear Engineering Department, University of Tripoli.

[32] Yii Mei-Wo, (2014), Determination Performance of Gamma Spectrometry Co-Axial Hpge Detector In Radiochemistry And Environment Group, Nuclear Malaysia, Seminar R & D, 14 -16.

[33] Steffen Hauf, et. al., (2015), Radioactive Decays in Geant4, IEEE Transactions on Nuclear Science, DOI:10.1109/TNS.2013.2270894.

[34] Hubert L. Oczkowski, (2001), Calibration standard for use in gamma spectrometry and luminescence dating, Journal on Methods and Applications of Absolute Chronology, geochronometria Vol. 20, pp 31-38.

[35] International atomic energy agency, (2017), Determination and interpretation of characteristic limits for radioactivity measurements, IAEA Analytical Quality in Nuclear Applications Series No. 48.

[36] Abdallah Ibrahim Abd El-Mageed, et. al., (2014), Natural radioactivity and radiological hazards of some building materials of Aden, Yemen, Journal of Geochemical Exploration 140 4145.

[37] Reza pourimani, (2018), Radiological Assessment of the Artificial and Natural Radionuclide Concentrations of Wheat and Barley Samples in Karbala, Iraq, Iran J Med Phys 2018; 15:126-131. 10.22038/ijmp.2017.24190.1238.

[38] CAEN Sys, (2017), Systems and Spectroscopy Solutions, www.caensys.com.

[39] A. Faanu, O. K. Adukpo, et. al., (2016), Natural radioactivity levels in soils, rocks and water at a mining concession of Perseus gold mine and surrounding towns in Central Region of Ghana, a springer journal, DOI 10.1186/s40064-016-1716-5.

[40] Hoang Duc Tam, et. al., (2017), Optimization of the Monte Carlo simulation model of NaI(Tl) detector by Geant4 code, Applied Radiation and Isotopes, 130, 7579.

[41] A. A. Mowlavi, et. al., (2005), Calculation of Intrinsic Efficiency of NaI(Tl) Detector Using MCNP Code, International Journal of Pure and Applied Physics ISSN 0973-1776 Vol.1, No.2, pp. 129-136, Research India Publications, http://www.ripublication.com

[42] A. Elanique, (2017), Monte Carlo modelling of a NaI(Tl) scintillator detectors using MCNP simulation code, J. Mater. Environ. Sci., Volume 8, Issue 12, Page 4560-4565.

[43] T. Hosseini, et. al, (2006), Assessment of radionuclides in imported foodstuffs in Iran, Iran. J. Radiat. Res. pp. 149-153.

[44] Ghazwa Alzubaidi, et. al, (2016), Assessment of Natural Radioactivity Levels and Radiation Hazards in Agricultural and Virgin Soil in the State of Kedah, North of Malaysia, http://dx.doi.org/10.1155/2016/6178103.

[45] UNSCAEN Sys, (2017), CER (2000, Vol. I) Sources and effects of ionizing radiation, United Nations Scientific Committee on the Effects of Atomic Radiation UNSCEAR 2000 Report to the General Assembly, Annex B.

[46] Ayham Assie, et. al., (2016), Determination of natural radioactivity by gamma spectroscopy in Balad soil, Iraq, Pelagia Research Library Advances in Applied Science Research, 7(1):35-41.

[47] A. EL-TAHER, (2012), Assessment of natural radioactivity levels and radiation hazards for building materials used in qassim area, Saudi Arabia, Rom. Journ. Phys., Vol. 57, Nos. 34, P. 726735.

[48] http://weppi.gtk.fi/publ/foregsatlas/text/K.pdf

[49] Mark Bediako and Eric Opoku Amankwah, (2015), Analysis of Chemical Composition of Portland Cement in Ghana, http://dx.doi.org/10.1155/2015/349401.

[50] CD. Barton & A.D. Karathanasis, (2002), Clay minerals, Encyclopedia of Soil Science, Marcel Dekker, Inc.

[51] A. El-Taher and S. Makhluf, (2011), Radiological significance of Egyptian limestone and alabaster used for construction of dwellings, Indian Journal of Pure & Applied Physics, Vol. 49, pp. 157-161.

[52] U.S. Geological Survey Fact Sheet , (1997), Radioactive Elements in Coal and Fly Ash: Their Environmental Effects, Science for changing Word, FS-163-97.

[53] U. S. National Energy Strategy, (1991/1992), Executive Summary and Sustainable Energy Strategy, (1995), Chapter 7, pp 1-4.

[54] Xian-Yong, et. al., (2015), Coal-Based Products and Their Uses, https://www.researchgate.net/publication/285591902.

[55] B. P. Mazzilli, et. al., (2006), Radioactivity of coal and ashes from Figueira coal power plant in Brazil, Journal of Radioanalytical and Nuclear Chemistry, Vol. 270, No.3, 597602.

[56] Robert D., Crangle Jr., (2013), Pumice and Pumicite, U.S. Geological survey minerals year book.

[57] Ahmed Hassan Korna, et. al., (2014), Natural radioactivity levels and radiation hazards for gypsum materials used in Egypt, Vol.6, No.1, 5-13, http://dx.doi.org/10.4236/ns.2014.61002.

[58] B. E. zdis, et. al., (2017), Assessment of natural radioactivity in cements used as building materials in Turkey, J Radioanal Nucl Chem, 311:307316, DOI 10.1007/s10967-016-5074-0.

[59] Estokova A., Palascakova L., 2013, Study of Natural Radioactivity of Slovak Cements, Chemical Engineering transactions, 32,1675-1680.

[60] M. Nain, et. al., (2006), Alpha radioactivity in Indian cement samples, Iran. J. Radiat. Res. 3 (4): 171-176.

[61] Faweya Ebenezer Babatope, (2009), Radiation dose estimation from the radioactivity analysis of cement used in Nigeria, Jurnal fizik malaysia, volume 30, number 1 - 4.

[62] D.O. Kpeglo, et. al., (2011), Natural Radioactivity and its Associated Radiological Hazards in Ghanaian Cement, Research Journal of Environmental and Earth Sciences 3(2): 160-166.

[63] Muktha K, et, al., (2016), Comparative Study on OPC and PPC Composites with Foundry Sand as Partial Replacement for Fine Aggregate, Conference Paper, DOI: 10.13140/RG.2.1.1227.9448.

[64] A El-Taher & S. Makhluf, (2011), Radiological significance of Egyptian limestone and alabaster used for construction of dwellings, Indian Journal of Pure & Applied Physics, Vol. 49, pp. 157-161.

[65] T.M. Cioroianu, F. Bunus et. al., (2000), Environmental considerations on uranium and radium from phosphate fertilizers, Bucharest, 215-224.

[66] Mesay Adugna Kassa, (2017), Review on Environmental Effects of Ethiopian Floriculture Industry, Asian Research Journal of Agriculture, DOI: 10.9734/ARJA/2017/31884.

[67] Ione Makiko Yamazaki, Luiz Paulo Geraldo, (2003), Uranium content in phosphate fertilizers commercially produced in Brazil, Applied Radiation and Isotopes, 59, 133136.

[68] Atkure Defar, Ahmed Ali, (2013), Occupational induced health problems in floriculture workers in Sebeta and surrounding areas, West Shewa, Oromia, Ethiopia, Ethiop. J. Health, 64-71.

[69] Mulugeta Getu Sisay, (2009), Ethiopian Floriculture and Its Impact on the Environment: Regulation, Supervision and Compliance, 3(2) Mizan Law Review, 240-270.

[70] Gudeta Degytnu Tilahun, (2012), Socio-economic and Environmental Impact of Floriculture Industry in Ethiopia, Humboldt University of Berlin (Germany), MSc thesis.

Appendix I
Peak locate report

Peak Locate Analysis Report 7/27/2019 11:03:46 AM Page 1

****
***** P E A K L O C A T E R E P O R T *****
****

Detector Name: B13010
Sample Title: Soil Sample
Peak Locate Performed on: 7/27/2019 11:03:46 AM
Peak Locate From Channel: 180
Peak Locate To Channel: 8192
Peak Search Sensitivity: 3.00

Peak No.	Centroid Channel	Centroid Uncertainty	Energy (keV)	Peak Significance
1	190.65	0.2341	46.60	6.15
2	258.95	0.1814	63.29	10.15
3	306.20	0.0914	74.84	40.60
4	315.53	0.0772	77.12	54.45
5	332.09	0.3054	81.17	4.89
6	344.64	0.1722	84.23	9.51
7	356.74	0.1128	87.19	24.25
8	367.93	0.1327	89.92	19.10
9	380.40	0.1283	92.97	14.30
10	407.46	0.2400	99.58	5.92
11	431.58	0.2476	105.48	4.57
12	470.85	0.2968	115.08	3.26
13	528.14	0.1559	129.08	13.29
14	588.77	0.2850	143.90	3.82
15	629.96	0.2174	153.96	6.65
16	668.48	0.3660	163.38	3.05
17	760.98	0.1154	185.99	21.76
18	826.47	0.3408	201.99	3.30
19	856.02	0.1203	209.22	20.05
20	976.29	0.0556	238.61	93.05
21	989.22	0.1105	241.77	18.71
22	1058.79	0.2899	258.77	3.24
23	1105.58	0.1354	270.21	13.32
24	1134.79	0.1607	277.34	10.97
25	1207.95	0.0764	295.23	47.79
26	1227.72	0.1222	300.06	17.96
27	1246.02	0.3437	304.53	3.24
28	1341.99	0.1380	327.98	14.51
29	1384.08	0.0826	338.27	40.48
30	1439.90	0.0639	351.92	65.07
31	1675.22	0.1557	409.43	10.57
32	1795.51	0.2791	438.83	3.23
33	1853.10	0.3027	452.90	3.32
34	1877.26	0.3200	458.81	3.00
35	1894.46	0.1198	463.01	16.58
36	1965.72	0.2784	480.43	3.86
37	2089.72	0.0966	510.73	24.26
38	2300.74	0.2132	562.30	5.76
39	2386.06	0.0650	583.16	55.28
40	2492.85	0.0635	609.26	56.70
41	2722.15	0.2242	665.30	4.87

Peak No.	Centroid Channel	Centroid Uncertainty	Energy (keV)	Peak Significance
42	2895.81	0.2993	707.74	3.55
43	2975.52	0.0948	727.22	23.71
44	3090.46	0.2054	755.31	4.72
45	3123.19	0.2672	763.31	3.69
46	3143.76	0.1331	768.34	12.74
47	3159.69	0.1939	772.23	6.30
48	3200.86	0.2903	782.29	3.59
49	3214.37	0.1577	785.60	8.25
50	3252.42	0.1209	794.90	14.83
51	3298.36	0.2100	806.13	4.94
52	3396.26	0.2362	830.05	3.55
53	3419.59	0.1587	835.75	8.65
54	3436.31	0.2022	839.84	4.36
55	3520.87	0.1111	860.51	17.34
56	3537.26	0.3074	864.51	3.00
57	3699.11	0.2402	904.07	3.71
58	3728.01	0.0665	911.13	46.77
59	3822.12	0.1434	934.13	10.44
60	3946.94	0.1094	964.64	17.42
61	3964.34	0.0775	968.89	32.96
62	4095.94	0.2526	1001.06	3.49
63	4474.73	0.2750	1093.63	3.18
64	4543.58	0.2466	1110.46	4.06
65	4583.64	0.0916	1120.25	23.30
66	4725.72	0.1915	1154.97	5.10
67	4939.34	0.2600	1207.18	3.52
68	5065.47	0.1237	1238.01	12.00
69	5241.38	0.2169	1281.00	3.89
70	5637.06	0.1170	1377.70	13.48
71	5734.04	0.1862	1401.41	4.84
72	5760.89	0.1567	1407.97	7.75
73	5976.84	0.0375	1460.75	124.86
74	6119.94	0.1673	1495.72	6.58
75	6174.81	0.1564	1509.13	7.17
76	6296.30	0.2326	1538.83	3.13
77	6315.01	0.2539	1543.40	3.30
78	6466.10	0.2193	1580.32	3.95
79	6498.29	0.1185	1588.19	13.19
80	6515.34	0.1869	1592.36	5.36
81	6631.01	0.1502	1620.63	6.72
82	6671.87	0.1446	1630.62	8.27
83	6702.81	0.2178	1638.18	4.25
84	6797.73	0.1724	1661.38	5.05
85	6866.95	0.2670	1678.29	3.09
86	7077.24	0.1205	1729.69	11.81
87	7219.78	0.0817	1764.53	24.31
88	7423.98	0.2764	1814.43	3.36
89	7559.70	0.1410	1847.60	8.33

? = Adjacent peak noted

Appendix II
Peak analysis report

***** P E A K A N A L Y S I S R E P O R T *****

Detector Name: B13010
Sample Title: Soil Sample
Peak Analysis Performed on: 7/27/2019 11:03:53 AM
Peak Analysis From Channel: 180
Peak Analysis To Channel: 8192

	Peak No.	ROI start	ROI end	Peak centroid	Energy (keV)	FWHM (keV)	Net Peak Area	Net Area Uncert.	Continuum Counts
F	1	185-	196	190.46	46.55	0.89	8.84E+002	61.28	5.37E+003
F	2	253-	264	258.91	63.28	0.92	1.27E+003	71.76	6.93E+003
M	3	302-	388	306.24	74.85	0.94	7.75E+003	114.59	7.84E+003
m	4	302-	388	315.50	77.11	0.95	1.03E+004	108.84	8.75E+003
m	5	302-	388	344.80	84.27	0.96	7.80E+002	40.51	7.89E+003
m	6	302-	388	356.77	87.20	0.96	5.21E+003	106.28	7.53E+003
m	7	302-	388	367.92	89.92	0.96	3.68E+003	112.50	6.61E+003
m	8	302-	388	380.44	92.98	0.97	3.72E+003	82.74	6.79E+003
F	9	399-	415	407.14	99.51	0.98	6.76E+002	64.08	8.34E+003
F	10	425-	439	431.63	105.49	0.99	6.45E+002	65.56	7.87E+003
F	11	464-	479	471.03	115.12	1.00	3.78E+002	63.40	8.27E+003
F	12	524-	532	528.10	129.07	1.02	1.43E+003	73.14	4.81E+003
F	13	582-	597	588.98	143.95	1.03	4.69E+002	65.05	8.24E+003
F	14	624-	636	629.90	153.95	1.05	6.19E+002	66.47	6.60E+003
F	15	754-	769	760.96	185.98	1.08	3.45E+003	84.62	7.26E+003
F	16	849-	865	856.04	209.22	1.10	2.52E+003	77.13	6.97E+003
M	17	969-	998	976.37	238.63	1.13	2.75E+004	178.21	5.68E+003
m	18	969-	998	988.77	241.66	1.13	4.67E+003	87.30	5.06E+003
F	19	1097-	1115	1105.78	270.26	1.16	1.93E+003	66.14	5.39E+003
F	20	1130-	1144	1134.84	277.36	1.16	1.00E+003	58.57	4.29E+003
M	21	1200-	1250	1207.92	295.22	1.18	7.72E+003	102.19	4.20E+003
m	22	1200-	1250	1227.73	300.06	1.18	1.87E+003	64.53	3.68E+003
F	23	1332-	1348	1341.88	327.96	1.20	1.39E+003	58.79	3.79E+003
F	24	1377-	1393	1384.15	338.29	1.21	5.60E+003	89.46	3.86E+003
F	25	1429-	1449	1439.84	351.90	1.22	1.38E+004	126.77	4.20E+003
F	26	1670-	1682	1675.18	409.42	1.26	7.54E+002	48.32	2.22E+003
F	27	1791-	1805	1795.66	438.86	1.28	1.90E+002	38.14	2.15E+003
M	28	1845-	1901	1853.53	453.01	1.29	2.03E+002	39.09	2.33E+003
m	29	1845-	1901	1894.41	463.00	1.30	1.69E+003	55.10	2.05E+003
F	30	1960-	1974	1965.73	480.43	1.31	1.46E+002	37.04	1.95E+003
F	31	2078-	2100	2089.66	510.72	1.99	4.50E+003	82.57	3.11E+003
F	32	2295-	2310	2301.17	562.41	1.36	2.85E+002	37.08	1.77E+003
F	33	2377-	2397	2386.08	583.16	1.37	9.77E+003	105.95	2.28E+003
F	34	2481-	2504	2492.90	609.27	1.39	1.08E+004	110.23	2.38E+003
F	35	2716-	2733	2722.46	665.38	1.42	2.45E+002	35.07	1.73E+003
F	36	2969-	2986	2975.52	727.22	1.45	2.47E+003	58.11	1.35E+003
F	37	3083-	3102	3090.86	755.41	1.46	3.20E+002	34.37	1.62E+003
M	38	3114-	3171	3123.50	763.39	1.47	1.76E+002	32.60	1.50E+003
m	39	3114-	3171	3143.58	768.30	1.47	1.02E+003	43.10	1.41E+003
m	40	3114-	3171	3159.88	772.28	1.47	4.42E+002	35.30	1.34E+003
M	41	3195-	3223	3200.82	782.29	1.48	9.37E+001	30.40	1.14E+003
m	42	3195-	3223	3214.35	785.59	1.48	5.23E+002	37.14	1.45E+003

	Peak No.	ROI start	ROI end	Peak centroid	Energy (keV)	FWHM (keV)	Net Peak Area	Net Area Uncert.	Continuum Counts
F	43	3242	3264	3252.43	794.90	1.48	1.12E+003	44.31	1.66E+003
F	44	3290	3306	3298.11	806.07	1.49	2.34E+002	32.19	1.24E+003
M	45	3388	3448	3396.58	830.13	1.50	2.11E+002	31.43	1.24E+003
m	46	3388	3448	3419.22	835.66	1.50	5.02E+002	36.03	1.42E+003
m	47	3388	3448	3436.57	839.90	1.50	3.12E+002	33.78	1.38E+003
F	48	3511	3542	3520.81	860.49	1.51	1.25E+003	45.64	2.16E+003
M	49	3691	3739	3699.10	904.07	1.53	1.67E+002	31.62	1.25E+003
m	50	3691	3739	3727.97	911.12	1.54	7.27E+003	90.79	1.33E+003
F	51	3810	3831	3821.82	934.06	1.55	6.15E+002	37.14	1.39E+003
M	52	3935	3976	3946.98	964.65	1.56	1.42E+003	47.47	1.27E+003
m	53	3935	3976	3964.36	968.90	1.56	4.19E+003	71.38	1.29E+003
F	54	4089	4102	4095.95	1001.06	1.58	1.08E+002	30.20	1.01E+003
F	55	4537	4550	4543.47	1110.43	1.62	1.27E+002	31.43	1.03E+003
F	56	4571	4596	4583.56	1120.23	1.63	2.33E+003	58.29	2.02E+003
F	57	4715	4738	4725.48	1154.92	1.64	3.28E+002	35.25	1.81E+003
F	58	4930	4947	4939.38	1207.19	1.66	1.90E+002	34.63	1.51E+003
F	59	5057	5079	5065.51	1238.02	1.68	9.28E+002	46.25	2.14E+003
F	60	5231	5250	5241.42	1281.01	1.69	2.25E+002	30.00	1.11E+003
F	61	5626	5651	5637.29	1377.76	1.73	7.45E+002	33.18	6.12E+002
M	62	5726	5772	5734.14	1401.43	1.74	2.00E+002	22.52	4.39E+002
m	63	5726	5772	5760.80	1407.95	1.74	3.55E+002	25.66	4.89E+002
F	64	5962	5991	5976.81	1460.74	1.76	5.52E+004	235.28	6.06E+002
F	65	6112	6133	6120.47	1495.85	1.77	2.06E+002	19.64	2.79E+002
F	66	6164	6185	6174.68	1509.10	1.78	2.52E+002	21.56	3.31E+002
M	67	6290	6322	6296.38	1538.85	1.79	6.91E+001	15.04	2.16E+002
m	68	6290	6322	6315.45	1543.50	1.79	4.58E+001	14.35	2.22E+002
M	69	6458	6530	6467.05	1580.56	1.80	1.65E+002	16.84	1.75E+002
m	70	6458	6530	6498.14	1588.15	1.81	6.53E+002	28.42	2.23E+002
m	71	6458	6530	6515.10	1592.30	1.81	2.26E+002	19.58	2.47E+002
F	72	6619	6641	6630.69	1620.55	1.82	2.61E+002	20.82	2.73E+002
M	73	6661	6710	6671.79	1630.60	1.82	3.09E+002	20.98	1.91E+002
m	74	6661	6710	6702.84	1638.18	1.82	6.33E+001	13.79	1.71E+002
F	75	6788	6808	6797.69	1661.37	1.83	1.72E+002	16.72	1.58E+002
F	76	6860	6873	6867.20	1678.35	1.84	3.68E+001	11.81	1.08E+002
F	77	7063	7091	7077.02	1729.63	1.85	5.36E+002	25.78	2.28E+002
F	78	7204	7235	7219.70	1764.50	1.86	2.36E+003	49.71	1.64E+002
F	79	7547	7575	7559.63	1847.58	1.89	3.46E+002	21.32	1.98E+002

M = First peak in a multiplet region
m = Other peak in a multiplet region
F = Fitted singlet

Appendix III
Nuclide ISO 11929 report and Gamma spectrum analysis

```
ISO11929 MDA Report                                              7/27/2019  11:05:31

*************************************************************************
*****                  N U C L I D E   I S O  1 1 9 2 9   R E P O R T
*************************************************************************

       Nuclide   MDA      Decision  Conf Int  Conf Int  Wt. Mean  Wt. Mean  Best
       Name              Level     Lower Lmt Upper Lmt Activity  Act Unc   Activ
             (Bq /kg  )(Bq /kg  )(Bq /kg  )(Bq /kg  )(Bq /kg  )(Bq /kg  )(Bq /k

+      K-40     7.2E+000  3.6E+000  1.2E+003  1.4E+003  1.3E+003  6.1E+001  1.3E+
+ >    MN-54    0.0E+000  0.0E+000  8.2E-001  1.2E+000  1.0E+000  9.7E-002  1.0E+
+ >    TI-208   0.0E+000  0.0E+000  9.0E+002  4.1E+003  2.5E+003  8.3E+002  2.5E+
+ >    BI-212   0.0E+000  0.0E+000  3.4E+001  4.4E+001  3.9E+001  2.6E+000  3.9E+
+ >    PB-212   0.0E+000  0.0E+000  4.3E+001  5.9E+001  5.1E+001  4.2E+000  5.1E+
+      BI-214   1.4E+000  6.8E-001  3.6E+001  4.2E+001  3.9E+001  1.4E+000  3.9E+
+      PB-214   1.3E+000  6.1E-001  3.4E+001  4.3E+001  3.9E+001  2.4E+000  3.9E+
+      AC-228   2.6E+000  1.3E+000  8.1E+001  9.9E+001  9.0E+001  4.5E+000  9.0E+

       + = Nuclide identified during the nuclide identification
       > = Calculated MDA is zero due to zero counts in the region, or
           the region is outside the spectrum, or MDA has not been calculated
       ? = MDA calculation has failed
       Errors quoted at  1.000 sigma
Ethiopian Radiation Protection Authority Laboratory
*************************************************************************
*****        G A M M A   S P E C T R U M    A N A L Y S I S         *****
*************************************************************************


Filename: C:\GENIE2K\CAMFILES\HAILU New\H.02.CNF

Report Generated On             : 7/27/2019  11:05:33 AM

Sample Title                    : Soil Sample
Sample Description              :
Sample Identification           : ERTL/H.02/19
Sample Type                     : Soil
Sample Geometry                 : 538G-E

Peak Locate Threshold           :  3.00
Peak Locate Range (in channels) :   180 -  8192
Peak Area Range (in channels)   :   180 -  8192
Identification Energy Tolerance :    1.000 keV

Sample Size                     :  4.850E-001 kg

Sample Taken On                 :
Acquisition Started             : 7/16/2019   5:51:57 PM

Live Time                       :    36000.0 seconds
Real Time                       :    36138.9 seconds

Dead Time                       :   0.38 %

             Energy Calibration Used Done On       : 6/24/2019
             Efficiency Calibration Used Done On   : 7/27/2019
             Efficiency ID                         : SAMPLE_NANALYSIS
```